Analysis of Higher-Order Soliton Compression for Formation of Ultra-Short Pulses

By

Shah Md. Salimullah

MASTER OF SCIENCE IN ELECTRICAL AND ELECTRONIC ENGINEERING

Department of Electrical and Electronic Engineering

BANGLADESH UNIVERSITY OF ENGINEERING AND TECHNOLOGY

16 August, 2015

The thesis titled **"Analysis of Higher-Order Soliton Compression for Formation of Ultra-Short Pulses"** submitted by Shah Md. Salimullah, Student No: 0413062220, Session: April, 2013, has been accepted as satisfactory in partial fulfillment of the requirement for the degree of MASTER OF SCIENCE IN ELECTRICAL AND ELECTRONIC ENGINEERING on 16 August, 2015.

BOARD OF EXAMINERS

1._____

Dr. Mohammad Faisal
Associate Professor
Department of Electrical and Electronic Engineering, — Chairman
Bangladesh University of Engineering and Technology (BUET) — (Supervisor)
Dhaka – 1000, Bangladesh

2._____

Dr. Taifur Ahmed Chowdhury
Professor and Head — Member
Department of Electrical and Electronic Engineering, — (Ex-officio)
Bangladesh University of Engineering and Technology (BUET)
Dhaka – 1000, Bangladesh

3._____

Dr. Md. Saiful Islam
Professor
IICT, Bangladesh University of Engineering and Technology (BUET) — Member
Dhaka – 1000, Bangladesh

4._____

Dr. Intekhab Alam
Assistant Professor
Dept. of EEE, United International University — Member
UIU Bhaban, House#80, Satmosjid Road, — (External)
Dhanmondi, Dhaka -1209

CANDIDATE'S DECLARATION

It is hereby declared that this thesis or any part of it has not been submitted elsewhere for the award of any degree or diploma and that all sources are acknowledged.

Signature of the Candidate

_____

Shah Md. Salimullah

DEDICATION

To my beloved parents

ACKNOWLEDGEMENT

First of all, I would like to thank Allah for giving me the ability to complete this thesis work.

I would like to express my sincere gratitude to my supervisor, Dr. Mohammad Faisal. This thesis would not have been completed without his support and guidance. I would like to express my great thanks and gratefulness for his instructions, continuous encouragement, valuable discussions, and careful review during the period of this research. His keen sight and a wealth of farsighted advice and supervision have always provided me the precise guiding frameworks of this research. I have learned many valuable lessons and concepts of Optical fiber Communication from him through my study, which I have utilized to develop my abilities to work innovatively and to boost my knowledge. His constant encouragement gave me the confidence to carry out my work.

I would like to thank all my teachers. They gave the knowledge and directions that have helped me throughout my life. I express my gratitude to my teachers from Bangladesh University of Engineering and Technology. The knowledge I learned from the classes in my M.Sc. levels were essential for this thesis.

Last but not the least, I would like to thank by parents and my family. Their unconditional support made it possible for me to finish this thesis.

ABSTRACT

In this study, propagation of ultrashort fundamental and higher-order soliton pulse has been studied in details for both communication and medical applications. Although so many researchers already have studied the propagation of ultrashort pulse, the effect of self-steepening and Raman scattering are not so far taken into consideration in same study yet. But in addition to group-velocity dispersion and self-phase modulation, third order dispersion as higher-order dispersive effect, self-steepening and intrapulse Raman scattering as higher-order nonlinear effects are of great concern for ultrashort pulses. Considering all the effects mentioned above, soliton pulse propagation operating at a speed of 400 Gb/s and 1 Tb/s in different types of optical fiber like standard single mode fiber, nonzero dispersion shifted fiber, large effective area fiber, multiclad dispersion flattening fiber and multiclad dispersion shifted fiber has been investigated. Multiclad dispersion shifted fiber has been proposed to be a flexible and effective means for ultrashort soliton propagation for high speed communication applications.

At the same time compressed ultrashort soliton has become prominent in removal of tissue as well as cancer cell treatment. The compressed ultrashort soliton has spatial dimension (nm-pm range) lower than that of cancer cell size, hence it causes no side effect other then removing the specific affected tissue. To get ultrashort soliton of specific spatial range a good compressor is needed. Dispersion decreasing fiber has been proposed to be a good compressor (calculated pulse width after compression is 90fs and spatial dispersion is 722.6pm) of ultrashort soliton instead of dispersion compensating fiber and fiber Bragg grating for medical applications. For radiotherapy of cancer treatment the laser beam spot size is in mm^2. Recently in 2014 the beam spot size has been used as 70-100nm^2 for nanosurgical tools and removal of tissue as well as ablation of cancer cell. But for precision ablation like Corneal sculpting, neuron disruption (brain: seizure control), Stapedectomy (ear: hearing restoration), bone resection near nerve, Transmyocardial revascularization (heart: improved output, pain) we need to go for more small beam spot. Here in this study we have proposed fiber based soliton pulse of beam spot size as 2nm^2 - 722pm^2 range that can be used for both precision ablation and soliton therapy in cancer treatment.

Contents

List of Publications:

1. Shah Md. Salimullah*, Mohammad Faisal, ―Femtosecond Soliton Formation by Higher-Order Soliton Compression in Linear Dispersion Decreasing Fiber," paper no. 5066 (paper code: H-11), 20th Microoptics Conference (MOC'15), Fukuoka, Japan, Oct. 25 - 28, 2015. (Accepted and yet to be presented on 27 October, 2015)

List of Abbreviations

CPM	Cross phase modulation
DCF	Dispersion compensating fiber
DDF	Dispersion decreasing fiber
FBG	Fiber Bragg grating
FWHM	Full width at half maximum
GVD	Group velocity dispersion
IRS	Intrapulse Raman scattering
LEAF	Large effective area fiber
MCDFF	Multiclad dispersion flattening fiber
MCDSF	Multiclad dispersion shifted fiber
NLSE	Nonlinear Schrödinger equation
NZDSF	Non-zero dispersion shifted fiber
SBS	Stimulated Brillouin scattering
SPM	Self-phase modulation
SRS	Stimulated Raman scattering
SS	Self-steepening
SSFM	Split-step Fourier method
SSMF	Standard single mode fiber
TOD	Third order dispersion

Chapter 1

Introduction

1.1 Introduction

Soliton pulse has become a subject of tremendous investigation and thorough analysis for the past few decades [1-5]. It offers the possibility of a dynamic balance between group-velocity dispersion (GVD) and self-phase modulation (SPM), the two effects that limit the performance of non-soliton systems. The term ‗soliton‘‘ is used in optics to describe a localized pulse that travels without a change in shape, an entity which the mathematics community refers to as a solitary wave. Historically speaking, solitons were defined as those solutions which asymptotically preserve their speed and amplitude upon interaction. There are two types of soliton, one is fundamental and other is higher-order soliton. These happen with the combination of dispersive length and nonlinear length of the fiber. Generally soliton governs by the nonlinear Schrödinger equation and we can get the solution of this equation using different methods. In split-step Fourier method total length of the fiber is divided into small one and a combination of dispersion and nonlinearity is maintained. When dispersive length is equal to the nonlinear length only then fundamental soliton is formed. If dispersive length is four times greater than nonlinear length, second order soliton is formed. And thus the higher-order soliton can be got.

Interest in optical solitons has grown steadily in recent decades. The field has considerable potential for technological applications, and it presents many exciting research problems both from a fundamental and an applied point of view. New optical devices are in various stages of development; soliton information processing looms on the horizon. At the same time, basic research in nonlinear optical phenomena maintains its vitality. Although many technological applications of optical solitons are being actively pursued, including soliton switching, pulse compression, wavelength conversion and corresponding physical problems which feature optical solitons are second-harmonic generation, three-wave interactions, self-induced transparency, together with gap solitons, incoherent solitons, etc. One of the areas of nonlinear optics which has attracted considerable attention in the last twenty years is the field of soliton communication systems. Over the past fifty years, soliton research has been conducted in fields as diverse as particle physics, molecular biology, quantum mechanics,

geology, meteorology, oceanography, astrophysics and cosmology [6]. But the area of soliton research which is technologically most significant is currently the study of solitons in optical fibers, where the sought-after goal is to use soliton pulses as the information carrying __bits‘‘ in optical fibers. Optical communications is a wonderful example of how the interplay between mathematics and more applied research has generated significant technological advances: Historically, soliton research and optical communications started as two separate fields. In the last thirty-five years, however, technological advances in conventional transmission systems have often inspired parallel developments in soliton systems Soliton based communication systems are leading candidates for ultra-high-speed long-haul lightwave transmission links. Fundamental Soliton Trains for High-Bit-Rate Optical Fiber Communication Lines had shown by Pave1 V. Mamyshev [1]. One channel 100 Gbits/s with amplifier spacing 120km has been shown by Ren´e-Jean Essiambre and Govind P. Agrawal in 1996 [2]. Consequently Timing jitter of ultrashort solitons in high-speed communication systems has shown by the same authors [3]. The IEEE 802.15.3c standard operates at the 60 GHz frequency band, and it is applicable for a short distance optical communication such as indoor systems, where the higher transmission data rate can be performed using a high frequency band of the output optical soliton pulses [4]. Consequently high-capacity soliton transmission for indoor and outdoor communications using integrated ring resonators has been shown very recently [5].

At the same time ultrashort soliton pulse have an amazing array of possible applications in the health and medicine industry. In recent years ultrashort soliton pulse has become the subject of numerous studies because of the potential use of it in medical applications. Modern bio-photonics and microscopy techniques like coherent anti-stokes Raman Scattering (CARS) microscopy, optical coherence tomography [7] etc. are extremely related with ultrashort soliton pulse that are used for identification of chemical and biological species. The ultrafast pulses have found multifunctional usage in biology and medicine [8, 9]. The ability of precise and accurate cutting quality on different materials makes the femtosecond pulse a promising multifunctional surgery tool for refractive surgery [10], surgery on the inner ear [11], dentistry [12, 13], and cardiovascular surgery [14]. To accomplish this medical applications highly stable and high power pulse are needed. Ultrashort soliton pulse could be the best choice to the case mentioned above.

1.2 Motivation

The soliton phenomenon was first described in 1834 [15] by John Scott Russell (1808–1882) who observed a solitary wave in the Union Canal in Scotland. He reproduced the phenomenon in a wave tank and named it the "Wave of Translation". Scott Russell spent some time making practical and theoretical investigations of these waves. He built wave tanks at his home and noticed some key properties:

(i) The waves are stable, and can travel over very large distances (normal waves would tend to either flatten out, or steepen and topple over)

(ii) The speed depends on the size of the wave, and its width on the depth of water.

(iii) Unlike normal waves they will never merge – so a small wave is overtaken by a large one, rather than the two combining.

(iv) If a wave is too big for the depth of water, it splits into two, one big and one small.

Scott Russell's experimental work seemed at odds with Isaac Newton's and Daniel Bernoulli's theories of hydrodynamics. George Biddell Airy and George Gabriel Stokes had difficulty accepting Scott Russell's experimental observations because they could not be explained by the existing water wave theories. Their contemporaries spent some time attempting to extend the theory but it would take until the 1870s before Joseph Boussinesq and Lord Rayleigh published a theoretical treatment and solutions. In 1895 Diederik Korteweg and Gustav de Vries provided what is now known as the Korteweg–de Vries equation, including solitary wave and periodic cnoidal wave solutions [16].

In 1965 Norman Zabusky of Bell Labs and Martin Kruskal [17] of Princeton University first demonstrated soliton behavior in media subject to the Korteweg–de Vries equation (KdV equation) in a computational investigation using a finite difference approach. They also showed how this behavior explained the puzzling earlier work of Fermi, Pasta and Ulam. In 1967, Gardner, Greene, Kruskal and Miura discovered an inverse scattering transform enabling analytical solution of the KdV equation [18]. The work of Peter Lax on Lax pairs and the Lax equation has since extended this to solution of many related soliton-generating systems. Note that solitons are, by definition, unaltered in shape and speed by a collision with other solitons [19]. So solitary waves on a water surface are near-solitons, but not exactly – after the interaction of two (colliding or overtaking) solitary waves, they have changed a bit in amplitude and an oscillatory residual is left behind [20-22]. Much experimentation has been done using solitons in fiber optics applications. Solitons in a fiber optic system are

described by the Manakov equations. Solitons' inherent stability make long-distance transmission possible without the use of repeaters, and could potentially double transmission capacity as well [19]. Akira Hasegawa of AT&T Bell Labs was the first to suggest that solitons could exist in optical fibers, due to a balance between self-phase modulation and anomalous dispersion [19]. Also in 1973 Robin Bullough made the first mathematical report of the existence of optical solitons. He also proposed the idea of a soliton-based transmission system to increase performance of optical telecommunications. From the Universities of Brussels and Limoges– made the first experimental observation of the propagation of a dark soliton, in an optical fiber in 1987. It was 1988, Linn Mollenauer and his team transmitted soliton pulses over 4,000 kilometers using a phenomenon called the Raman effect, named after Sir C. V. Raman who first described it in the 1920s, to provide optical gain in the fiber.
A Bell Labs research team in 1991 transmitted solitons error-free at 2.5 gigabits per second over more than 14,000 kilometers, using erbium optical fiber amplifiers (spliced-in segments of optical fiber containing the rare earth element erbium). Pump lasers, coupled to the optical amplifiers, activate the erbium, which energizes the light pulses. Revolutionary findings got by Thierry Georges and his team in 1998 at France Telecom R&D Center, who demonstrated a composite data transmission of 1 terabit per second (1,000,000,000,000 units of information per second), combining optical solitons of different wavelengths (wavelength-division multiplexing),The above impressive experiments have not translated to actual commercial soliton system deployments however, in either terrestrial or submarine systems, chiefly due to the Gordon–Haus (GH) jitter. The GH jitter requires sophisticated, expensive, compensatory solutions that ultimately make dense wavelength-division multiplexing (DWDM) soliton transmission in the field unattractive, compared to the conventional non-return-to-zero/return-to-zero paradigm. Further, the likely future adoption of the more spectrally efficient phase-shift-keyed/QAM formats makes soliton transmission even less viable, due to the Gordon–Mollenauer effect. Consequently, the long-haul fiber optic transmission soliton has remained a laboratory curiosity. Cundiff predicted the existence of a vector soliton in a birefringence fiber cavity passively mode locking through SESAM in 2000 [23]. The polarization state of such a vector soliton could either be rotating or locked depending on the cavity parameters. In 2008 D. Y. Tang et al. observed a novel form of higher-order vector soliton from experiments and numerical simulations. Different types of vector solitons and the polarization state of vector solitons have been investigated by his group [24]. The rapid increase in popularity of bandwidth-consuming applications such as internet video, cloud storage, over-the-top (OTT), and social networking requires large

volumes of data to be transmitted over long distances. This has fueled the historically exponential growth of data traffic volumes in the worldwide telecommunication network, and based on current trends it is likely to continue to drive an unsurpassed need for transmission capacity over the next decade. After 40 Gb/s the industry-wide drive to develop the optical components, subsystems and systems required to upgrade long haul and ultra long-haul networks to 100 G line rates instead of 160Gb/s. With the further maturation of high speed digital-to-analog converter (DAC), Nyquist wavelength-division-multiplexing (N-WDM) super-channels with much higher spectrum efficiency (SE) based digital signal processing (DSP) at both transmitter and receiver sides has attracted a great deal of interest for the transmission of 100G beyond [25–33]. Actually the trend is varying like 40Gb/s, 100Gb/s, 224Gb/s, 400Gb/s, 448Gb/s, 512Gb/s, 1Tb/s [34-40] To meet the demand for large traffic volume and its increasing dynamic nature, propagation of ultrashort soliton pulse is a promising solution. In order to increase the bit rate to more than 100 Gbit/s for a single carrier wavelength, the soliton pulse width should be in the sub-picosecond i.e femtosecond region. Transmission of 20Gb/s data over distances of 20000km was achieved using dispersion managed solitons in 1999 [41]. A new technique adiabatic soliton trapping for achieving sub-picosecond i.e femtosecond optical soliton communication over long distances was proposed. And the author said it will cover around 100Gb/s [42]. Next in 2005 distortionless 50 km fiber transmission for, 500 fs pulses, using dispersion compensating fiber and a programmable pulse shaper as a spectral phase equalizer was demonstrated [43]. In 2006, constrained coding was proposed as a method to increase the data rate in dispersion-managed soliton (DMS) communication systems [44]. And most recently research on ultrashort soliton for communication purpose is of greatest interest [45, 46].

In case of ultrashort pulse, all higher-order dispersive and nonlinear effects like third order dispersion, self-steepening, intrapulse Raman scattering are of great concern. Although so many researchers already have studied the propagation of ultrashort pulse [47], [48], [49], [50], [51], most of them neglected either the effect of self-steepening or Raman scattering. In an experiment, 830-fs pulses with peak powers up to 530 W were explored in fibers up to 1 km long without considering fiber loss [49]. In an experiment, the combination of a DCF and a frequency-resolved, programmable, dispersion compensator compensated second order dispersion and TOD simultaneously over a 30-nm-wide wavelength range [52]. This scheme allowed transmission of a 0.2-ps pulse train with 22-nm bandwidth over a distance of 85 km. In a later experiment, 0.25-ps could be transmitted over 139 km when dispersion up to fourth

order was compensated using a DCF with a negative slope [53]. A single high-speed channel at 640 Gb/s (obtained through time-division multiplexing) has been transmitted over 92km by compensating group-velocity dispersion (GVD) and TOD [54]. In this experiment only TOD is in consideration as the higher-order effect. But with decrease in pulse width the higher-order effects become dominant. And if higher-order nonlinear effects are considered then the propagation distance becomes reduced.

Getting motivations from these facts, in this study we will explore the propagation of ultrashort soliton pulse (fundamental and higher-order) considering higher-order dispersive and nonlinear effects like third order dispersion, self-steepening, intrapulse Raman scattering through different optical fiber. At the same time a comparative study will be given for ultrashort soliton compression in Dispersion Decreasing Fiber (DDF), Dispersion Compensating Fiber (DCF) and Fiber Bragg Grating (FBG). More specifically how we can use our compressed pulse in medical applications will also be observed.

1.3 Objectives

The objectives of this thesis are:

i. To investigate the propagation characteristics of ultrashort fundamental and higher-order soliton for 400 Gb/s and 1Tb/s in different optical fibers like standard single mode fiber (SSMF), nonzero dispersion shifted fiber (NZDSF), large effective area fiber (LEAF), Multiple-clad dispersion flattening fiber (MCDFF) and Multiple-clad dispersion shifted fiber (MCDSF) for communication applications.

ii. To explore the compression of ultrashort fundamental and higher-order soliton pulse in dispersion compensating fiber (DCF), fiber Bragg grating (FBG) and dispersion decreasing fiber (DDF).

iii. To observe the medical applications of compressed ultrashort soliton pulse and find ―soliton therapy" as a viable technique for cancer cell treatment.

The outcome of this thesis is to propose the best possible fiber for ultrashort soliton propagation for communication applications and to explore the suitability of DDF as ultrashort soliton compressor instead of DCF and FBG for different applications like industrial applications, medical applications etc. MCDSF is proven to be a flexible, compact and effective waveguide for ultrashort soliton propagation.

1.4 Thesis Orientation

This thesis is divided in chapters for presenting a structured view of the developed work. In this introductory chapter the main purposes and motivations of the work is presented. Since this is a thesis where numerical analysis is key terms, chapter 2 explains the higher-order linear and nonlinear effects. In chapter 3, we start with the general concept of ultrashort soliton both fundamental and higher-order. Then we have given an overview of mathematical background where the evolution of nonlinear Schrödinger equation (NLSE) is analyzed for ultrashort soliton.

In chapter 4 the details simulation setup with necessary values of relevant parameters are presented. Different characteristics are shown like higher-order dispersive and nonlinear effects on ultrashort soliton. Chapter 5 deals with the compression of ultrashort soliton both fundamental and higher-order. A comparison between DDF, DCF and FBG is demonstrated. Chapter 6 comprises conclusions regarding all of the previous chapters. This chapter also suggests the possible future opportunities and scopes of this study.

Chapter 2

Linear and Nonlinear Effects in Optical Fiber

2.1 Introduction

In optics the terms linear and nonlinear, mean intensity independent and intensity dependent phenomena respectively. Nonlinear effects in optical fibers occur due to change in the refractive index of the medium with optical intensity and, inelastic scattering phenomena. The power dependence of the refractive index is responsible for the Kerr-effect. Depending upon the type of input signal, the Kerr-nonlinearity manifests itself in three different effects such as Self-Phase Modulation (SPM), Cross-Phase Modulation (CPM) and Four-Wave Mixing (FWM). At high power level, the inelastic scattering phenomenon can induce stimulated effects such as Stimulated Brillouin-Scattering (SBS) and Stimulated Raman-Scattering (SRS). The intensity of scattered light grows exponentially if the incident power exceeds a certain threshold value. The difference between Brillouin and Raman scattering is that the Brillouin generated phonons (acoustic) are coherent and give rise to a macroscopic acoustic wave in the fiber, while in Raman scattering the phonons (optical) are in coherent and no macroscopic wave is generated. Except for SPM and CPM, all nonlinear effects provide gains to some channel at the expense of depleting power from other channels. SPM and CPM affect only the phase of signals and can cause spectral broadening, which leads to increased dispersion [55-59]. Among the higher-order nonlinear effects Self-Steepening (SS) results from the intensity dependence of the group velocity [60]–[63] and the effect of Intrapulse Raman Scattering (IRS) happens by the overlap of the power spectrum of the short pulse with its own Raman gain.

This chapter is organized as follows:

The basics of nonlinear effects in optical fiber are discussed in Section 2.2. Self-phase modulation, cross-phase modulation, four-wave mixing, stimulated Raman scattering and stimulated Brillouin scattering are described in sub-sections 2.2.1.1, 2.2.1.2, 2.2.1.3, 2.2.1.4, and 2.2.1.5 respectively.

2.2 Linear and Nonlinear Effects

In fiber optic communication systems, linear impairments are due to the fiber loss, chromatic dispersion (CD) or group-velocity dispersion (GVD), third order dispersion (TOD) etc. Light

traveling in an optical fiber loses power over distance. When the optical communication systems operated at higher bitrates such as 10 Gbp/s and above and/or at higher transmitter powers, it is important to consider the effects of nonlinearities. In the case of WDM systems, nonlinear effects can become important even at moderate powers and bitrates. The nonlinear effects that we consider in this section arise owing to the dependence of the refractive index on the intensity of the applied electric field, which in turn is proportional to the square of the field amplitude. At sufficiently high optical intensities, non-linear refraction occurs in the core (Kerr effect), which is the variation of the index of refraction with light intensity. This makes nonlinear effects a critical concern in optical networks since long-haul transmission commonly relies on high power lasers to transmit optical pulses over long spans to overcome attenuation. Nonlinear Effects are comprised of first-order and higher-order effects. The linear and nonlinear effects that affect the shape of an optical pulse are as follows:

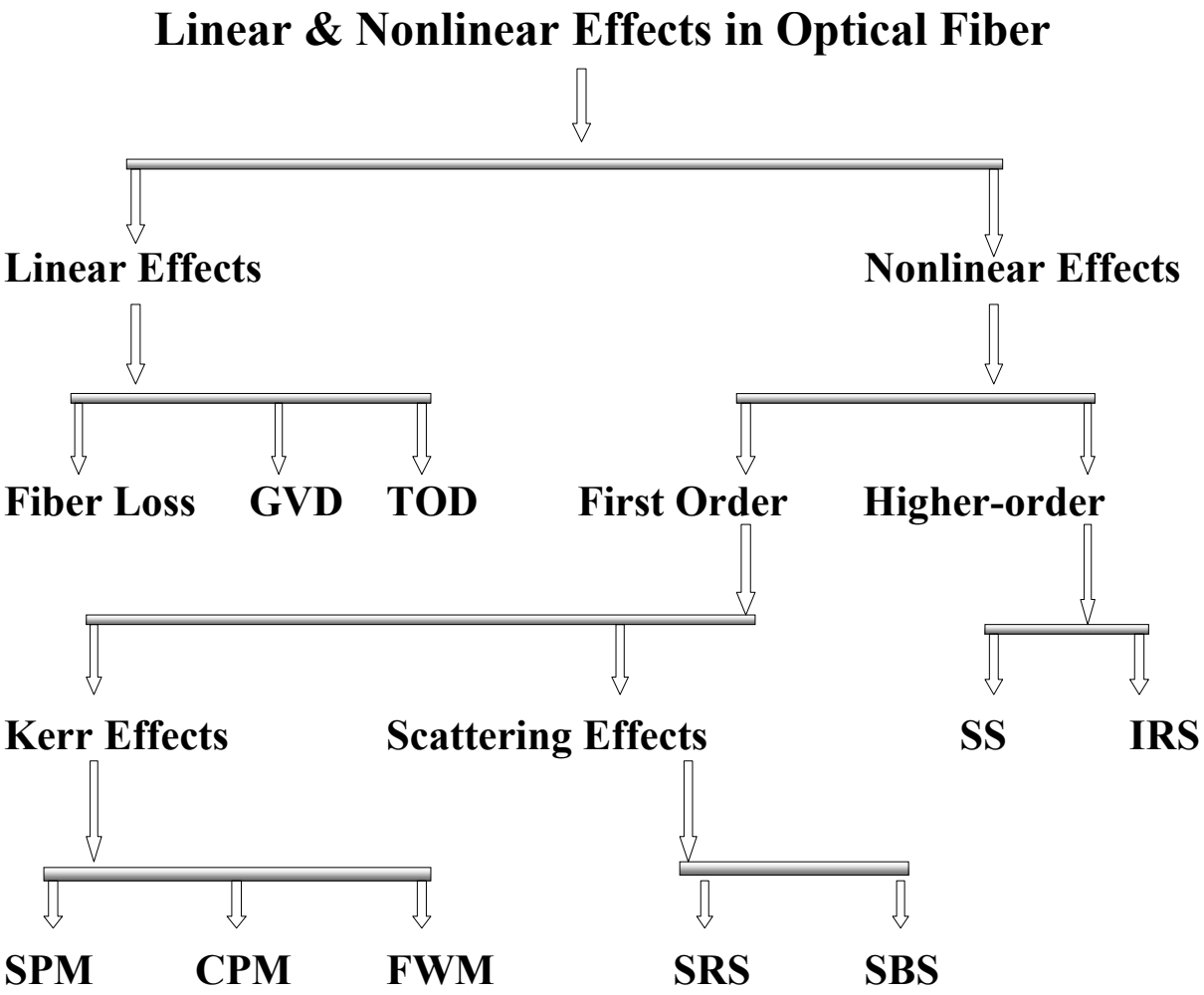

Fig. 2.1: Classification of linear and nonlinear effects in fiber.

1. Linear effects
   - Fiber Loss
   - Group-velocity dispersion (GVD)
   - Third order dispersion (TOD)
2. Nonlinear effects

   i) First Order

   A) Kerr Effects
      - Self-phase modulation (SPM)
      - Cross-phase modulation (CPM)
      - Four wave mixing (FWM)

   B) Scattering Effects
      - Stimulated Raman scattering (SRS)
      - Stimulated Brillouin scattering (SBS)

   ii) Higher-order
      - Self-steepening (SS)
      - Intrapulse Raman scattering (IRS)

2.2.1 Fiber Loss

Light traveling in an optical fiber loses power over distance. The loss of power depends on the wavelength of the light and on the propagating material. For silica glass, the shorter wavelengths are attenuated the most. The lowest loss occurs at the 1550-nm wavelength, which is commonly used for long-distance transmissions. Transmission of light by fiber optics is not 100% efficient. There are several reasons for this including absorption by the core and cladding (caused by the presence of impurities) and the leaking of light from of the cladding. The loss of power in light in an optical fiber is measured in decibels (dB). Fiber optic cable specifications express cable loss as attenuation per 1-km length as dB/km. This value is multiplied by the total length of the optical fiber in kilometers to determine the fiber's total loss in dB.

2.2.2 Group-velocity dispersion (GVD)

Chromatic dispersion or group-velocity dispersion (GVD) is primarily the cause of performance limitation in the long haul fiber optic communication systems. Dispersion is the spreading out of a light pulse in time as it propagates down the fiber. As a result short pulses

broaden which leads to significant intersymbol interference (ISI), and therefore, severely degrades the performance. Single mode fibers effectively eliminate inter-modal dispersion by limiting the number of modes to just one through a much smaller core diameter. However, the pulse broadening still occurs in SMFs due to intra-modal dispersion which is described as follows. When an electromagnetic wave interacts with the bound electrons of a dielectric, the medium response depends on the optical frequency *(ω)*. This property manifests through the frequency dependence of the refractive index *n (ω)*. Because the velocity of light is determined by *c/n(ω),* the different frequency components of the optical pulse would travel at different speeds. This phenomenon is called group-velocity dispersion or chromatic dispersion to emphasize its frequency dependent nature. Assuming the spectral width of the pulse to be $\Delta\omega$, at the output of the optical fiber, the pulse broadening can be estimated as

$$\Delta T \approx L\frac{d^2\beta}{d\omega^2}\Delta\omega = L\beta_2\Delta\omega. \tag{2.1}$$

Where $\beta_2 = {d^2\beta}/{d\omega^2}$ is known as GVD Parameter and

L is the fiber length. It can be seen from eqn. (2.1), that the amount of pulse broadening is determined by the spectral width of pulse, $\Delta\omega$. The dispersion induced spectrum broadening would be very important even without nonlinearity for high data-rate transmission systems (> 2.5 Gb/s), and it could limit the maximum error-free transmission distance. The effects of dispersion can be described by expanding the mode propagation constant, β at any frequency ω in terms of the propagation constant and its derivatives at some reference frequency ω_0 using Taylor Series,

$$\beta(\omega) = \beta_0 + \beta_1(\omega-\omega_0) + \frac{1}{2}\beta_2(\omega-\omega_0)^2 + \ldots \tag{2.2}$$

Here $\beta_m(\omega) = \left[\frac{d^m\beta}{d\omega^m}\right]_{\omega=\omega_0}$ (m=0, 1, 2, ……) (2.3)

It is easy to get first-order and second-order derivatives from Eqns. (2.2) and (2.3)

$$\beta_1 = \frac{1}{c}\left[n + \omega\frac{dn}{d\omega}\right] = \frac{1}{v_g} \tag{2.4}$$

and

$$\beta_2 = \frac{1}{c}\left[2\frac{dn}{d\omega} + \omega\frac{d^2n}{d\omega^2}\right] \approx \frac{\lambda^3}{2\pi c^2}\frac{d^2n}{d\lambda^2}, \tag{2.5}$$

where c is the speed of light vacuum and λ is the wavelength. β_1 is the inverse group velocity, and β_2 is the second order dispersion coefficient. If the signal bandwidth is much smaller than the carrier frequency ω_0, we can truncate the Taylor series after the second term on the right hand side. As the spectral width of the signal transmitted over the fiber increases, it may be necessary to include the higher-order dispersion coefficients such as β_3 and β_4. The wavelength where $\beta_2 = 0$ is called zero dispersion wavelength λ_D. Dispersion parameter, D, is another parameter related to the difference in arrival time of pulse spectrum. The relationship between D, β_1 and β_2 can be found as following

$$D = \frac{d\beta_1}{d\lambda} = -\frac{2\pi c}{\lambda^2}\beta_2 \approx -\frac{\lambda}{c}\frac{d^2n}{d\lambda^2} \tag{2.6}$$

From Eq. (2.6) it can be understood that D has the opposite sign with β_2. If $\lambda < \lambda_D$, $\beta_2 < 0$ (or $D > 0$), It is said that optical signal exhibit anomolous dispersion. In the anomolous dispersion regime high-frequency components of optical signal travel faster than low-frequency components. On the contrary, When $\lambda > \lambda_D$, $\beta_2 > 0$ (or $D < 0$), it is said to exhibit normal dispersion. In the normal dispersion regime high frequency components of optical signal travels slower than low-frequency components. The normal dispersion regime is of considerable interest for the study of nonlinear effects, because it is in this regime that optical fibers support solitons through a balance between the dispersive and nonlinear effects. The impact of the group-velocity dispersion can be conventionally described using the dispersion length which is defined as

$$L_D = \frac{T_0^2}{\beta_2} \tag{2.7}$$

where T_0 is the temporal pulse width. This length provides a scale over which the dispersive effect becomes significant for pulse evolution along a fiber. Dispersion and specially GVD play an important role in signal transmission over fibers. The interaction between dispersion and nonlinearity is an important issue in light wave system design.

2.2.3 Third Order Dispersion (TOD)

The dispersion-induced pulse broadening happens due to the lowest-order GVD term proportional to β_2. Although the contribution of this term dominates in most cases of practical interest, it is sometimes necessary to include the third-order term proportional to β_3. If the pulse wavelength nearly coincides with the zero-dispersion wavelength λ_D, $\beta_2 \approx 0$; the $\beta_3$term then provides the dominant contribution to the GVD effects. Reflectivity, ρ of optical fiber provides important information like the delay, dispersion and dispersion slope. Let us define θ = angle (ρ), then the first derivative with angular frequency ω is directly proportional to ω this term can be identified as time delay [64],

$$= \frac{d\theta}{d\omega} = -\frac{\lambda^2}{2\pi c}\frac{d\theta}{d\lambda}$$

is usually represented in units of picoseconds. Since the dispersion D (in ps/nm) is the rate of change of delay with wavelength, we get

$$D = \frac{d}{d\lambda}$$
$$= \frac{2}{\lambda} - \frac{\lambda^2}{2\pi c}\frac{d^2\theta}{d\lambda^2}$$
$$= \frac{\lambda^2}{2\pi c}\frac{d^2}{d\lambda^2}$$

The TOD parameter β_3 can be deduced from the above equation

$$\beta_3 = \left(\frac{\lambda^2}{2\pi c}\right)^2 \left(\frac{2D}{\lambda} + \frac{dD}{d\lambda}\right)$$

The effect of TOD is to introduce spectral asymmetry without affecting the two-peak structure. In the absence of TOD, a symmetric two-peak spectrum is expected. In dispersion-managed fiber links, β_2 is large locally but nearly vanishes on average. The effects of TOD play an important role in such links, especially for short optical pulses. The spectral and temporal evolution depends on whether the dispersion-compensating fiber (DCF) is placed before or after the the standard fiber (pre- or post compensation). In the case of post

compensation, the pulse develops an oscillating tail because of TOD and exhibits spectral narrowing. The effect of TOD in case ultrashort fundamental soliton through MCDSF fiber is shown in the following figure where the trailing edge of pulse is obvious.

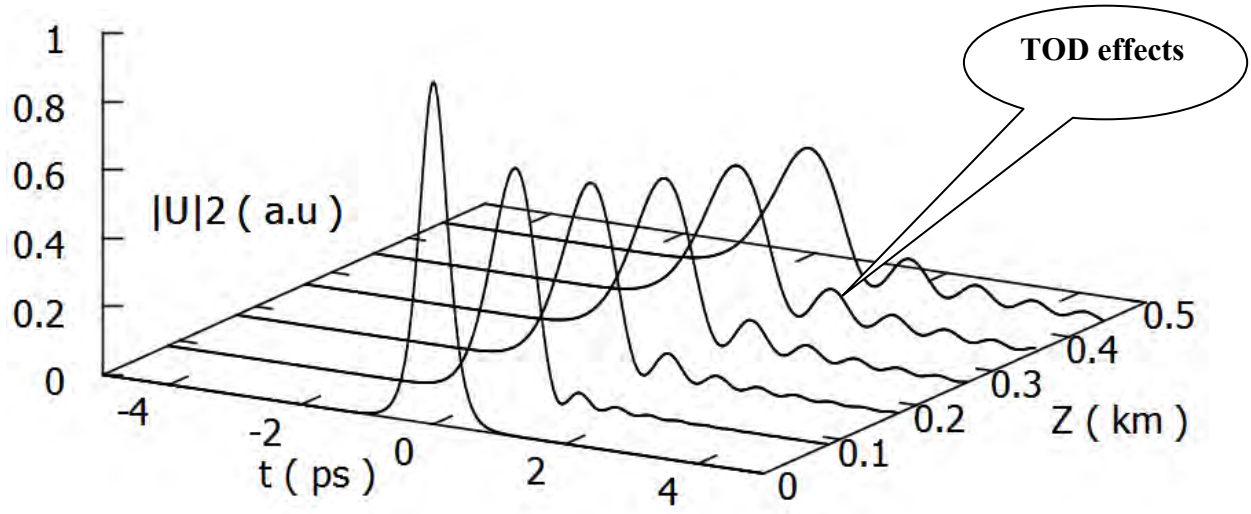

Fig. 2.2: Effect of TOD on (input pulse width - 500fs) fundamental soliton in MCDSF.

2.2.4 First Order Effects

First order effects consist of Kerr effects and Scattering effects where Kerr comprises the following:

(i) Self-phase modulation (SPM)

(ii) Cross phase modulation (CPM), and

(iii) Four wave mixing (FWM).

And scattering effects comprises the following:

(i) Stimulated Raman scattering (SRS)

(ii) Stimulated Brillouin scattering (SBS)

2.2.4.1 Self-Phase Modulation (SPM)

Self-phase modulation (SPM) is due to the power dependence of the refractive index of the fiber core. SPM refers the self-induced phase shift experienced by an optical field during its propagation through the optical fiber; change of phase shift of an optical field is given by

$$\phi(z,\tau) = \left(\frac{2\pi}{\lambda} n_0 z + \frac{2\pi}{\lambda} n_2 |E|^2 z_{eff} \right) = \phi_L + \phi_{NL} \qquad (2.8)$$

Here $k_0 = \frac{2\pi}{\lambda}$ and E is the electric field of the transmitted pulse, ϕ_L is the linear part and ϕ_{NL} is the nonlinear part that depends on intensity. Here z_{eff} is the effective transmission distance taking into account of the fiber attenuation, and it is given by

$$z_{eff} = \frac{1 - e^{-\alpha z}}{\alpha}$$

The first term in Eqn. (2.8) is just a linear phase shift, and depends only on the transmission distance z. On the other hand, the second term in (2.8) depends not only on the transmission distance z by way of z_{eff}, but also the intensity variation of the signal E itself. Therefore, this effect is called self-phase modulation (SPM). The intensity dependence of refractive index causes a nonlinear phase shift, which is proportional to the intensity of the signal. It should be noted that z_{eff} is less than z . This implies that fiber attenuation reduces the effect of nonlinear phase shift. SPM alone broadens the signal spectrum, but does not affect the intensity profile of the signal. The spectral broadening effect can be understood from the fact that the time-dependent phase variation causes instantaneous frequency deviation $\delta\omega(\tau)$, which is given by

$$\delta\omega(\tau) = -\frac{\partial\varphi}{\partial\tau} = \frac{2\pi n_2 z_{eff}}{\lambda}\frac{\partial E(\tau)}{\partial\tau} \qquad (2.9)$$

Eqn. (2.9) suggests that the magnitude of instantaneous frequency deviation increases with distance and the intensity variation of the signal. Thus different parts of the pulse undergo a different phase shift, which gives rise to chirping of the pulses. The SPM-induced chirp affects the pulse broadening effects of dispersion. The spectrum broadening effect caused by SPM may result in inter-channel cross talk among channels in WDM systems. The combined effect of dispersion and SPM strongly depends on the sign of dispersion (the sign of D). In terms of the sign of dispersion, the operating wavelength region is divided into two regimes: normal dispersion and anomalous dispersion regimes. The normal dispersion regime corresponds to the wavelength range in which dispersion D is negative (β_2 is positive) whereas the anomalous dispersion regime is the wavelength region in which D is positive (β_2 is negative). For the propagation of an optical pulse, the SPM enhances the effect of dispersion when the operating wavelength is in the normal dispersion regime. That is, the pulse is broadened more severely than under the effect of dispersion alone in the normal dispersion regime.

2.2.4.2 Cross Phase Modulation (CPM)

Cross phase modulation (CPM) is very similar to SPM except that it involves two pulses of light, whereas SPM needs only one pulse. In Multi-channel WDM systems, all the other interfering channels also modulate the refractive index of the channel under consideration, and therefore its phase. This effect is called CPM. CPM refers the nonlinear phase shift of an optical field induced by co-propagating channels at different wavelengths; the nonlinear phase shift be given as

$$\phi_{NL} = n_2 k_0 L\left(|E_1|^2 + 2|E_2|^2\right)$$

Where, E_1 and E_2 are the electric fields of two optical waves propagating through the same fiber. In CPM, two pulses travel down the fiber, each changing the refractive index as the optical power varies. If these two pulses happen to overlap, they will introduce distortion into the other pulses through CPM. Unlike, SPM, fiber dispersion has little impact on CPM. Increasing the fiber effective area will improve CPM and all other fiber nonlinearities.

2.2.4.3 Four-Wave Mixing (FWM)

The intensity dependence of refractive index not only causes nonlinear phase shift but also gives rise to the process by which signals at different wavelengths are mixed together producing new signals at new wavelengths. This process is known as four-wave mixing (FWM). The processes (SPM and CPM) causing the nonlinear phase shift but energy transfer occurs in the FWM process. When signals at frequencies f_i , f_j, *and* f_k propagate along an optical fiber, the nonlinear interactions among those signals by mean of FWM result in the generation of new signals at $f_{ijk} = f_i + f_j - f_k$

The energies from the interacting signals are transferred to those newly-generated signals at frequencies f_{ijk}. In the simplest case when only two signals at frequencies f_1 and f_2 are involved, the FWM generates new signals at $2f_1 - f_2$ and $2f_2 - f_1$ as demonstrated in Fig. 2.3. The number of FWM-generated signals grows rapidly with the number of involved signals

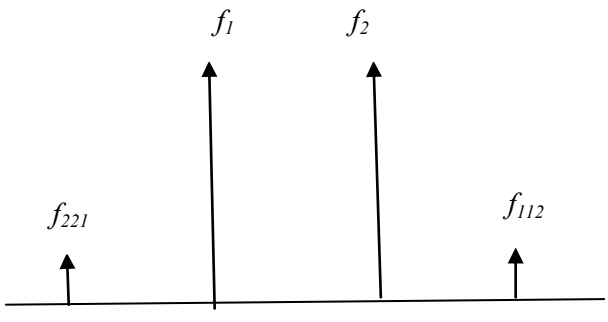

Fig. 2.3: Illustrations of FWM process of two signals at frequencies f_1 and f_2

When N signals are involved in the FWM process, the number of FWM generated signals is given by

$$M = \frac{N^2(N-1)}{2}$$

For example, when 10 signals are four-wave mixed together, 450 signals are generated. In WDM systems, not only does the FWM cause power depletion on the participating channels, but it also results in cross talk among channels. The cross talk comes from the fact that some of the FWM-generated signals can have the same frequencies as the WDM channels when all channels are equally spaced in frequency.

2.2.4.4 Stimulated Raman Scattering (SRS)

If two or more signals at different wavelengths are injected into a fiber, SRS causes power to be transmitted from lower wavelength channels to the higher wavelength channels. The incident light interacts with the molecular vibrations in a fiber and scattered light is generated, down-shifted by the Stokes frequency. The magnitude of the peak gain coefficient scales inversely with the pump wavelength. For a single injected channel, the amplification of spontaneous Raman scattered light can cause depletion of the signal light. In general, the criterion used to determine the level of scattering effects is the threshold power P_{th} defined as the input power level that can induce the scattering effect so that half of the power (3-dB power reduction) is lost at the output of an optical fiber of length z. The threshold power P_{th} is given by

$$P_{th} = {32\alpha A_{eff}}\Big/{g_R}$$

Where, α and A_{eff} are the attenuation coefficient and effective core area of an optical fiber, respectively, and g_R is the Raman gain coefficient. For a 1.55-μm single channel system employing a standard single-mode optical fiber, P_{th} is found to be of the order of 1 W. Commonly, the transmitted power is well below 1 W; thus, the effect of SRS is negligible in single-channel systems.

The effect of Raman scattering is different when two or more signals travel along an optical fiber. When two optical signals separated by the Stokes frequency travel along an optical fiber, the SRS would result in the energy transfer from the higher frequency signal to the lower frequency signal. That is, one signal experiences excess loss whereas another signal gets amplified. The signal that is amplified is called the probe signal whereas the signal that

suffers excess loss is called the pump signal. The effectiveness of the energy transfer depends on the frequency difference (Stokes frequency) between the pump and probe signals.

2.2.4.5 Stimulated Brillouin Scattering (SBS)

In the stimulated scattering processes, the optical fiber acts as a nonlinear medium and plays an active role through the participation of molecular vibrations. When a powerful light wave travels through a fiber it interacts with acoustical vibration modes in the glass. This causes a scattering mechanism to be formed that reflects much of the light back to the source. SBS corresponds to the interaction of the optical waves with the acoustic waves that occur in the fiber. A contra directional scattering at frequencies smaller than the incident frequency takes place. The threshold of this non-linear effect depends on the source spectral width and on the power density in the fiber.

The SBS threshold power is given by Y. Aoki, et al. [65] as:

$$P_{thr}=\frac{21A_{eff}}{g_B L_{eff}}\left[1+\frac{\Delta v_p}{\Delta v_B}\right]$$

Where Δv_p and Δv_B are the line-widths of the input laser and the Brillouin line, A_{eff} and L_{eff} are the effective core area and the effective length of the fiber, and g_B is the Brillouin gain in the fiber.

2.2.5 Higher-Order Nonlinear Effects

For ultrashort optical pulses of width < 1 ps, it is necessary to include the higher-order nonlinear effects which comprises of two.

i. Self-steepening (SS)
ii. Intrapulse Raman scattering (IRS).

2.2.5.1 Self-Steepening (SS)

The propagation of ultrashort optical soliton pulses with pulse width ≤1ps in a single-mode fiber is described by the generalized nonlinear Schrödinger wave equation taking into consideration of the higher-order dispersive and nonlinear effects as [66]

$$\frac{\partial A}{\partial z}+\frac{\alpha}{2}A+\frac{i\beta_2}{2}\frac{\partial^2 A}{\partial T^2}-\frac{\beta_3}{6}\frac{\partial^3 A}{\partial T^3}=i\gamma\left(|A|^2A+\frac{i}{\omega_0}\frac{\partial}{\partial T}|A|^2A-T_R A\frac{\partial|A|^2}{\partial T}\right) \quad (2.10)$$

where A is the slowly varying complex envelop of the soliton pulse, z is distance propagated by the pulses and T is the time measured in a frame of reference moving with the pulse at the group velocity υ_g ($T = t - z/\upsilon_g$), α is the absorption coefficient, β_2 and β_3 are, respectively, the second-and third-order dispersions. T_R is the response time related to the slope of the Raman gain [24], the term having the factor $1/\omega_0$ is related to the Self-steepening effect [66] and nonlinearity coefficient is γ that results in SPM is related to the nonlinear refractive index n_2 by

$$\gamma = \frac{n_2 \omega_0}{c A_{eff}} \tag{2.11}$$

Where A_{eff} is the effective core area of the fiber. At the same time, we introduce normalized amplitude U as

$$A(z,\tau) = \sqrt{P_0} exp(-\alpha z/2) U(z,\tau) \tag{2.12}$$

Where P_0 is the peak power of the incident pulse. The exponential factor in Eq. (2.12) accounts for fiber loss. Hence the Eq. (2.10) takes the following form after considering $A = kU$ from Eq. 2.12, where $k = \sqrt{P_0} exp(-\alpha z/2)$ and neglecting fiber loss

$$\frac{\partial\, kU}{\partial z} + \frac{i\beta_2}{2}\frac{\partial^2\, kU}{\partial T^2} - \frac{\beta_3}{6}\frac{\partial^3\, kU}{\partial T^3} = i\gamma\left(k^2.|U|^2.k.U + \frac{i}{\omega_0}\frac{\partial}{\partial T}\, k^2.|U|^2.k.U - T_R.k.U\frac{\partial\, k^2.|U|^2}{\partial T}\right)$$

Or,

$$\frac{\partial U}{\partial z} + \frac{i\beta_2}{2}\frac{\partial^2 U}{\partial T^2} - \frac{\beta_3}{6}\frac{\partial^3 U}{\partial T^3} = i\gamma\left(k^2.|U|^2U + \frac{i}{\omega_0}\frac{\partial}{\partial T}\, k^2.|U|^2U - T_R U\frac{\partial\, k^2.|U|^2}{\partial T}\right)$$

Or,

$$\frac{\partial U}{\partial z} + \frac{i\beta_2}{2}\frac{\partial^2 U}{\partial T^2} - \frac{\beta_3}{6}\frac{\partial^3 U}{\partial T^3} = i\gamma.k^2\left(|U|^2U + \frac{i}{\omega_0}\frac{\partial}{\partial T}|U|^2U - T_R U\frac{\partial|U|^2}{\partial T}\right)$$

Or,

$$\frac{\partial U}{\partial z}+\frac{i\beta_2}{2}\frac{\partial^2 U}{\partial T^2}-\frac{\beta_3}{6}\frac{\partial^3 U}{\partial T^3}=i\gamma.\left(\sqrt{P_0}exp(-\alpha z/2)\right)^2\left(|U|^2U+\frac{i}{\omega_0}\frac{\partial}{\partial T}|U|^2U-T_RU\frac{\partial|U|^2}{\partial T}\right)$$

Or,

$$\frac{\partial U}{\partial z}+\frac{i\beta_2}{2}\frac{\partial^2 U}{\partial T^2}-\frac{\beta_3}{6}\frac{\partial^3 U}{\partial T^3}=i\gamma.P_0exp(-\alpha z)\left(|U|^2U+\frac{i}{\omega_0}\frac{\partial}{\partial T}|U|^2U-T_RU\frac{\partial|U|^2}{\partial T}\right)$$

Now introducing a time scale normalized to the input pulse width T_0 as $\tau = T/T_0$ we get from above equation is given below

$$\frac{\partial U}{\partial z}+\frac{i\beta_2}{2L_D}\frac{\partial^2 U}{\partial \tau^2}-\frac{\beta_3}{6L'_D}\frac{\partial^3 U}{\partial \tau^3}=i\frac{e^{-\alpha z}}{L_{NL}}\left(|U|^2U+is\frac{\partial}{\partial \tau}|U|^2U-\tau_RU\frac{\partial|U|^2}{\partial \tau}\right) \quad (2.13)$$

WhereL_D, L_{D}, and $L_{NL}$are the three length scales stands for second order dispersive, third order dispersive and nonlinear length defined as

$$L_D=\frac{T_0^2}{|\beta_2|},L_{D}=\frac{T_0^3}{|\beta_3|}\,,\ L_{NL}=\frac{1}{\gamma P_0}. \quad (2.14)$$

The parameters $s$and τ_R govern the effects of self-steepening and intrapulse Raman scattering, respectively, and are defined as

$$\tau_R=\frac{T_R}{T_0}\,,\ s=\frac{\lambda}{2\pi cT_0} \quad (2.15)$$

Both of these effects are quite small for picoseconds pulses but must be considered for ultrashort pulses with $T_0 < 1$ ps. Before solving Eq. (2.13) numerically, it is instructive to consider the dispersionless case by setting β_2=β_3 = 0. Equation (2.13) can be solved analytically in this specific case if we also set τ_R = 0 Defining a normalized distance as Z =z/L_{NL} and neglecting fiber losses (α = 0), Eq. (2.13) becomes

$$\frac{\partial U}{\partial Z}+s\frac{\partial}{\partial \tau}|U|^2U=i\,|U|^2U \quad (2.16)$$

Using $U=\sqrt{I}\exp(i\phi)$ in Eq. (2.16) and separating the real and imaginary parts, we obtain the following two equations:

$$\frac{\partial I}{\partial Z}+3sI\frac{\partial I}{\partial \tau}=0 \quad (2.17)$$

$$\frac{\partial \phi}{\partial Z} + sI\frac{\partial \phi}{\partial \tau} = I \tag{2.18}$$

Since the intensity equation (2.17) is decoupled from the phase equation (2.18), it can be solved easily using the method of characteristics. Its general solution is given by [67]

$$I(Z,\tau) = f(\tau - 3sIZ) \tag{2.19}$$

Where, we used the initial condition $I(0,\tau) = f(\tau)$, where $f(\tau)$, describes the pulse shape at z = 0. Equation (2.19) shows that each point τ moves along a straight line from its initial value, and the slope of the line is intensity dependent. This feature leads to pulse distortion. As an example, consider the case of a Gaussian pulse for which

$$I(0,\tau) = f(\tau) = \exp(-\tau^2) \tag{2.20}$$

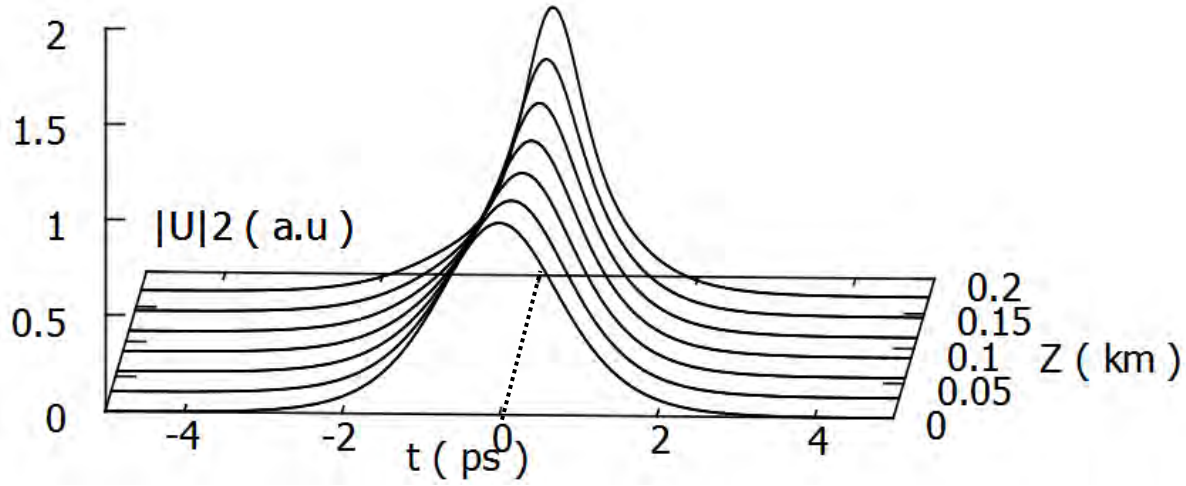

Fig. 2.4: Self-steepening of a Sech pulse with pulse width of 500fs in NZDSF fiber.

From Eq. (2.19), the pulse shape at a distance Z is obtained by using

$$I(Z,\tau) = \exp[-(\tau - 3sIZ)^2] \tag{2.21}$$

The implicit relation for $I(Z,\tau)$ should be solved for each τ to obtain the pulse shape at a given value of Z. Fig. 2.4 shows the pulse shapes with the effect of self-steepening. As the pulse propagates inside the fiber, it becomes asymmetric, with its peak shifting toward the

trailing edge. As a result, the trailing edge becomes steeper and steeper with increasing Z. Physically, the group velocity of the pulse is intensity dependent such that the peak moves at a lower speed than the wings.

2.2.5.2 Intrapulse Raman Scattering (IRS)

Intrapulse Raman scattering plays the most important role among the higher-order nonlinear effects. Its effects on solitons are governed by the last term in Eq. (2.13) and were observed experimentally in 1985 [68]. The need to include this term became apparent when a new phenomenon, called the soliton self-frequency shift, was observed in 1986. To isolate the effects of intrapulse Raman scattering, it is useful to set $\beta_3 = 0$ and $s = 0$ in Eq. (2.13). Pulse evolution inside fibers is then governed by

$$i\frac{\partial U}{\partial z} + \frac{1}{2}\frac{\partial^2 U}{\partial \tau^2} + |U|^2 U = \tau_R U \frac{\partial |U|^2}{\partial \tau} \tag{2.22}$$

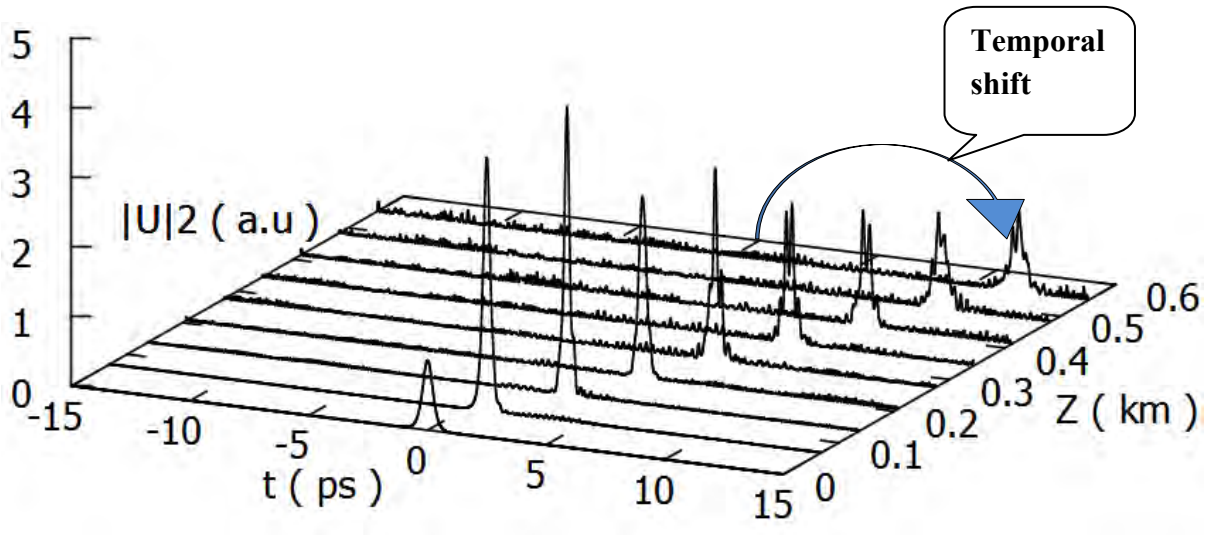

Fig. 2.5: Effect of intrapulse Raman scattering in case of 500fs soliton in LEAF fiber (Temporal Evolution).

The effect of intrapulse Raman scattering on higher-order solitons is similar to the case of self-steepening. In particular, even relatively small values of τ_R lead to the decay of higher-order solitons into its constituents. Fig. 2.5 shows such a decay for a second-order soliton (N = 2) by solving Eq. (2.22) numerically with $\tau_R = 0.01$. At the same time it is clear from the

Fig. 2.6 that within 600m distance there is a shift of energy happens. The short pulse shows an energy shift towards a specific wavelength and the long pulse is shifting towards another wavelength. This is what the physical significance of IRS effect on ultrashort pulse propagation.

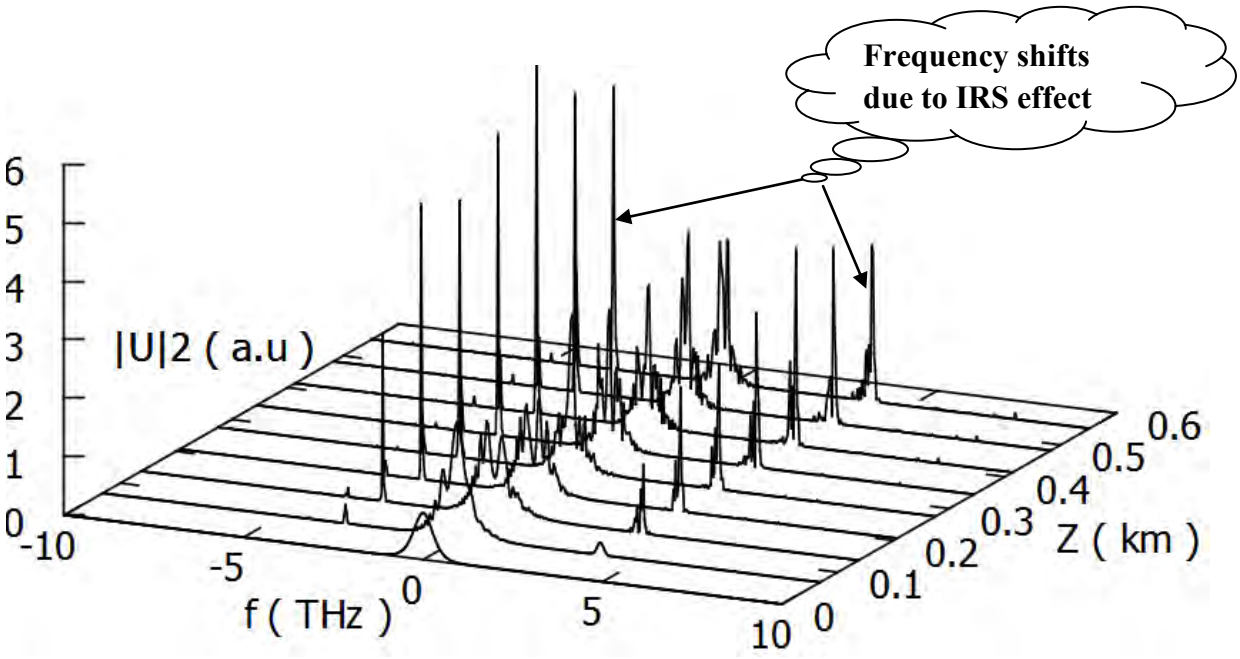

Fig. 2.6: Effect of intrapulse Raman scattering in case of 500fs soliton in LEAF fiber (Spectral Evolution).

2.3 Conclusion

This chapter briefly discuss about nonlinear effects of optical fiber. The physical impairments of optical fiber transmission can be categorized into two main parts: linear and nonlinear. Linear barriers include fiber loss and dispersion, on the other hand nonlinear part comprises SPM, CPM, FWM, SRS, SBS, SS and IRS effects.

Chapter 3

Numerical Analysis of Ultrashort Soliton

3.1 Introduction

The history of solitons, in fact, dates back to 1834, the year in which Scott Russell observed a heap of water in a canal that propagated undistorted over several kilometers. Here is a quote from his report published in 1844 [15],

―I was observing the motion of a boat which was rapidly drawn along a narrow channel by a pair of horses, when the boat suddenly stopped—not so the mass of water in the channel which it had put in motion; it accumulated round the prow of the vessel in a state of violent agitation, then suddenly leaving it behind, rolled forward with great velocity, assuming the form of a large solitary elevation, a rounded, smooth and well-defined heap of water, which continued its course along the channel apparently without change of form or diminution of speed. I followed it on horseback, and overtook it still rolling on at a rate of some eight or nine miles an hour, preserving its original figure some thirty feet long and a foot to a foot and a half in height. Its height gradually diminished, and after a chase of one or two miles I lost it in the windings of the channel. Such, in the month of August 1834, was my first chance interview with that singular and beautiful phenomenon which I have called the Wave of Translation."

Such waves were later called solitary waves. However, their properties were not understood completely until the inverse scattering method was developed. The term *soliton* was coined in 1965 to reflect the particle like nature of those solitary waves that remained intact even after mutual collisions [17]. Since then, solitons have been discovered and studied in many branches of physics including optics [69]–[70]. In the context of optical fibers, the use of solitons for optical communications was first suggested in 1973 [71]. The word ―soliton" has become so popular in recent years that a search on the Internet returns thousands of hits. Similarly, scientific databases reveal that hundreds of research papers are published every year with the word ―soliton" in their title. It should be stressed that the distinction between a soliton and a solitary wave is not always made in modern optics literature, and it is quite common to refer to all solitary waves as solitons.

3.2 Soliton

An optical soliton is a pulse that travels without distortion due to dispersion or other effects. They are a nonlinear phenomenon caused by self-phase modulation (SPM), which means that the electric field of the wave changes the index of refraction seen by the wave (Kerr effect). SPM causes a red shift at the leading edge of the pulse. Solitons occur when this shift is canceled due to the blue shift at the leading edge of a pulse in a region of anomalous dispersion, resulting in a pulse that maintains its shape in both frequency and time. Solitons are therefore an important development in the field of optical communications.

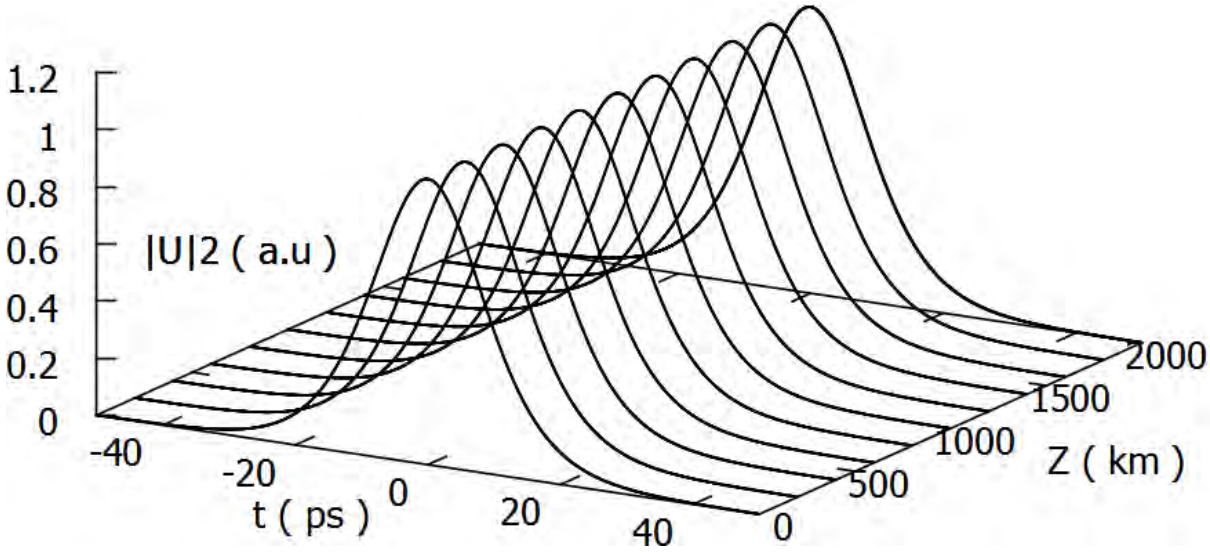

Fig. 3.1: Optical soliton formation.

From the above figure we are experiencing optical soliton formation within 2000Km of a fiber. Along this long distance GVD and SPM make a balance between each other and forms a pulse shape which becomes intact or unchanged with respect to propagation distance.

3.3 Fundamental and Higher-order Soliton

Basically two types of soliton survive in optical fiber. One is fundamental soliton and the other is higher-order solitons. In terms of normalized amplitude $U$with ξ and τ representing the normalized distance and time variables, the propagation Eq. (2.6) takes the form:

$$\frac{\partial U}{\partial \xi}+\frac{i}{2}\frac{\partial^2 U}{\partial \tau^2}-\frac{i}{6}\frac{\partial^3 U}{\partial \tau^3}=iN^2e^{-\alpha z}\left(|U|^2U+\frac{is}{\omega_0}\frac{\partial}{\partial \tau}|U|^2U-\tau_R U\frac{\partial |U|^2}{\partial \tau}\right) \quad (3.1)$$

Here, $U=\frac{A}{\sqrt{P_0}}$, $\xi=\frac{Z}{L_D}$, $\tau=\frac{T}{T_0}$ (3.2)

Where $T_0$is the width of the incident pulse, and for soliton it will be as follows

$$T_0 = \frac{T_{FWHM}}{1.763} \tag{3.3}$$

If the pulse width of the soliton is about T_0 < 1ps then it will be defined as ultrashort soliton. Parameter N characterizes the soliton order that provides the measure of the strength of the nonlinear response compared to the fiber dispersion, and is defined as

$$N^2 = \frac{L_D}{L_{NL}} = \frac{\gamma P_0 T_0^2}{|\beta_2|} \tag{3.4}$$

When fiber length L is such that $L << L_{NL}$ and $L << L_D$, neither dispersive nor nonlinear effects play a significant role during pulse propagation. The fiber plays a passive role in this regime and acts as a mere transporter of optical pulses (except for reducing the pulse energy because of fiber losses). This regime is useful for optical communication systems. When the fiber length is such that $L << L_{NL}$ but $L \sim L_D$, the pulse evolution is then governed by GVD, and the nonlinear effects play a relatively minor role. The dispersion-dominant regime is applicable whenever the fiber and pulse parameters are such that

$$N^2 = \frac{L_D}{L_{NL}} = \frac{\gamma P_0 T_0^2}{|\beta_2|} \ll 1 \tag{3.5}$$

When the fiber length L is such that $L << L_D$ but $L \sim L_{NL}$, in that case, pulse evolution in the fiber is governed by SPM that leads to spectral broadening of the pulse. The nonlinearity-dominant regime is applicable whenever

$$N^2 = \frac{L_D}{L_{NL}} = \frac{\gamma P_0 T_0^2}{|\beta_2|} \gg 1 \tag{3.6}$$

When the fiber length L is longer or comparable to both L_D and L_{NL}, dispersion and nonlinearity act together as the pulse propagates along the fiber. The interplay of the GVD and SPM effects can lead to a qualitatively different behavior compared with that expected from GVD or SPM alone. In the anomalous-dispersion regime ($\beta_2 < 0$), the fiber can support solitons. In the normal-dispersion regime ($\beta_2 > 0$), the GVD and SPM effects can be used for pulse compression.

In Eqn. (3.6) whenever $N = 1$, there will exist fundamental soliton and for other cases of $N = 2, 3, 4, 5, 6 \ldots$, the soliton will be called N^{th} order soliton shown in the following figure.

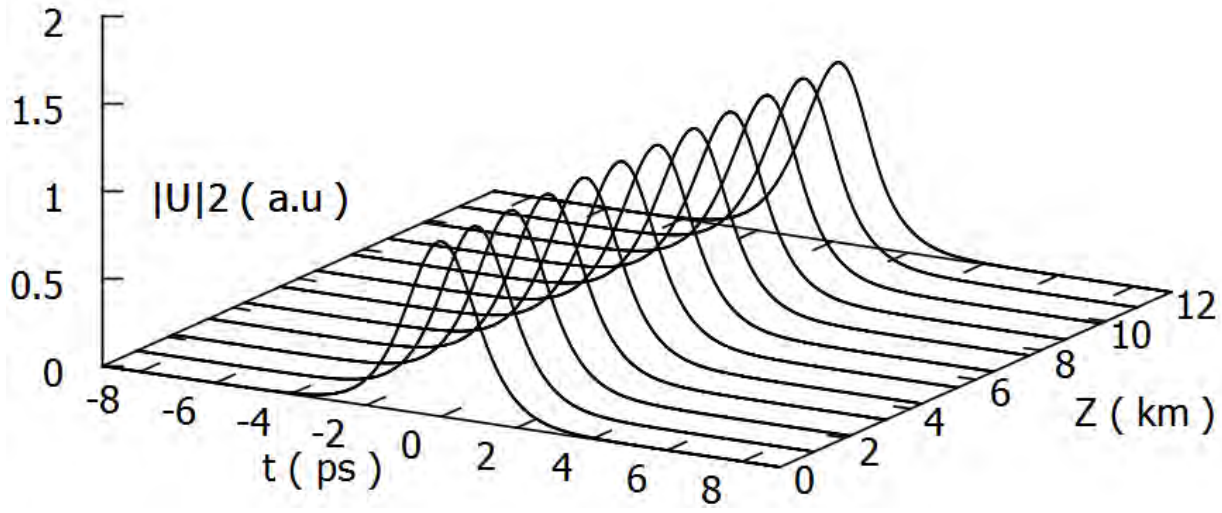

Fig. 3.2: Temporal evolution of fundamental (N = 1) soliton.

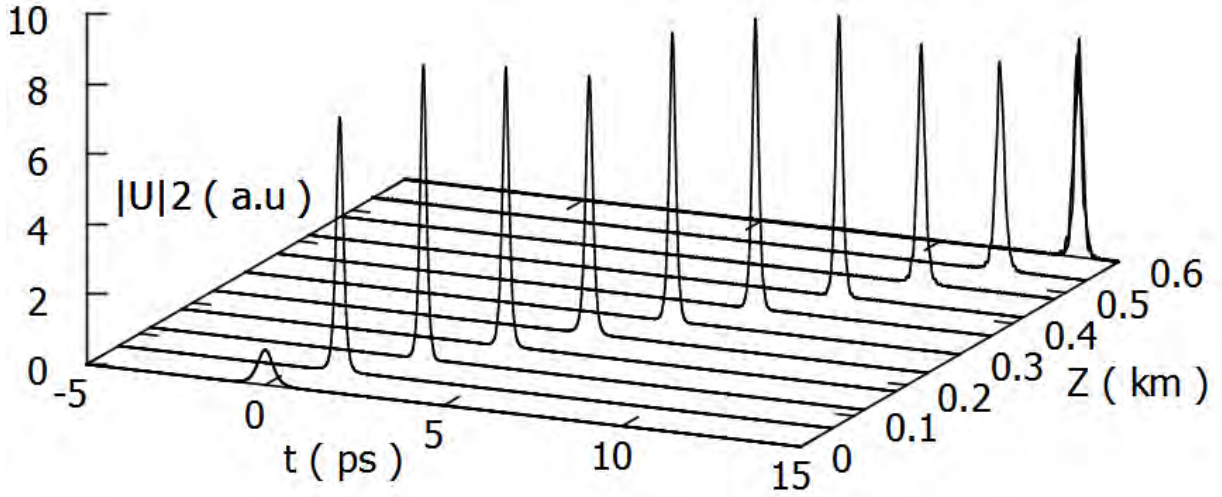

Fig.3.3: Temporal evolution of higher-order (N = 2) soliton.

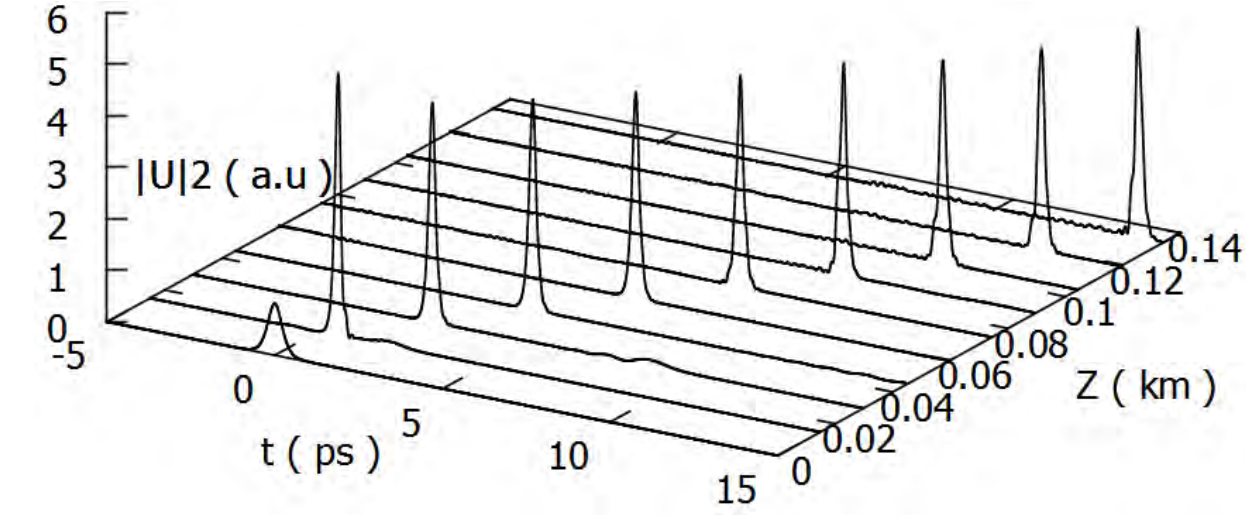

Fig. 3.4: Temporal evolution of ultrashort higher-order (N = 3) soliton propagation.

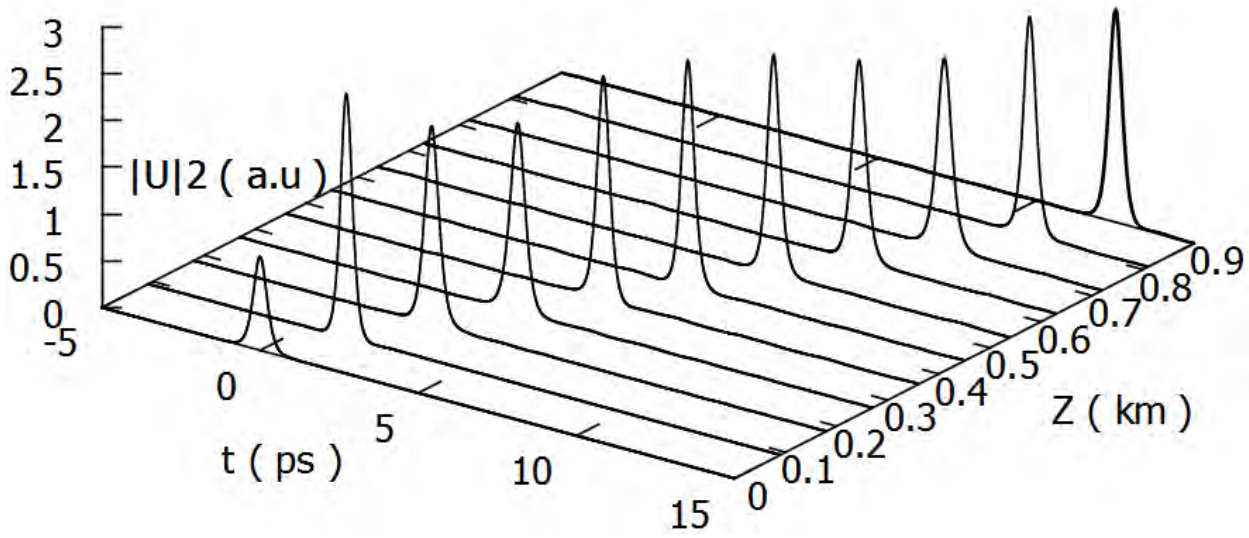

Fig. 3.5: Temporal evolution of ultrashort fractional order (N=1.7) soliton propagation.

In the case of a fundamental soliton, GVD and SPM balance each other in such a way that neither the pulse shape nor the pulse spectrum changes along the fiber length. In the case of higher-order solitons, SPM dominates initially but GVD soon catches up and leads to pulse contraction. As the pulse propagates along the fiber, it first contracts to a fraction of its initial width, splits into two distinct pulses and then merges again to recover the original shape at the end of the soliton period. This pattern is repeated over each section of length.

3.4 Conclusion

In this chapter we have given a brief discussion about the fundamental and higher-order ultrashort soliton with mathematical expression and figures as well. We get the key point that with change in the proportion of dispersion length and nonlinear length, the order of soliton varies. At the same time we will say ultrashort soliton only for that case when pulse width of the particular soliton is less than 1 ps.

Chapter 4

Characteristics of Ultrashort Soliton

4.1 Introduction

In this portion we have observed different characteristics of ultrashort fundamental and higher-order soliton. Soliton of pulse width greater than 1 ps can survive in any environment but as we go for ultrashort soliton, we find some obstacles due to the effect of higher-order dispersive (TOD) and nonlinear effects (SS, IRS). With all this effect propagation behaviour of soliton in different optical fiber has been investigated.

4.2 Soliton for Ultra-High Speed Communication

Although the trend in increasing the data rate per channel was structured as 10Gb/s, 40Gb/s, 160Gb/s etc., but recently it is no longer varying like that. The per channel data rate is varying randomly like 40Gb/s, 100Gb/s, 224Gb/s, 400Gb/s, 448Gb/s, 512Gb/s, 1Tb/s [34-40] and even more. To meet the demand for large traffic volume and its increasing dynamic nature, ultrashort soliton pulse is a promising solution. In order to increase the bit rate to more than 100Gbit/s for a single carrier wavelength, the soliton pulse width should be in the sub-picosecond i.e. femtosecond region. Transmission of 20Gb/s data over distances of 20000km was achieved using dispersion managed solitons in 1999 [41]. A new technique, adiabatic soliton trapping for achieving sub-picosecond i.e. femtosecond optical soliton communication over long distances was proposed for 100Gb/s [42]. A single high-speed channel at 640Gb/s (obtained through time-division multiplexing) has been transmitted over 92km by compensating group-velocity dispersion (GVD) and TOD [54]. In this section we will observe the propagation characteristics of fundamental soliton through different types of optical fiber like standard single mode fiber (SSMF), nonzero dispersion shifted fiber (NZDSF), large effective area fiber (LEAF), multiclad dispersion flattening fiber (MCDFF) and multiclad dispersion shifted fiber (MCDSF) for 400Gb/s with a sech pulse. Higher-order dispersive and nonlinear effects have been taken into consideration. Here temporal and

spectral evolution and eye pattern of the pulse will be demonstrated. The parameters taken for the analysis are tabulated for different fiber as follows:

Table 4.1: Fiber Parameters

Fiber Parameters	Fiber Name					
	SSMF	NZDSF	DCF	CORNING LEAF	MCDSF	MCDFF
D (ps/nm/km)	16.6	4	-96.33	2	0.04	1
D_λ	0.0575	0.045	0.65	0.060	0.033	-0.0176
n_2 ($\times 10^{-20} m^2/W$)	2.3	3	2.5	3	2.5	3
A_{eff} (μm^2)	85	70	20	72	50	70

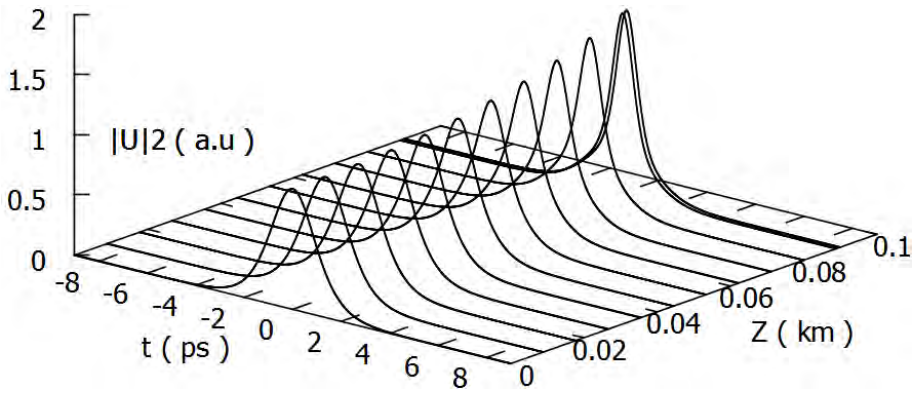

Fig. 4.1: Temporal evolution of 1.25ps fundamental soliton propagation in SSMF.

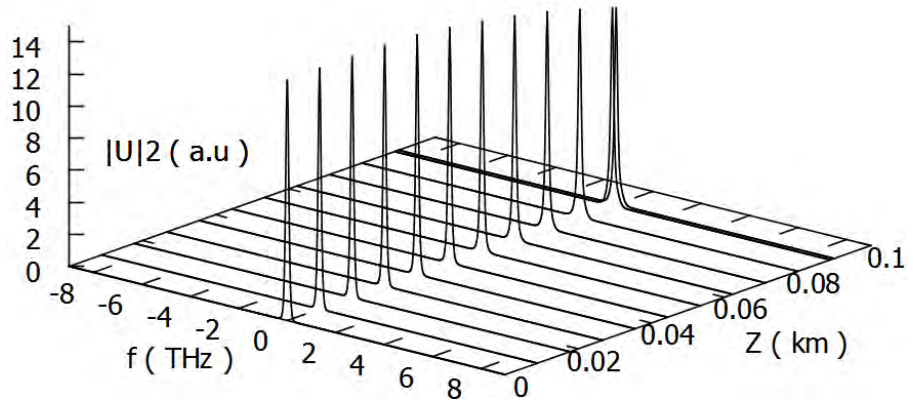

Fig. 4.2: Spectral evolution of 1.25ps fundamental soliton propagation in SSMF.

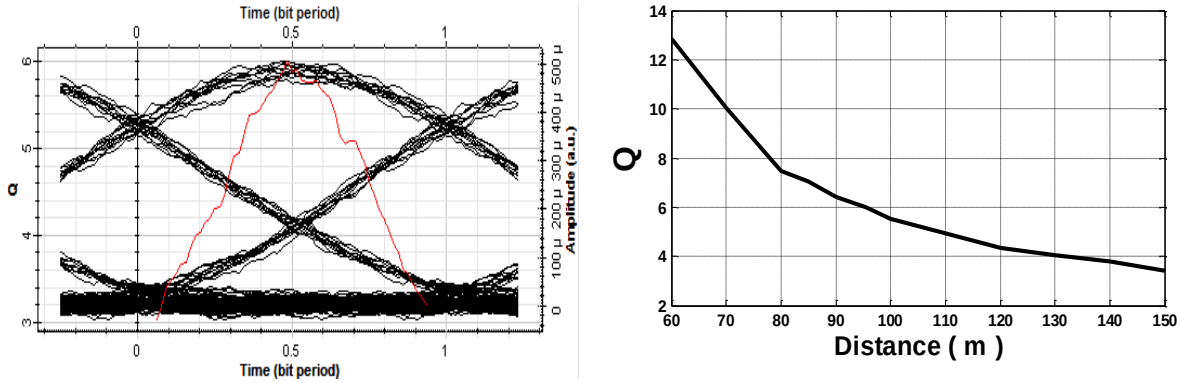

(a) (b)

Fig. 4.3: Eye pattern (a) and Q vs. distance curve (b) for propagation of soliton in SSMF (When Q = 6, distance = 0.0955km).

From Fig. 4.1 and Fig. 4.2 we can observe the propagation of fundamental soliton in SSMF fiber for per channel data rate of 400Gb/s. Although soliton pulse contains a balance between dispersive and nonlinear effects, in case of ultrashort (<1ps) range the balance exist for a short propagation distance. Minimum Q value required for eye pattern is about 6. Fig. 4.3(a) shows the eye pattern with the value of Q = 6. Keeping this Q value constant we have found that fundamental soliton propagates only 95.5m in SSMF. Beyond this distance higher-order effects like TOD, SS, IRS becomes severe and badly affects the smooth balance of dispersive and nonlinear effects. Fig. 4.3(b) screens distance vs. Q curve from where an inverse relationship between the distance and Q value can be observed.

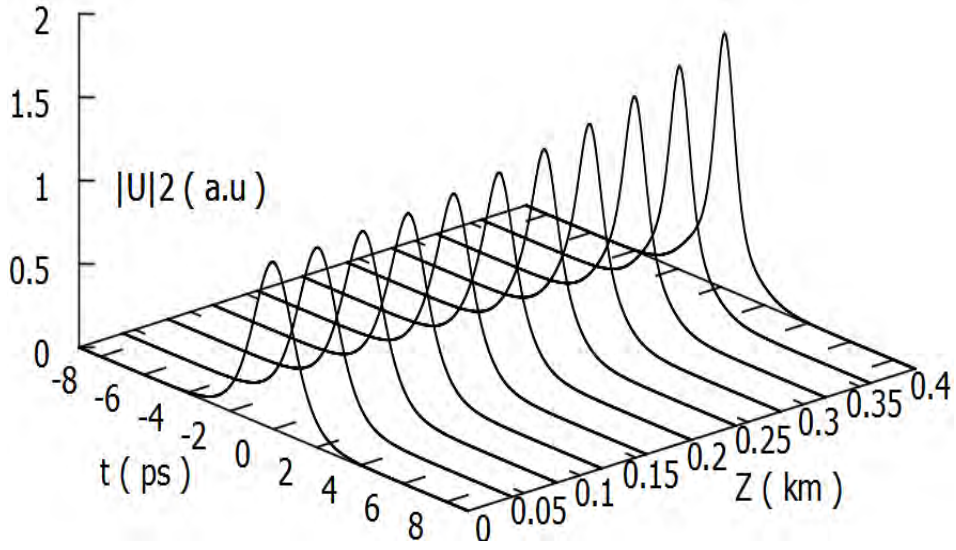

Fig. 4.4: Temporal evolution of 1.25ps fundamental soliton propagation in NZDSF.

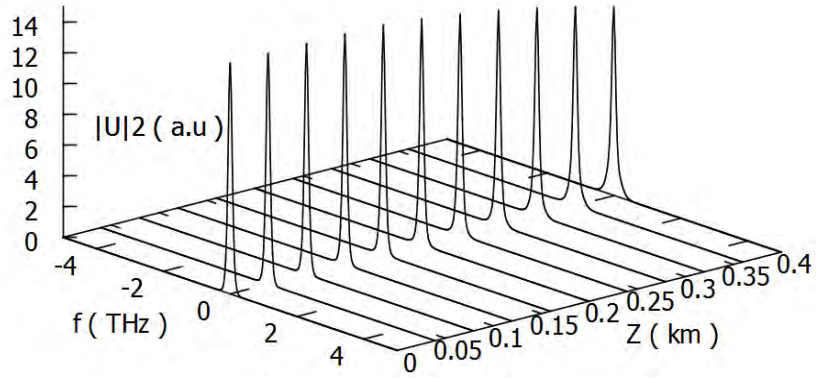

Fig. 4.5: Spectral evolution of 1.25ps fundamental soliton propagation in NZDSF.

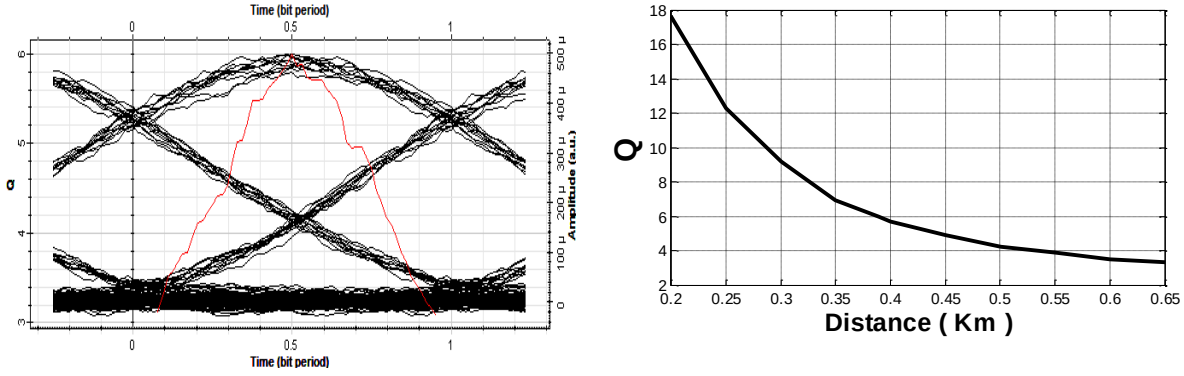

(a) (b)

Fig. 4.6: Eye pattern (a) and Q vs. distance curve (b) for propagation of soliton in NZDSF (When Q = 6, distance = 0.389km).

Fig. 4.4 and Fig. 4.5 shows the temporal and spectral wave shape of propagation of fundamental soliton in NZDSF fiber for per channel data rate of 400Gb/s. Propagation distance in NZDSF has been found to be 389m to keep the value, Q = 6. The eye pattern has shown in Fig. 4.6(a). Beyond this distance Q value inversely deviates with distance shown in Fig. 4.6(b).

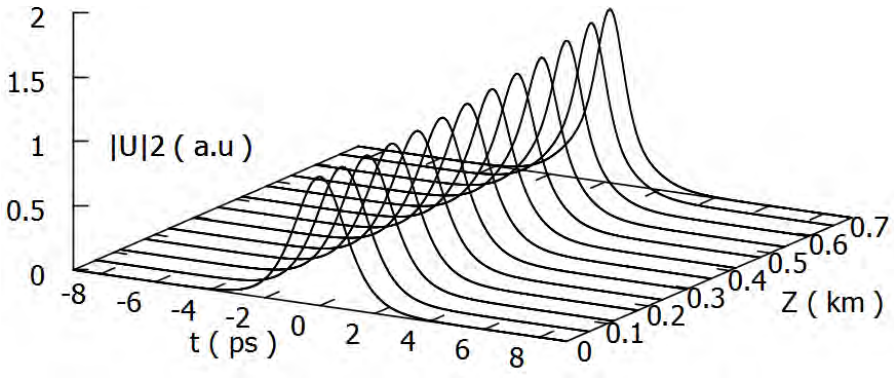

Fig. 4.7: Temporal evolution of 1.25ps fundamental soliton propagation in LEAF.

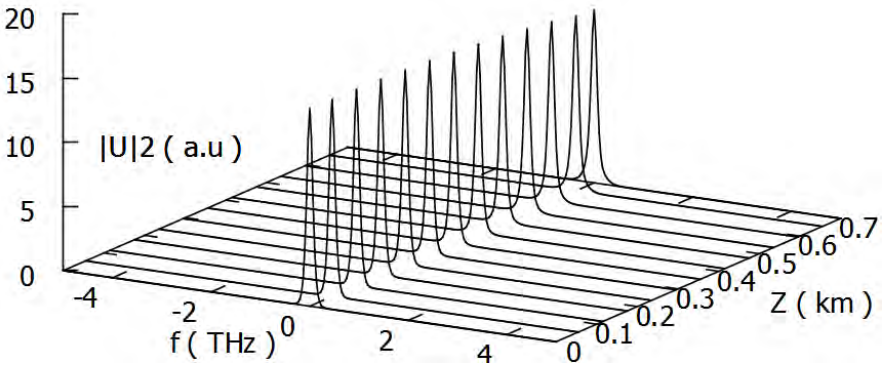

Fig. 4.8: Spectral evolution of 1.25ps fundamental soliton propagation in LEAF.

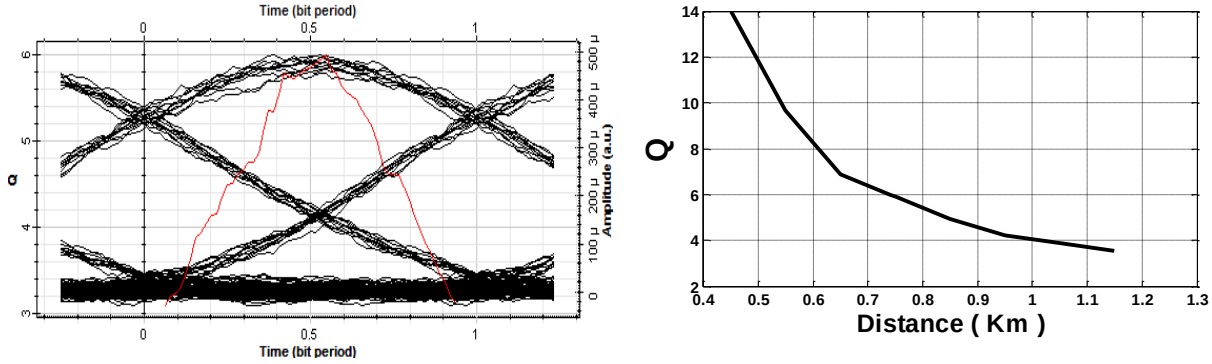

(a) (b)

Fig. 4.9: Eye pattern (a) and Q vs. distance curve (b) for propagation of soliton in LEAF (When Q = 6, distance = 0.739km).

From Fig. 4.7 and Fig. 4.8 we can observe the temporal and spectral wave shape of propagation of fundamental soliton in LEAF fiber for per channel data rate of 400Gb/s. After 739m propagation distance in LEAF the Q factor deteriorates beyond 6 shown in Fig. 4.9(b). The eye pattern has shown in Fig. 4.9(a).

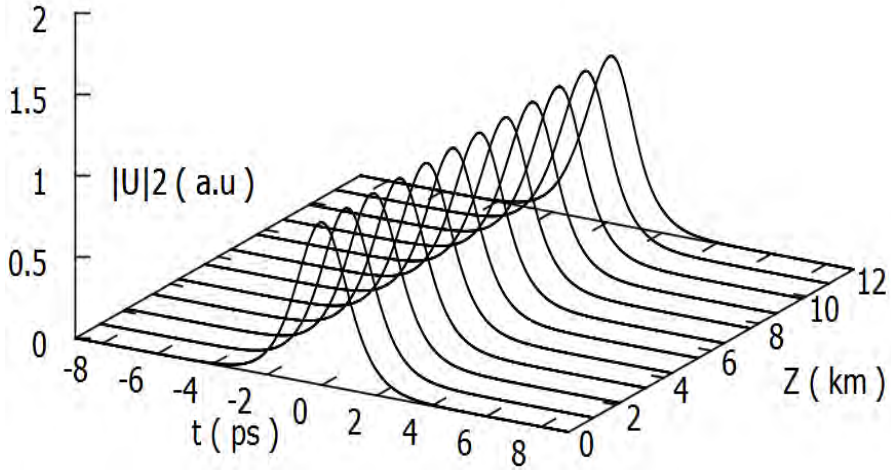

Fig. 4.10: Temporal evolution of 1.25ps fundamental soliton propagation in MCDSF.

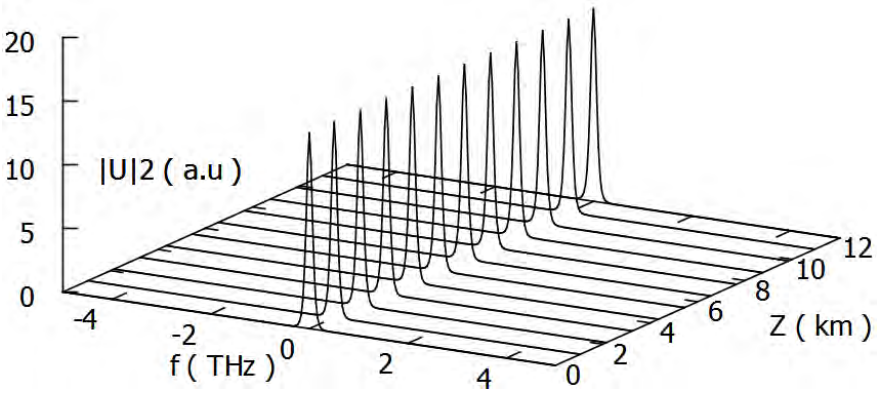

Fig. 4.11: Spectral evolution of 1.25ps fundamental soliton propagation in MCDSF.

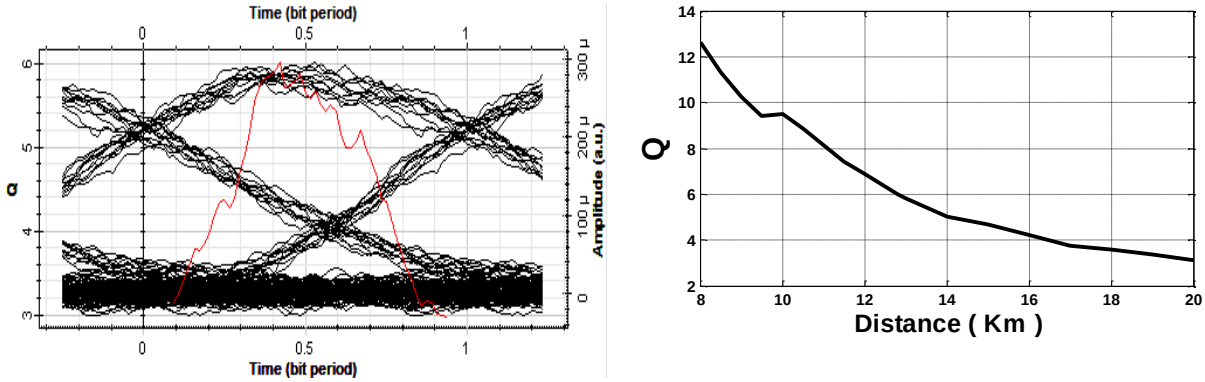

(a) (b)

Fig. 4.12: Eye pattern (a) and Q vs. distance curve (b) for propagation of soliton in MCDSF (When Q = 6, distance = 12.82km).

From Fig. 4.10 and Fig. 4.11 we can observe the temporal and spectral wave shape of propagation of fundamental soliton in MCDSF fiber for per channel data rate of 400Gb/s. MCDSF shows nice outcome of 12.82km propagation distance with the value of Q = 6 as well. The eye pattern has shown in Fig. 4.12(a). What happens after Q if the distance is varied has been explored in Fig. 4.12(b).

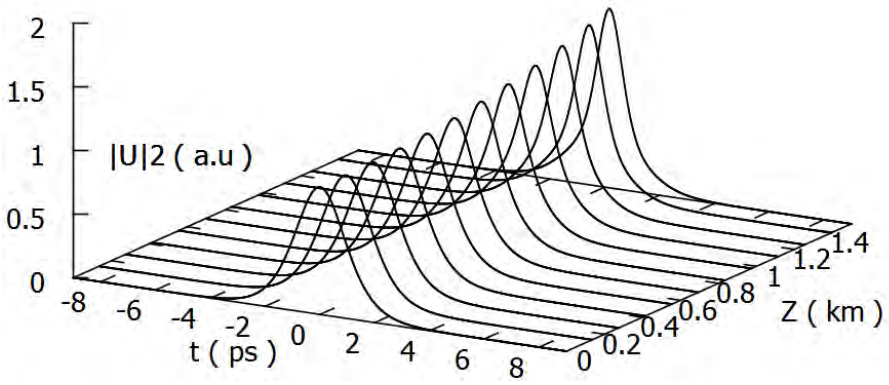

Fig. 4.13: Temporal evolution of 1.25ps fundamental soliton propagation in MCDFF.

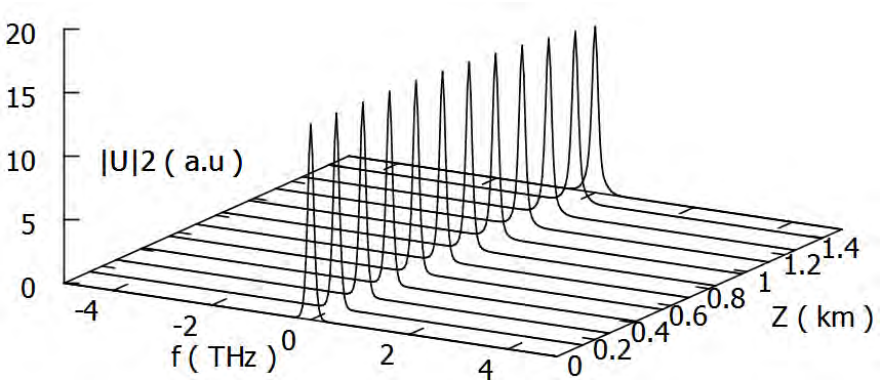

Fig. 4.14: Spectral evolution of 1.25ps fundamental soliton propagation in MCDFF.

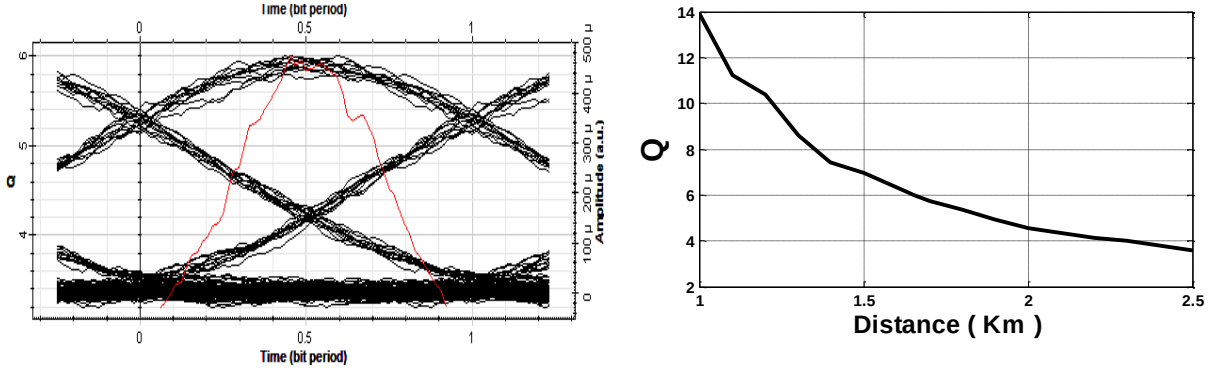

(a) (b)

Fig. 4.15: Eye pattern (a) and Q vs. distance curve (b) for propagation of soliton in MCDFF (When Q = 6, distance = 1.654km).

Fig. 4.13 and Fig. 4.14 show the temporal and spectral wave shape of propagation of fundamental soliton in MCDFF fiber for per channel data rate of 400Gb/s. For 1.654km propagation distance in MCDFF the Q factor = 6 as shown in Fig. 4.15(b). The eye pattern has shown in Fig. 4.15(a).

Table 4.2: Covering Distance in Different Fibers for Q = 6.

Fiber name	SSMF	NZDSF	LEAF	MCDSF	MCDFF
Q	6	6	6	6	6
Covering distance (km)	0.0955	0.389	0.739	12.82	1.654

If we make a comparative study observing the propagation behaviour in different optical fiber, from Fig. 4.10 it is obvious that with all higher order effects MCDSF fiber shows better

performance than that of any others (SSMF, NZDSF, LEAF and MCDFF). From all the data that has been tabulated in Table 4.2 we can easily say that MCDSF fiber will be the best one because soliton can propagate through MCDSF for 12.82km maintaining minimum Q value required for eye diagram.

4.3 Propagation Behaviour of Ultrashort Soliton for 1 Tb/s

We have observed propagation of ultrashort fundamental soliton for 1Tb/s of per channel data rate in SSMF, NZDSF, LEAF, MCDSF and MCDFF. We have explored our analysis with return to zero hyperbolic secant pulse of 50% duty cycle. The time-bandwidth product for sech pulse is always 0.32. In this section with temporal and spectral evolution of both fundamental and higher-order ultrashort soliton, the time-bandwidth product has also been calculated.

4.3.1 Propagation behaviour in SSMF

In the way to discuss the propagation behaviour of ultrashort fundamental and higher-order soliton this section is devoted only for SSMF fiber. Fig. 4.16 and Fig. 4.17 show the temporal and spectral evolution of fundamental soliton propagation in SSMF fiber. A small propagation distance maintaining soliton nature has been found here. The balance between GVD and SPM is very clear from temporal and spectral wave shape. This balance disrupts for more propagation distance due to the higher-order effects.

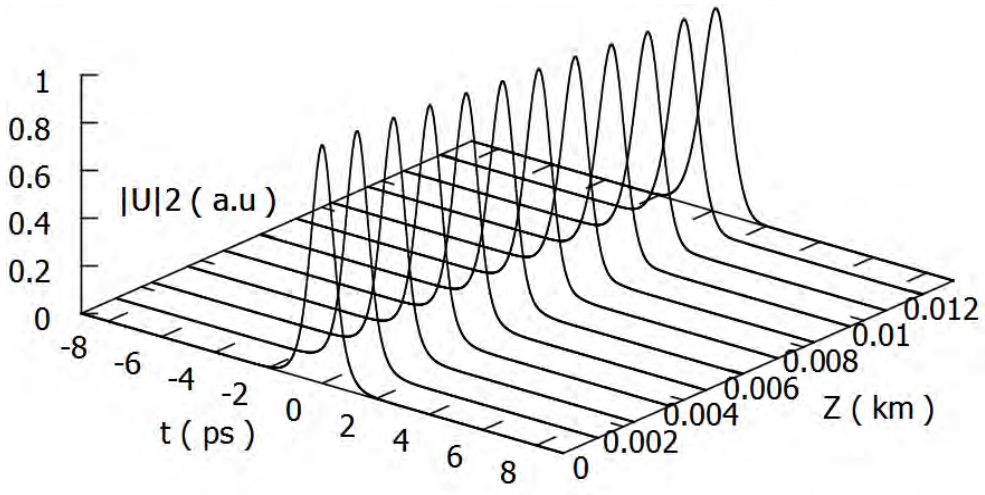

Fig. 4.16: Temporal evolution of ultrashort (FWHM = 500fs) fundamental (N = 1) soliton propagation in SSMF.

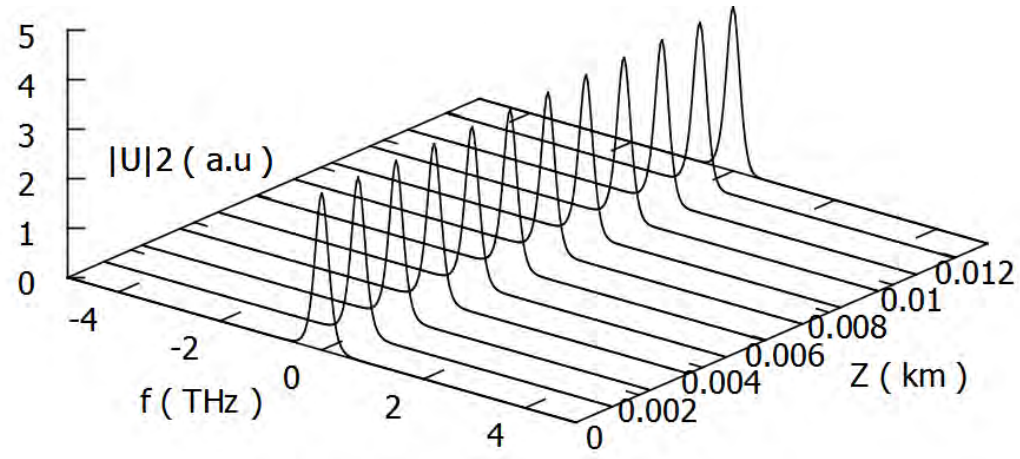

Fig. 4.17: Spectral evolution of ultrashort (FWHM = 500fs) fundamental (N = 1) soliton propagation in SSMF.

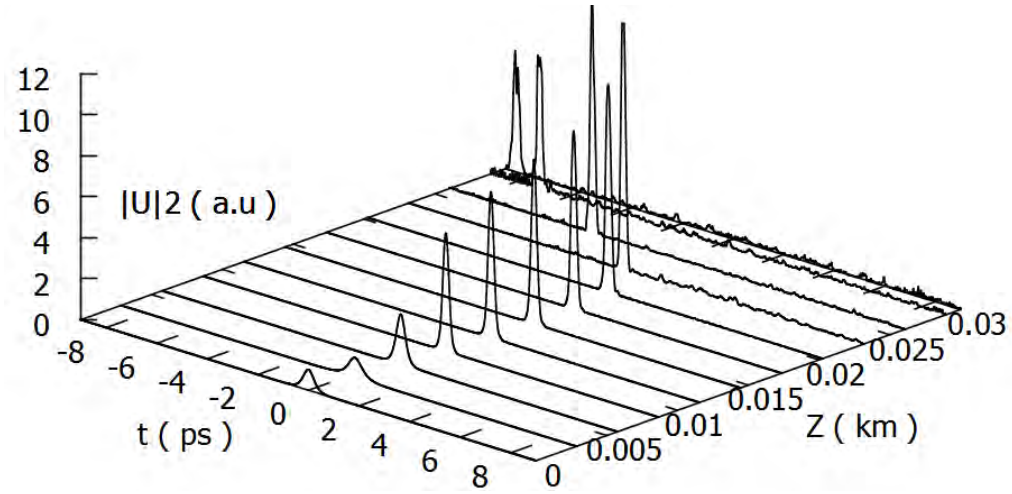

Fig. 4.18: Temporal evolution of ultrashort (FWHM = 500fs) higher-order (N=2) soliton propagation in SSMF.

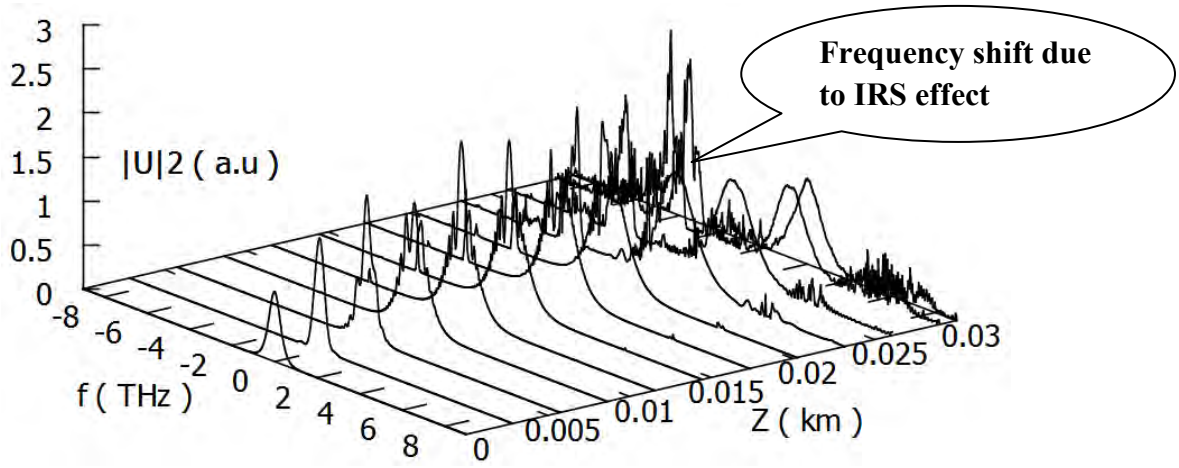

Fig. 4.19: Spectral evolution of ultrashort (FWHM = 500fs) higher-order (N=2) soliton propagation in SSMF.

Fig. 4.18 screens the temporal evolution whereas Fig. 4.19 shows the spectral evolution where we can observe the effect of IRS for second order soliton. After first 20m distance the time-bandwidth product remains 0.33 which has been tabulated in Table 4.3 later. After 20m distance from the spectral evolution it is clear that new pulses has been generated with different frequencies. This effect is more prominent in third order soliton and soliton self frequency shift is much more clear in Fig. 4.21. A temporal shift and pulse asymmetry has been found in case of third order soliton shown by Fig. 4.20. The more the ultrashort pulse is the more the higher-order effects happen. After first 4m distance the time-bandwidth product remains 0.31 which has been tabulated in Table 4.3 later. After 4m distance the temporal shift has been happened due to GVD and TOD effects. At the same time the effect of SS causes pulse asymmetry exposed in Fig. 4.21.

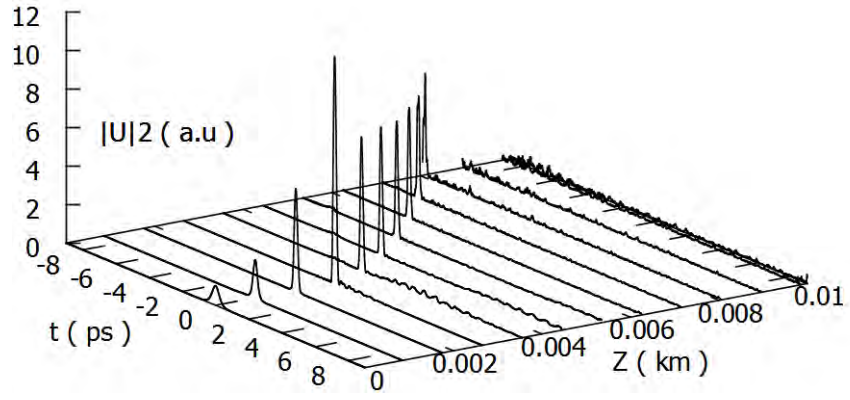

Fig. 4.20: Temporal evolution of ultrashort (FWHM = 500fs) higher-order (N=3) soliton propagation in SSMF.

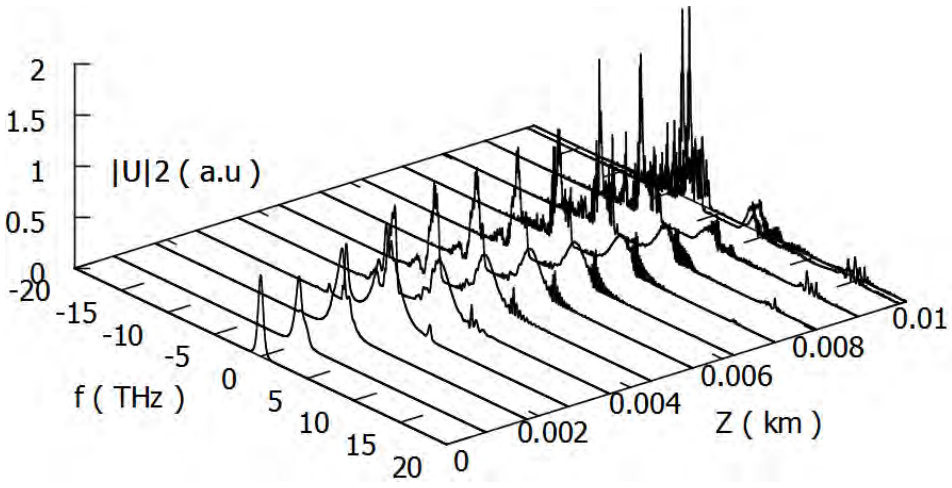

Fig. 4.21: Spectral evolution of ultrashort (FWHM = 500fs) higher-order (N=3) soliton propagation in SSMF.

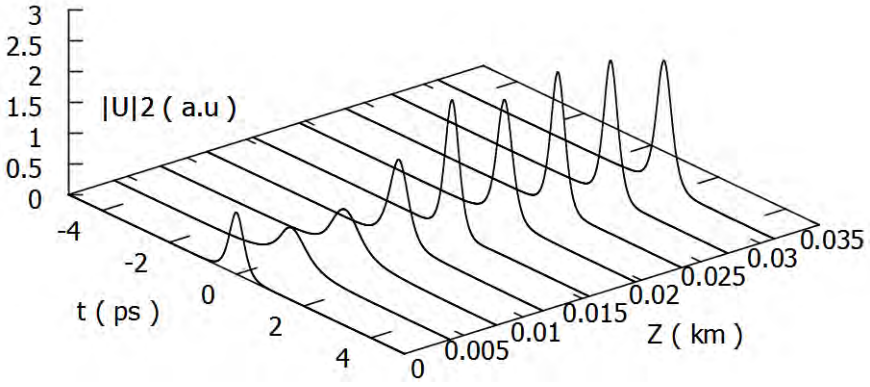

Fig. 4.22: Temporal evolution of ultrashort (FWHM = 500fs) fractional order (N=1.7) soliton propagation in SSMF.

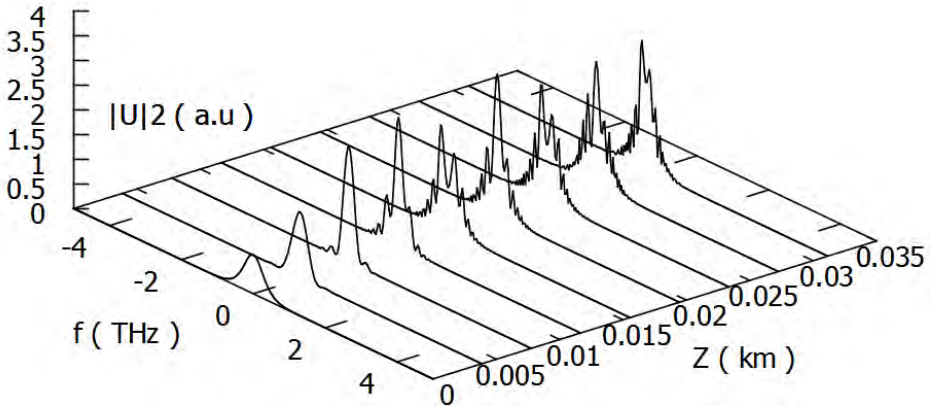

Fig. 4.23: Spectral evolution of ultrashort (FWHM = 500fs) fractional order (N=1.7) soliton propagation in SSMF.

We have found another fractional order soliton in Fig. 4.22 which shows better performance without being affected by higher-order terms. Only a small effect of TOD has been seen from the spectral evolution in Fig. 4.23. The time-bandwidth product has been revealed to be exact 0.32 as like for sech pulse in case of fractional order soliton tabulated in Table 4.3. Again different parameters like energy, peak power, soliton order with propagation distance has been exposed in Table 4.4.

Table 4.3: Propagation Distance in SSMF (to maintain time-bandwidth product = 0.32)

Soliton Order	Fiber Name	Covered Distance	Time-Bandwidth Product
1	SSMF	13m	0.32
2		20m	0.33
3		4m	0.31
1.7		35m	0.32

Table 4.4: Propagation Characteristics in SSMF

Fiber	SSMF	SSMF	SSMF	SSMF
Energy, E_0	0.137nJ	0.549nJ	1.24nJ	0.411nJ
Peak Power, P_0	242w	968w	2178w	725w
Soliton order, N	1	2	3	1.73 (Fractional)
Distance	13m	30m	10m	35m

4.3.2 Propagation behaviour in NZDSF

In this section we will explore the propagation behaviour of ultrashort fundamental and higher-order soliton in NZDSF fiber. As the order increases the higher-order effects become more prominent. A dynamic balance between GVD and SPM can be observed for fundamental ultrashort soliton from Fig. 4.24 and Fig. 4.25 for a propagation distance of 55m in NZDSF.

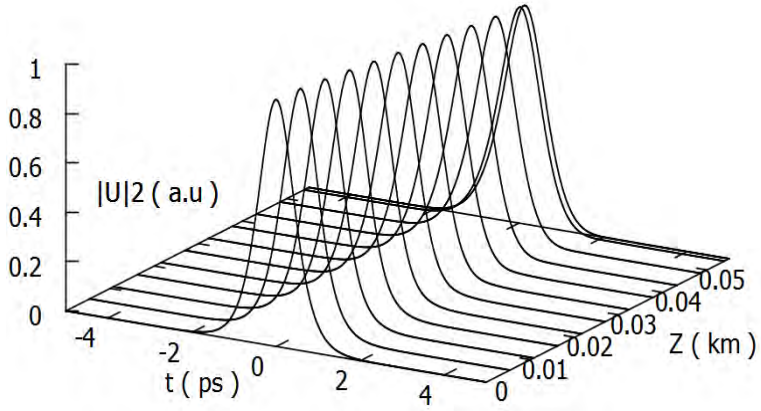

Fig. 4.24: Temporal evolution of ultrashort (FWHM = 500fs) fundamental (N = 1) soliton propagation in NZDSF.

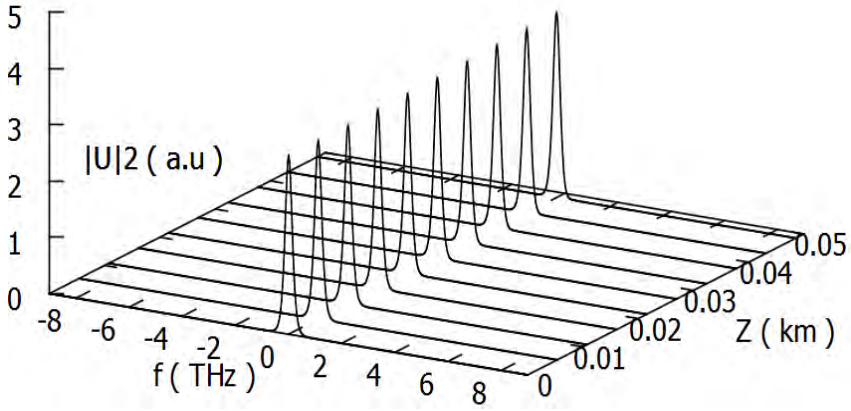

Fig. 4.25: Spectral evolution of ultrashort (FWHM = 500fs) fundamental (N=1) soliton propagation in NZDSF.

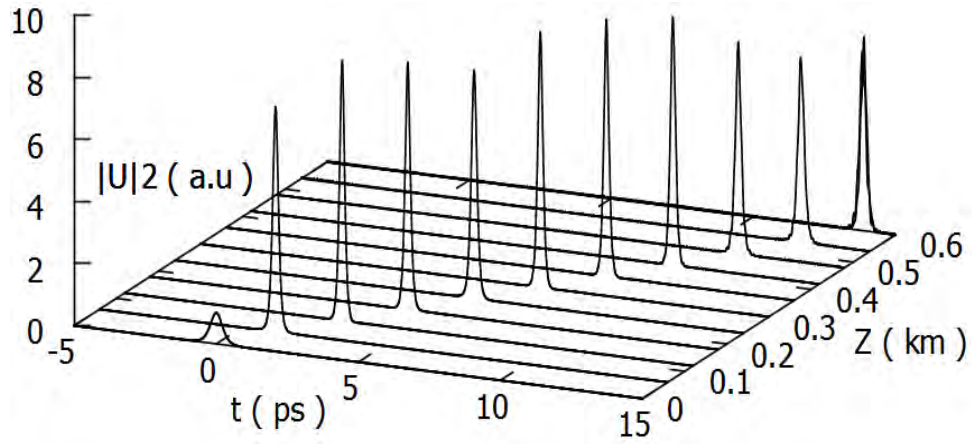

Fig. 4.26: Temporal evolution of ultrashort (FWHM = 500fs) higher-order (N = 2) soliton propagation in NZDSF.

In case of higher-order soliton a soliton self frequency shift and temporal shift has been also happened severely which is very clear from Fig. 4.26 and 4.27. The consequence of this temporal shift may cause great hamper in multichannel propagation. Basically this happens due to GVD and TOD parameters. Although soliton pulse propagates with the compromise of GVD and SPM, for higher-order soliton the effects of TOD, IRS and SS are there which hampers the dynamic balance. From Fig. 4.27 the frequency shifting and newer pulse generation at different frequencies is clear.

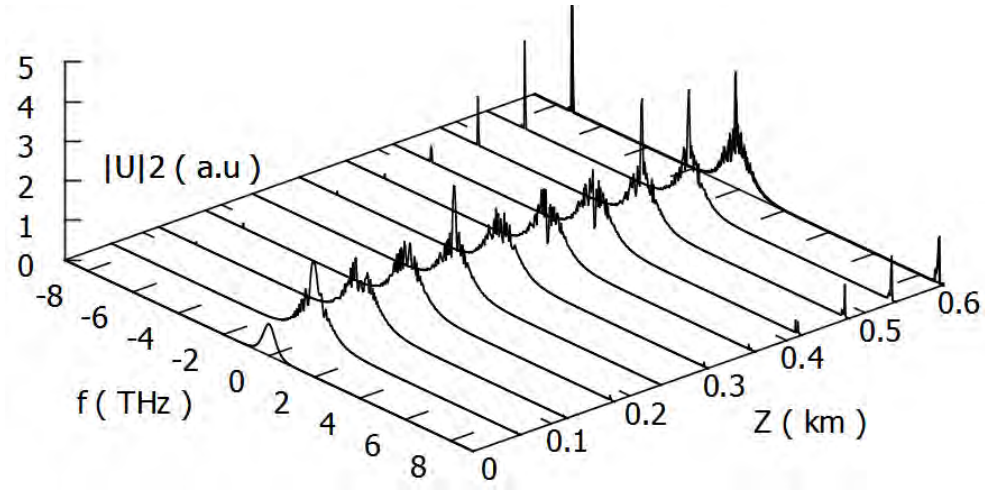

Fig. 4.27: Spectral evolution of ultrashort (FWHM = 500fs) higher-order (N = 2) soliton propagation in NZDSF.

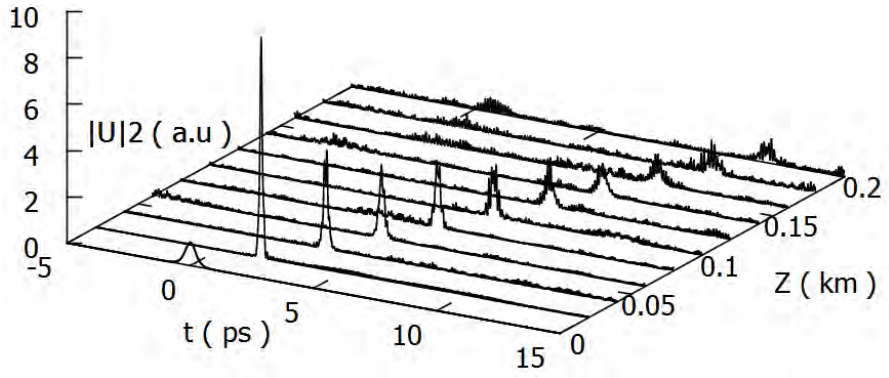

Fig. 4.28: Temporal evolution of ultrashort (FWHM = 500fs) higher-order (N = 3) soliton propagation in NZDSF.

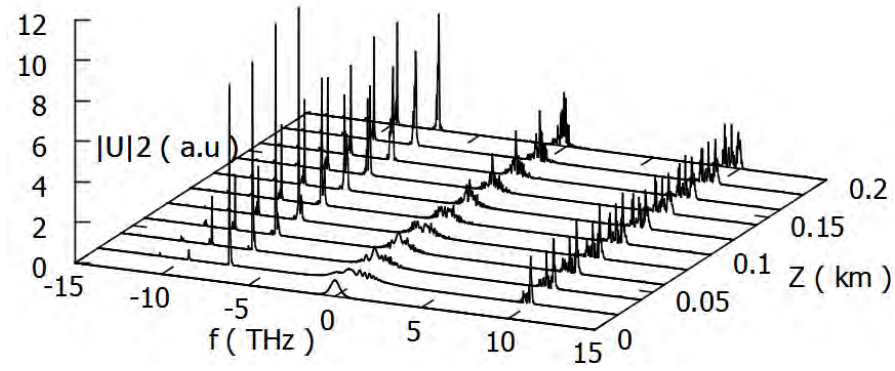

Fig. 4.29: Spectral evolution of ultrashort (FWHM = 500fs) higher-order (N = 3) soliton propagation in NZDSF.

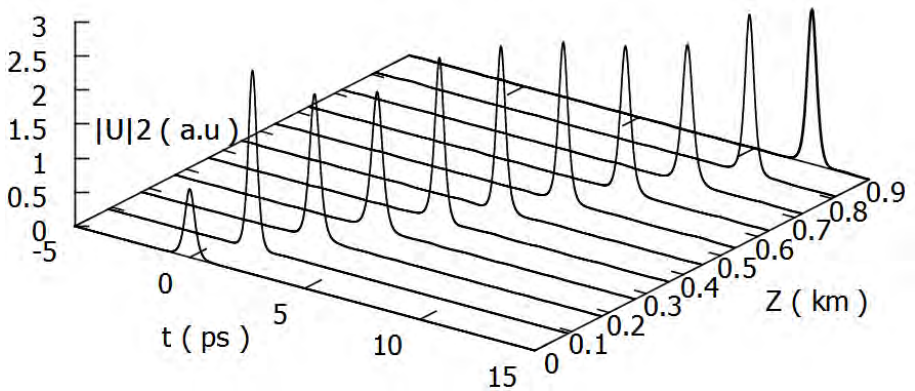

Fig. 4.30: Temporal evolution of ultrashort (FWHM = 500fs) fractional order (N=1.7) soliton propagation in NZDSF.

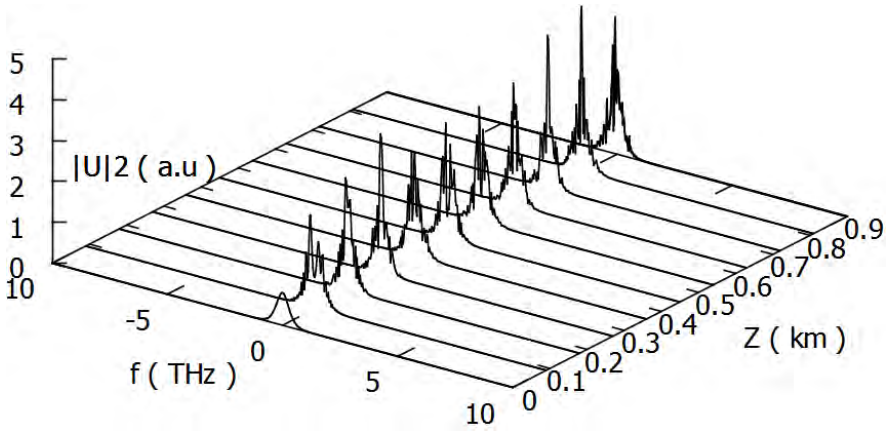

Fig. 4.31: Spectral evolution of ultrashort (FWHM = 500fs) fractional order (N=1.7) soliton propagation in NZDSF.

Fig. 4.28 and Fig. 4.29 show time domain and frequency domain wave shape of 3rd order soliton propagation respectively in NZDSF. The temporal shift and amplitude distortion is clear from Fig. 4.28 that is caused due to GVD and TOD. New frequency generation has been explored by Fig. 4.29 due to SS and IRS effect. Among all the results we can see the effect of SS and IRS is much more prominent in 3rd order soliton.

But in case of fractional order we have observed good propagation behaviour with Fig. 4.30 and Fig. 4.31. Although temporal shift of pulses has been found in Fig. 4.30 due to the effect of GVD and TOD, no new frequency generation has been found in frequency domain wave shape. That means SS and IRS effect are not so severe in fractional order soliton, whereas higher order soliton is affected by SS and IRS effect mostly what we have explored before. Time-bandwidth product for fundamental and higher-order soliton has been tabulated in Table 4.5 and Table 4.6 consists of the propagation distance, peak power for different order soliton and energy.

Table 4.5: Propagation Distance in NZDSF (to maintain time-bandwidth product = 0.32)

Soliton Order	Fiber Name	Covered Distance	Time-Bandwidth Product
1	NZDSF	55m	0.32
2		250m	0.315
3		50m	0.33
1.7		900m	0.32

Table 4.6: Propagation Characteristics in NZDSF

Fiber	NZDSF	NZDSF	NZDSF	NZDSF
Energy, E_0	0.02nJ	0.083nJ	0.189nJ	0.062nJ
Peak Power, P_0	37w	148w	333w	111w
Soliton order, N	1	2	3	1.73 (Fractional)
Distance	55m	600m	200m	900m

4.3.3 Propagation behaviour in LEAF

In this section we will explore the propagation behaviour of ultrashort fundamental and higher-order soliton in Corning LEAF fiber. A return to zero sech pulse of 50% duty cycle has been considered as input pulse. The covered distance maintaining soliton nature has been found about 100m for fundamental soliton in LEAF. Although no temporal shift in Fig. 4.32 and no new frequency generation in Fig. 4.33 have been observed, a small propagation distance has been covered in LEAF.

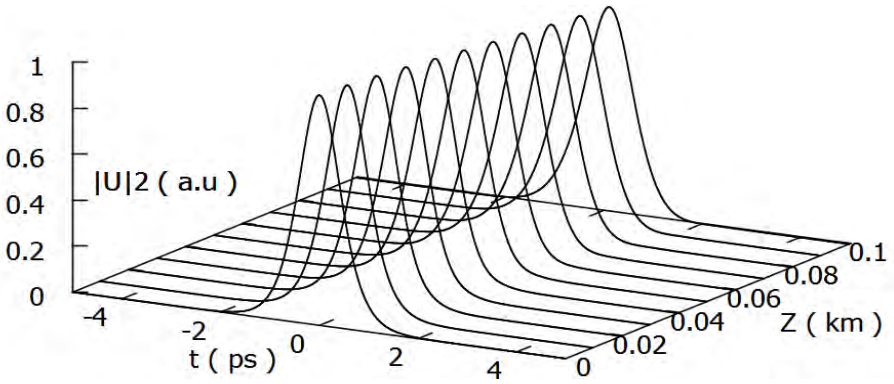

Fig. 4.32: Temporal evolution of ultrashort (FWHM = 500fs) fundamental (N = 1) soliton propagation in LEAF.

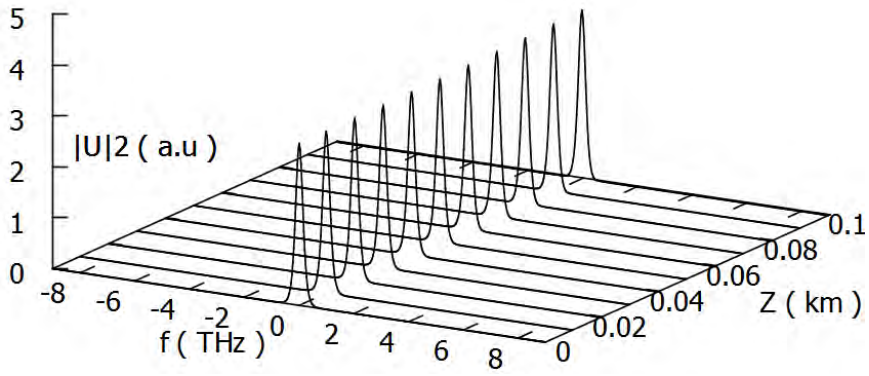

Fig. 4.33: Spectral evolution of ultrashort (FWHM = 500fs) fundamental (N = 1) soliton propagation in LEAF.

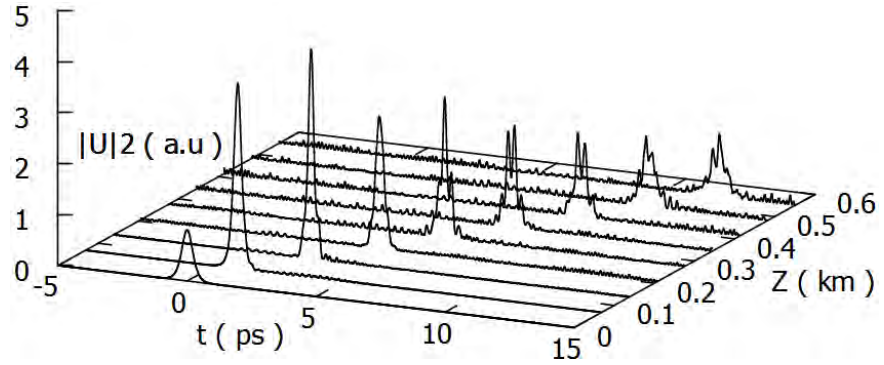

Fig. 4.34: Temporal evolution of ultrashort (FWHM = 500fs) higher-order (N = 2) soliton propagation in LEAF.

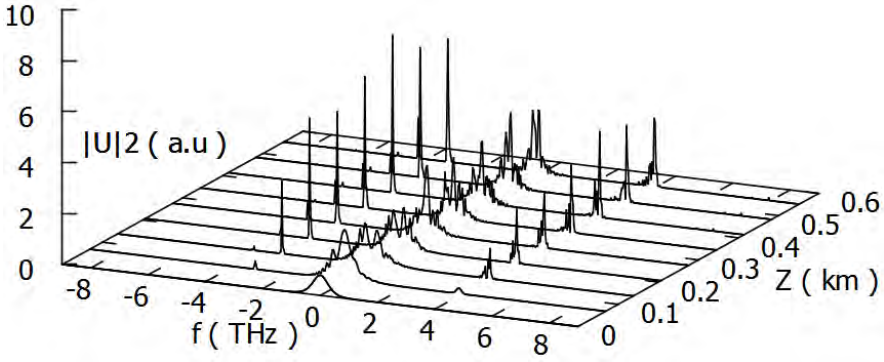

Fig. 4.35: Spectral evolution of ultrashort (FWHM = 500fs) higher-order (N = 2) soliton propagation in LEAF.

As the order increases the higher-order effects become more prominent. For second order soliton in LEAF, GVD and TOD effect can be observed by the temporal shift from Fig. 4.34. Soliton self frequency shift with new frequency generation and pulse asymmetry can also be observed as the consequence of the effect of SS and IRS from Fig. 4.35. In case of third order soliton GVD and TOD effects are similar like second order soliton shown in Fig. 4.36. But SS and IRS effects are less prominent than that of 2nd order soliton shown in Fig. 4.37.

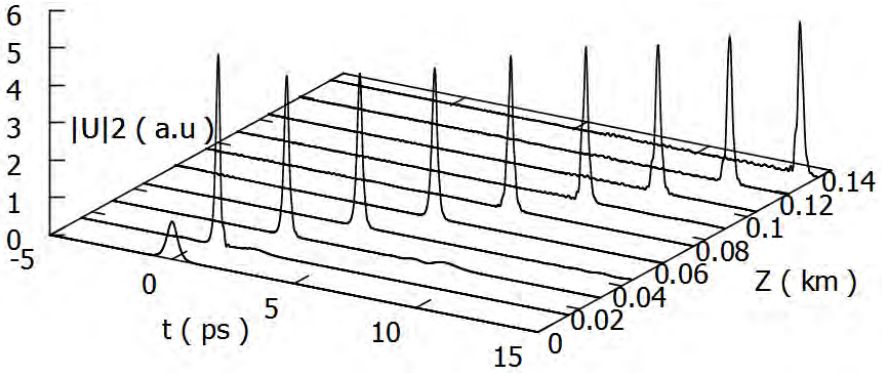

Fig. 4.36: Temporal evolution of ultrashort (FWHM = 500fs) higher-order (N = 3) soliton propagation in LEAF.

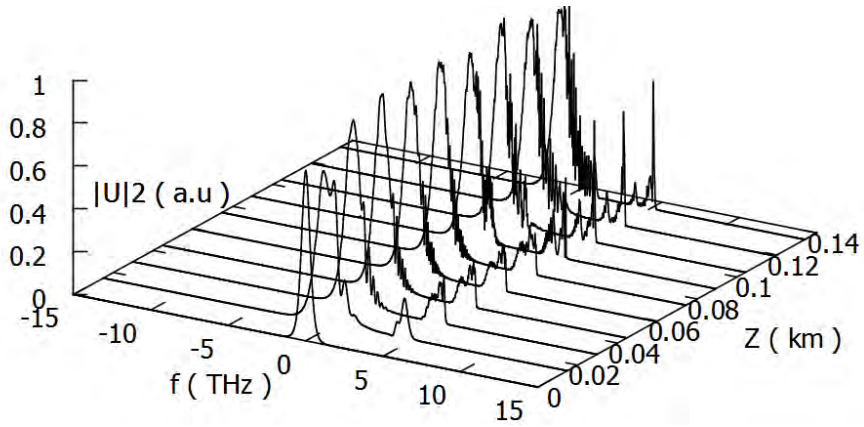

Fig. 4.37: Spectral evolution of ultrashort (FWHM = 500fs) higher-order (N = 3) soliton propagation in LEAF.

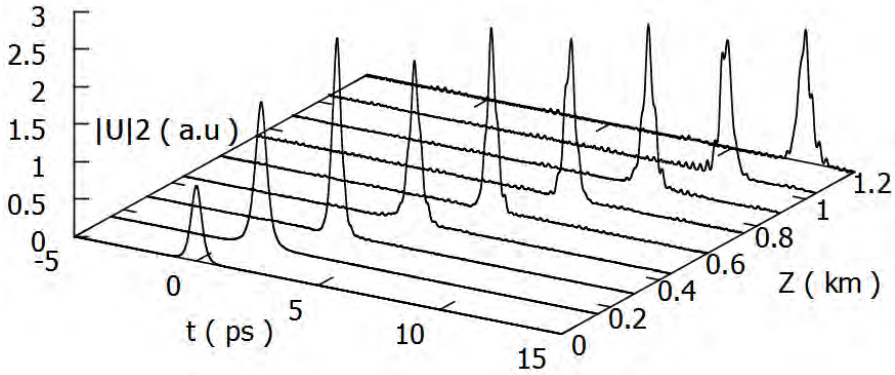

Fig. 4.38: Temporal evolution of ultrashort (FWHM = 500fs) fractional order (N=1.7) soliton propagation in LEAF.

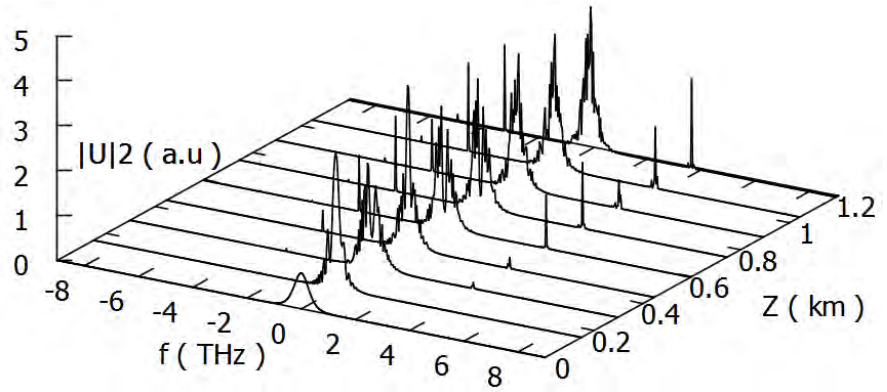

Fig. 4.39: Spectral evolution of ultrashort (FWHM = 500fs) fractional order (N=1.7) soliton propagation in LEAF.

In case of fractional order we have observed good propagation behaviour which propagates 1200m distance maintaining soliton nature shown in Fig. 4.38. A small SS and IRS effects can be observed from Fig. 4.39. The propagation distance, peak power for different order

soliton, energy has been tabulated in Table 4.8 and Table 4.7 has been revealed for time-bandwidth product.

Table 4.7: Propagation Distance in LEAF (to maintain time-bandwidth product = 0.32)

Soliton Order	Fiber Name	Covered Distance	Time-Bandwidth Product
1	LEAF	100m	0.32
2		280m	0.306
3		100m	0.31
1.7		1000m	0.32

Table 4.8: Propagation Characteristics in LEAF

Fiber	LEAF	LEAF	LEAF	LEAF
Energy, E_0	0.01nJ	0.043nJ	0.097nJ	0.032nJ
Peak Power, P_0	19w	76w	171w	57w
Soliton order, N	1	2	3	1.73 (Fractional)
Distance	100m	600m	140m	1200m

4.3.4 Propagation behaviour in MCDSF

In this section we will explore the propagation behaviour of ultrashort fundamental and higher-order soliton in MCDSF fiber. This fiber gives best performance among the others. About 2km has been covered by fundamental soliton in MCDSF without being affected by the higher order terms shown in Fig. 4.40. SS and IRS effects has not found during this distance shown in Fig. 4.41.

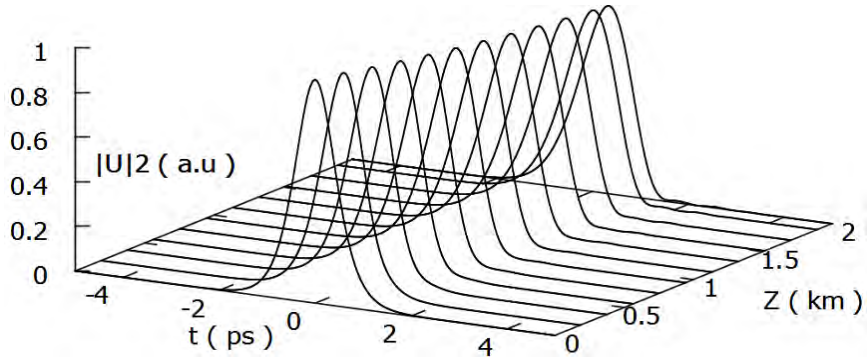

Fig. 4.40: Temporal evolution of ultrashort (FWHM = 500fs) fundamental (N = 1) soliton propagation in MCDSF.

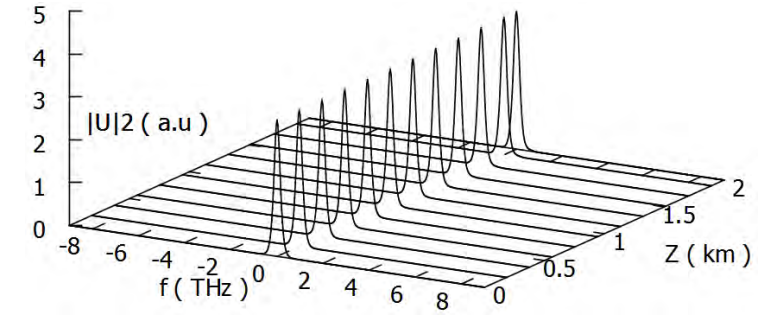

Fig. 4.41: Spectral evolution of ultrashort (FWHM = 500fs) fundamental (N = 1) soliton propagation in MCDSF.

For second order soliton in MCDSF, no temporal shift has been found but TOD effect can be observed by the trailing edge of the pulse from Fig. 4.42. A poor soliton self frequency shift with new frequency generation and pulse asymmetry can also be observed as the consequence of the small effect of SS and IRS shown in Fig. 4.43. Covered distance has been shown about 5km. After 3km the time-bandwidth product has been measured as 0.335 as shown later in Table 4.9. Beyond this propagation distance the time-bandwidth product goes beyond the fixed time-bandwidth product of sech pulse of 0.32.

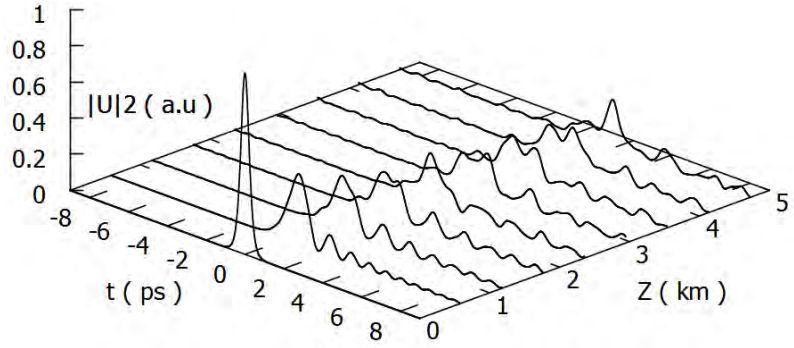

Fig. 4.42: Temporal evolution of ultrashort (FWHM = 500fs) higher-order (N = 2) soliton propagation in MCDSF.

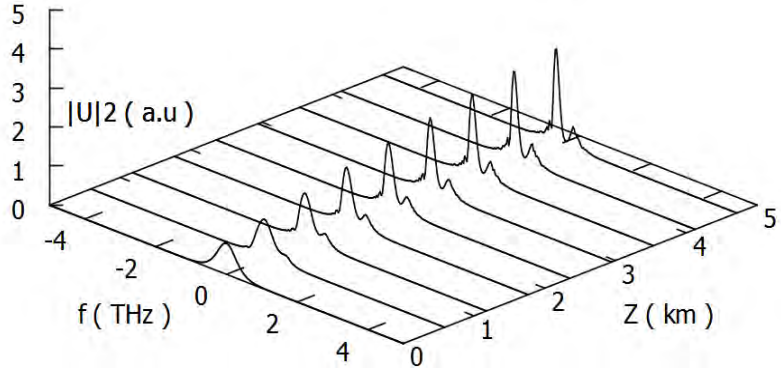

Fig. 4.43: Spectral evolution of ultrashort (FWHM = 500fs) higher-order (N = 2) soliton propagation in MCDSF.

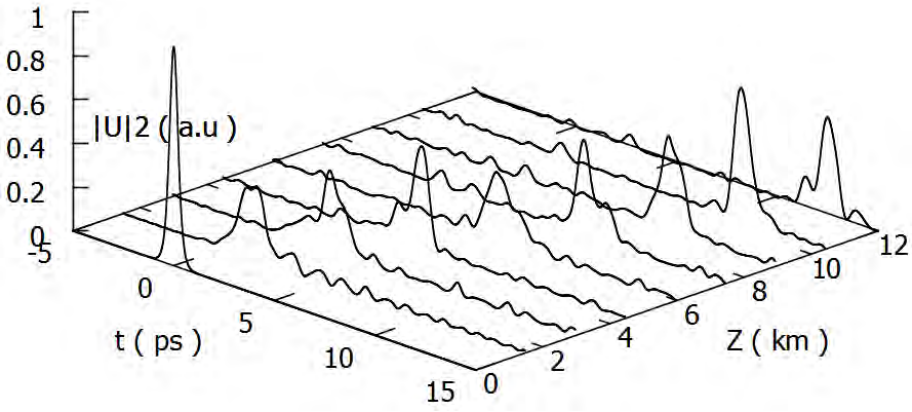

Fig. 4.44: Temporal evolution of ultrashort (FWHM = 500fs) higher-order (N = 3) soliton propagation in MCDSF.

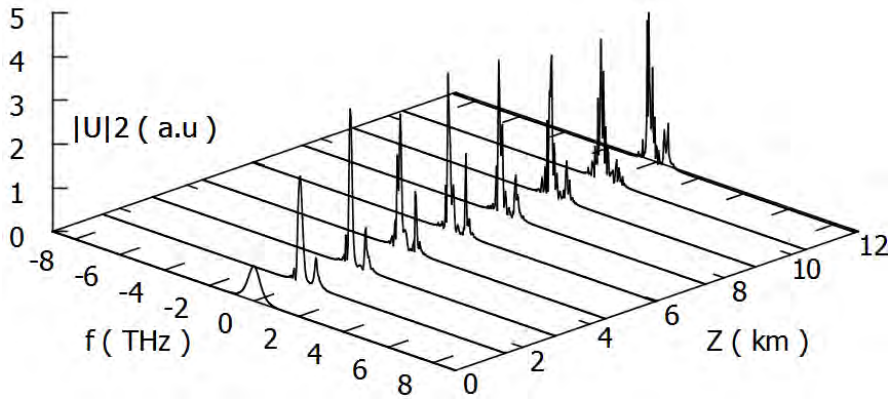

Fig. 4.45: Spectral evolution of ultrashort (FWHM = 500fs) higher-order (N = 3) soliton propagation in MCDSF.

As the order increases the higher-order effects become more prominent. For third order soliton in MCDSF, GVD and TOD effect can be observed by the temporal shift from Fig. 4.44. Soliton self frequency shift with new frequency generation and pulse asymmetry can also be observed as the consequence of the effect of SS and IRS from Fig. 4.45. Although covered distance has been shown about 12km, after 8km the time-bandwidth product has been measured as 0.31 as shown later in Table 4.9. Beyond this propagation distance the time-bandwidth product goes beyond the fixed time-bandwidth product of sech pulse of 0.32. In case of fractional order we have observed good propagation behaviour which propagates 9000m (9km) distance maintaining time-bandwidth product of 0.32 as shown in Fig. 4.46. A small SS and IRS effects can be observed from Fig. 4.47. The propagation distance, peak

power for different order soliton, energy has been tabulated in Table 4.10 and Table 4.9 has been revealed for time-bandwidth product.

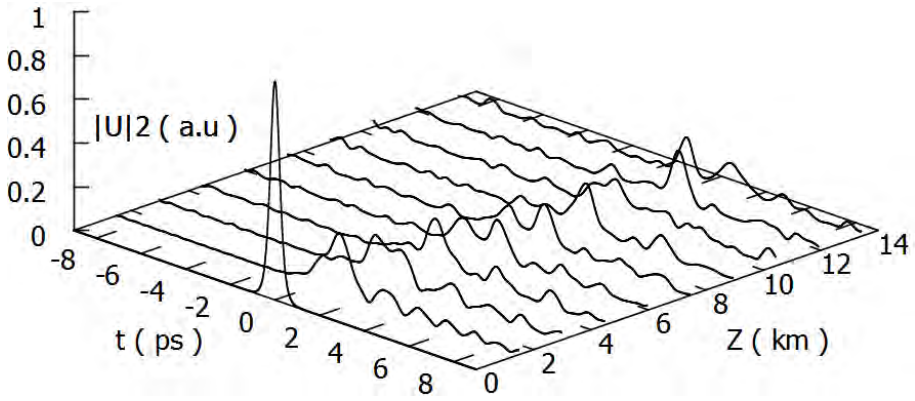

Fig. 4.46: Temporal evolution of ultrashort (FWHM = 500fs) fractional order (N = 1.7) soliton propagation in MCDSF.

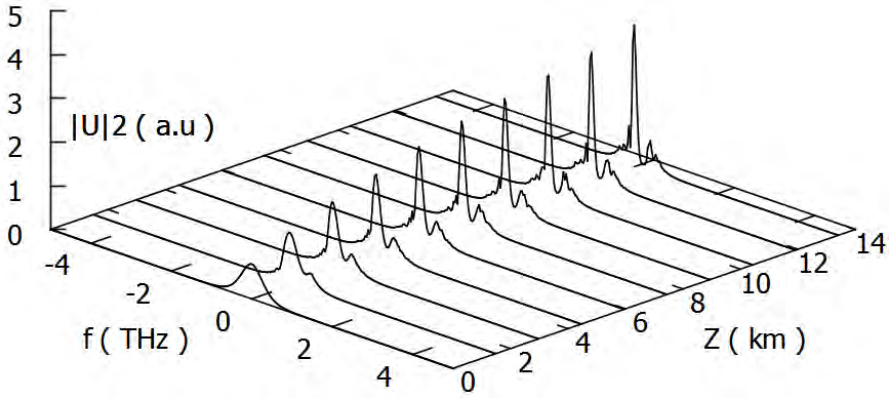

Fig. 4.47: Spectral evolution of ultrashort (FWHM = 500fs) fractional order (N = 1.7) soliton propagation in MCDSF.

Table 4.9: Propagation Distance in MCDSF (to maintain time-bandwidth product = 0.32)

Soliton Order	Fiber Name	Covered Distance	Time-Bandwidth Product
1	MCDSF	2000m	0.32
2		3000m	0.335
3		8000m	0.31
1.7		9000m	0.31

Table 4.10: Propagation Characteristics in MCDSF

Fiber	MCDSF	MCDSF	MCDSF	MCDSF
Energy, E_0	0.181pJ	0.72pJ	1.63pJ	0.54pJ
Peak Power, P_0	0.32w	1.28w	2.88w	0.96w

Soliton order, N	1	2	3	1.73 (Fractional)
Distance	2000m	5000m	12000m	14000m

4.3.5 Propagation behaviour in MCDFF

Different characteristics shown by MCDFF fiber will be discussed here in this section. About 200m has been covered by fundamental soliton in MCDFF without being affected by the higher order terms shown in Fig. 4.48. SS and IRS effects has not found during this distance shown in Fig. 4.49. The time-bandwidth product has been measured as 0.32 after this 200m propagation distance.

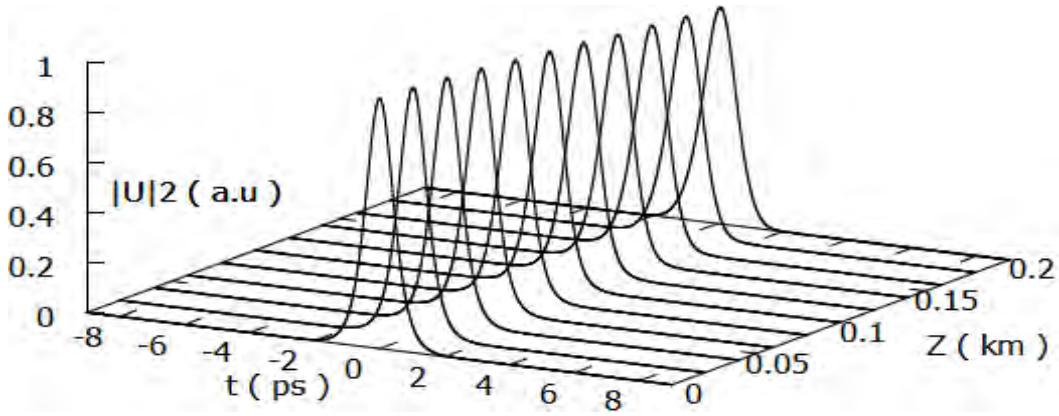

Fig. 4.48: Temporal evolution of ultrashort (FWHM = 500fs) fundamental (N = 1) soliton propagation in MCDFF.

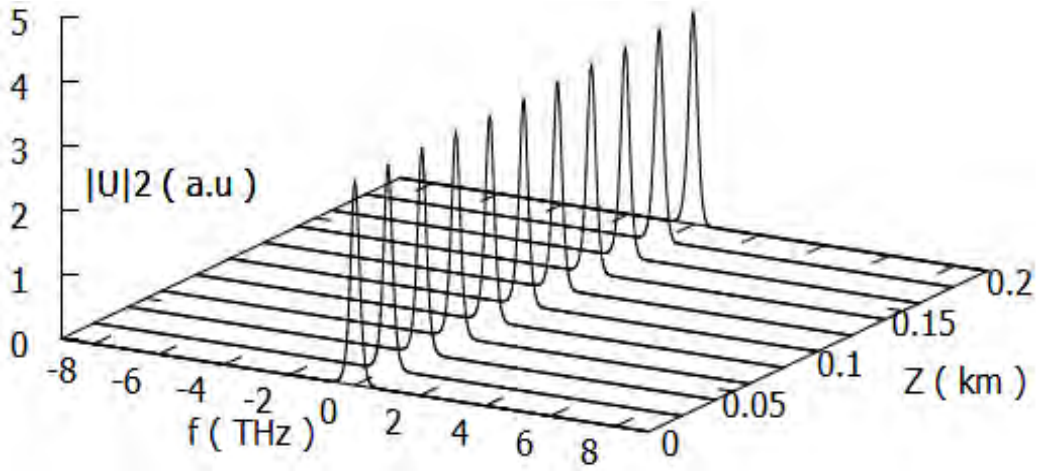

Fig. 4.49: Spectral evolution of ultrashort (FWHM = 500fs) fundamental (N = 1) soliton propagation in MCDFF.

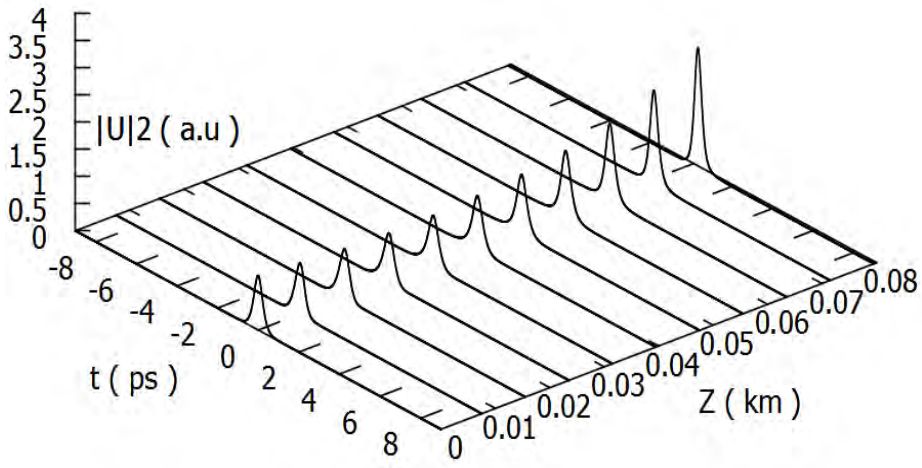

Fig. 4.50: Temporal evolution of ultrashort (FWHM = 500fs) higher-order (N = 2) soliton propagation in MCDFF.

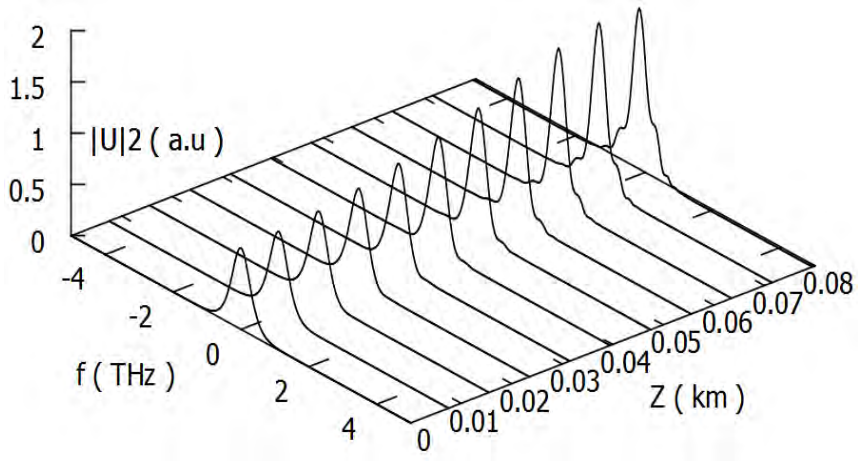

Fig. 4.51: Spectral evolution of ultrashort (FWHM = 500fs) higher-order (N = 2) soliton propagation in MCDFF.

For second order soliton in MCDFF, no temporal shift has been found i.e. GVD and TOD effects have been revealed as less prominent shown in Fig. 4.50. The spectrum has been found to be not affected by SS and IRS effect shown in Fig. 4.51 because soliton self frequency shift with new frequency generation and pulse asymmetry have been found absent in spectral evolution. Covered distance has been shown about 60m maintaining time-bandwidth product as 0.32. As the order increases the higher-order effects become more prominent. For third order soliton in MCDFF, GVD and TOD effect can be observed by the trailing edge of the pulse from Fig. 4.52. Soliton self frequency shift with new frequency

generation and pulse asymmetry can also be observed as the consequence of the effect of SS and IRS from Fig. 4.53. Although covered distance has been shown about 200m, after 80m the time-bandwidth product has been measured as 0.33 as shown later in Table 4.11. Beyond this propagation distance the time-bandwidth product goes beyond the fixed time-bandwidth product of sech pulse of 0.32.

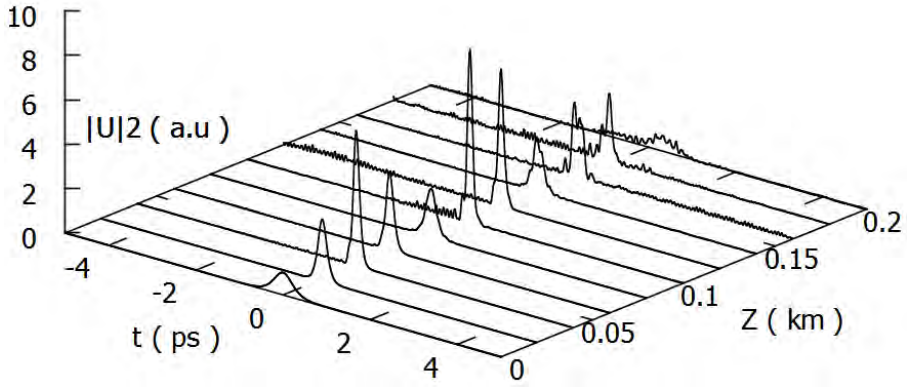

Fig. 4.52: Temporal evolution of ultrashort (FWHM = 500fs) higher-order (N = 3) soliton propagation in MCDFF.

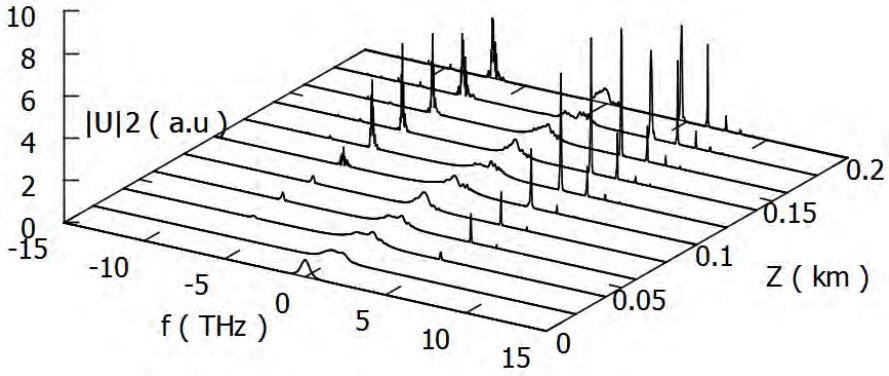

Fig. 4.53: Spectral evolution of ultrashort (FWHM = 500fs) higher-order (N = 3) soliton propagation in MCDFF.

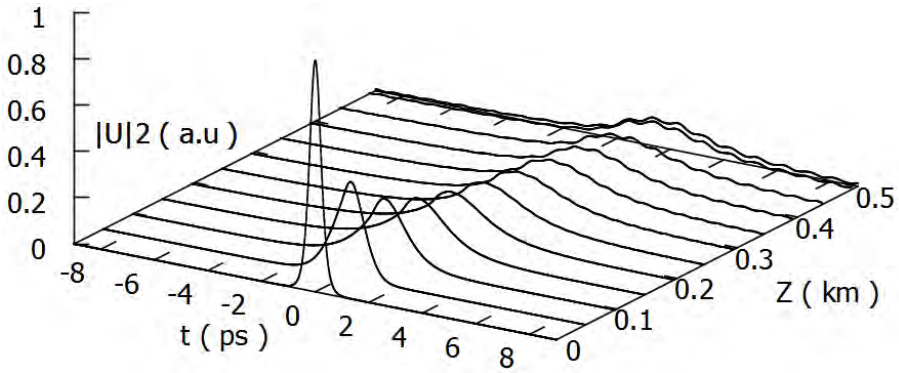

Fig. 4.54: Temporal evolution of ultrashort (FWHM = 500fs) fractional order (N = 1.7) soliton propagation in MCDFF.

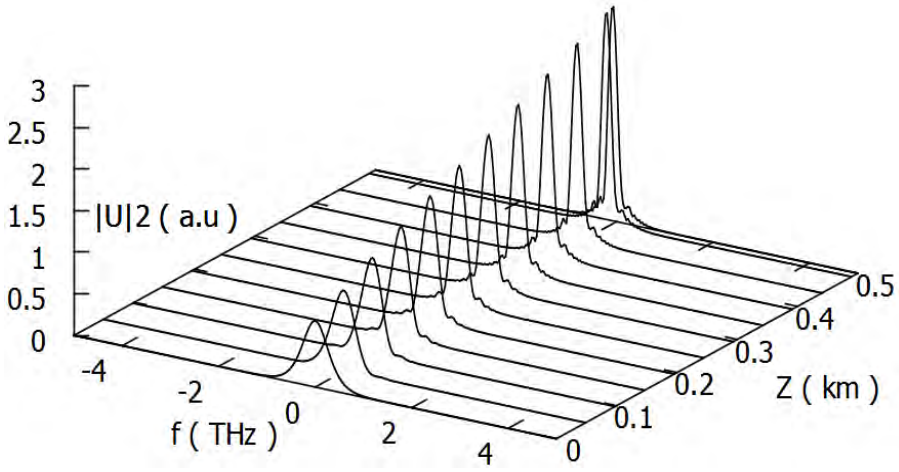

Fig. 4.55: Spectral evolution of ultrashort (FWHM = 500fs) fractional order (N = 1.7) soliton propagation in MCDFF.

In case of fractional order we have observed amplitude distortion due to high IRS and TOD effect and propagation distance has been found as 100m maintaining time-bandwidth product of 0.32 as shown in Fig. 4.54. A small IRS effects can be observed from Fig. 4.55. The propagation distance, peak power for different order soliton, energy has been tabulated in Table 4.12 and Table 4.11 has been revealed for time-bandwidth product.

Table 4.11: Propagation Distance in MCDFF (to maintain time-bandwidth product = 0.32)

Soliton Order	Fiber Name	Covered Distance	Time-Bandwidth Product
1	MCDFF	200m	0.32
2		60m	0.32
3		80m	0.33
1.7		100m	0.32

Table 4.12: Propagation Characteristics in MCDFF

Fiber	MCDFF	MCDFF	MCDFF	MCDFF
Energy, E_0	5.38pJ	21.55pJ	47.1pJ	9.07pJ
Peak Power, P_0	9.5w	38w	83w	16w
Soliton order, N	1	2	3	1.73 (Fractional)
Distance	200m	80m	200m	500m

4.4 Conclusion

In this chapter the simulation result based on propagation behavior of fundamental and higher-order ultrashort soliton has been demonstrated deliberately. From section 4.2 we can come to a decision that for fundamental soliton propagation with per channel data rate of 400Gb/s MCDSF fiber can be a great one with comparison to other fibers demonstrated. From section 4.3 we can say that ultrashort higher-order soliton propagation with per channel data rate of 1Tb/s MCDSF shows a good characteristics in case of 3^{rd} order soliton propagation in comparison to other fibers. An additional feature of section 4.3 has been demonstrating the behavior of fractional order soliton propagation.

Chapter 5

Compression of Ultrashort Soliton

5.1 Introduction

Compression of fundamental and higher-order soliton has been observed in DCF, DDF and FBG. Compression of ultrashort soliton can be performed with dispersion decreasing fiber, fiber Bragg grating and dispersion compensating fiber. We demonstrated a comparison among them that which one is better for compression. For this reason we have analysed the parameters like full width at half maximum, temporal and spectral evolution in case of both fundamental and higher-order ultrashort soliton.

5.2 Compression of Fundamental Soliton

Compression of ultrashort soliton can be performed with different techniques. We will hereby discuss ultrashort soliton compression using dispersion decreasing fiber, fiber Bragg grating and dispersion compensating fiber. The dispersion-decreasing fiber (DDF), first introduced in Ref. [72] that supports the lowest-order soliton despite the presence of optical loss. Group-velocity dispersion of this fiber decreases with distance, in accord with soliton attenuation that is due to the inherent optical loss of the fiber. DDF is used to avoid soliton broadening resulting from inherent optical loss of the fiber during the propagation of the pulse. Recent numerical and experimental results have shown [73] the possibility to generate parabolic pulses via a single DDF with normal dispersion.

Bragg gratings are extensively used in fiber optic communication systems. In general, any periodic perturbation in the propagating medium serves as a Bragg grating. This perturbation is usually a periodic variation of the refractive index of the medium. In this case, the Bragg gratings are ―written" in fibers. Bragg gratings written in fiber can be used to make a variety of devices such as filters, add/drop multiplexers and dispersion compensators. Nonlinear pulse propagation and compression have been reported in short period FBGs [74]-[77]. DCF

based soliton compression was previously studied [78]. Ultrashort soliton compression in DDF is also explored recently [48], [79].

But in our knowledge there was no attempt to perform a comparative study among the DDF, DCF and FBG. Motivated by this we will explore the suitability of DDF as ultrashort soliton compressor instead of DCF and FBG for medical applications. At first we have explored the temporal and spectral evolution of compressed soliton in a DCF and after then in a linear DDF of following dispersion profile [80] and finally FBG based soliton compression has been revealed.

$$\beta_{2n} = \beta_{2p}\left(1 + \frac{z}{\beta L} - \frac{z}{L}\right) \tag{5.1}$$

Whereβ_{2n} and β_{2p} are the changing group-velocity dispersion (GVD) and starting GVD respectively. Here$\beta = \frac{\beta_{2p}}{\beta_{2L}}$, β_{2L}=final GVD and L is the total fiber length. The fiber parameters used are as follows:

Table 5.1: Compression in DCF, FBG and DDF

Fiber Parameters	**Fiber Name**		
	SSMF	**DCF**	**FBG**
D(ps/nm/km)	16.6	-96.33	-632.6
D_{λ}	0.0575	0.65	0.65
n_2 ($\times 10^{-20} m^2/W$)	2.3	2.5	2.3
A_{eff}(μm^2)	85	20	500

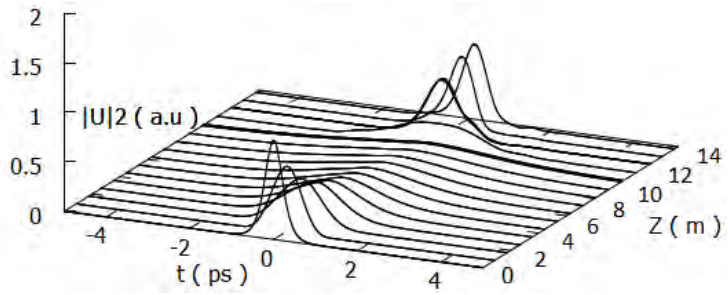

Fig. 5.1: Compression of fundamental soliton in DCF (Temporal Evolution).

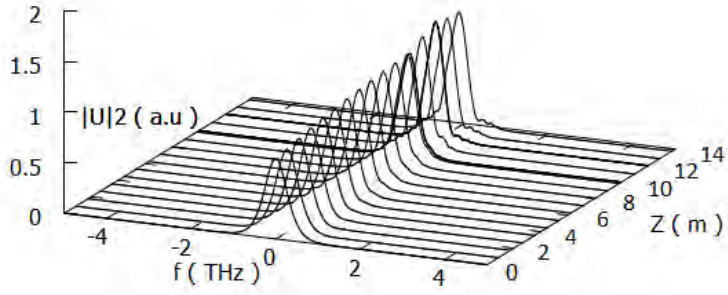

Fig. 5.2: Compression of fundamental soliton in DCF (Spectral Evolution).

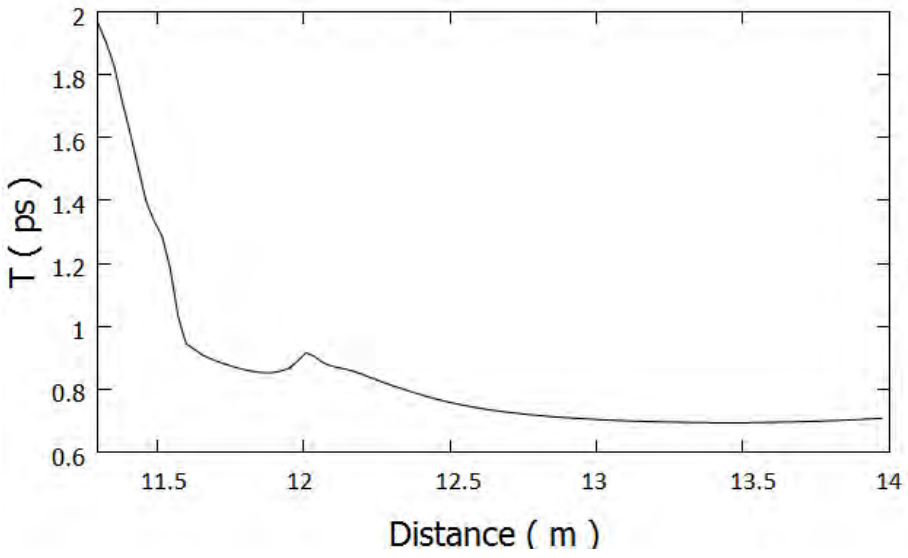

Fig. 5.3: Pulse width vs. distance curve for DCF (N=1).

In Fig. 5.1 pulse compression is shown using DCF. In this analysis 10m SSMF fiber and 2m DCF is used. Temporal evolution shows that 10m SSMF causes an expansion and the pulse expanded up to 2ps. Next 2m DCF compresses the pulse and turns it into 700fs. The FWHM has shown in Fig. 5.3, from where it is clear that the compression has been going on with increase in propagation distance of fundamental soliton.

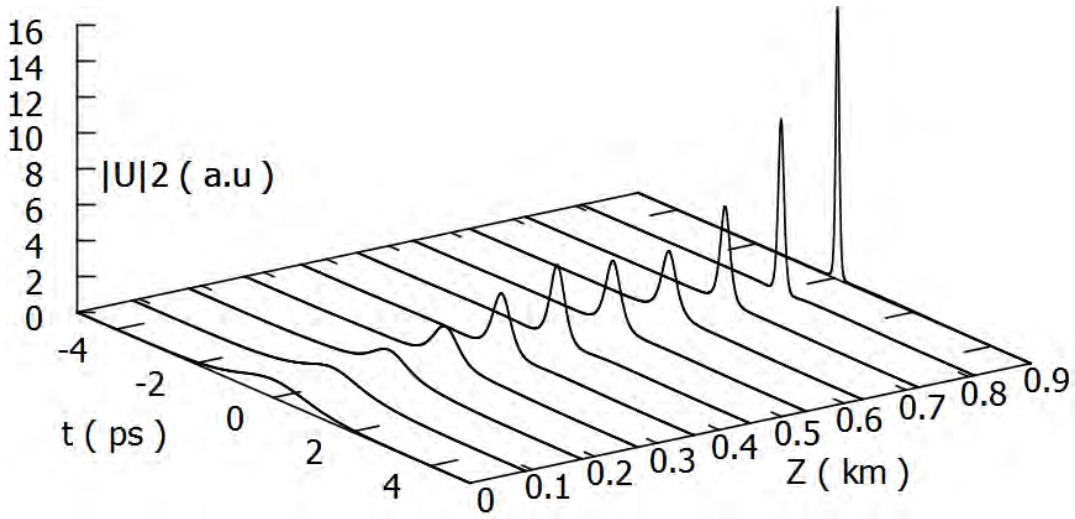

Fig. 5.4: Compression of fundamental soliton in DDF (Temporal Evolution).

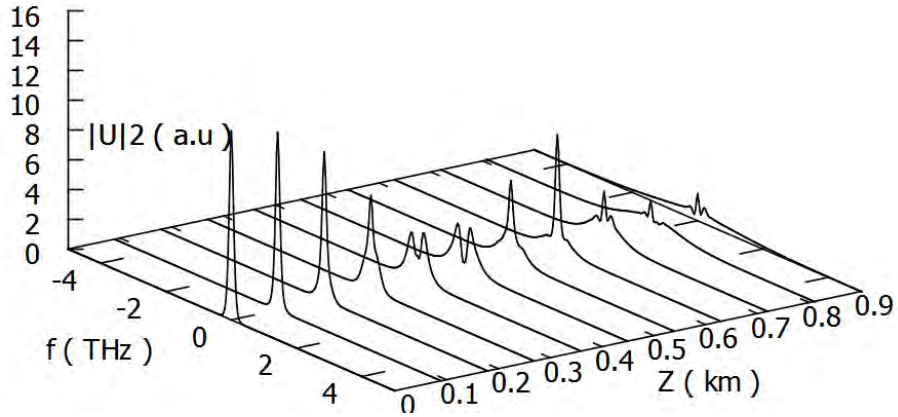

Fig. 5.5: Compression of fundamental soliton in DDF (Spectral Evolution).

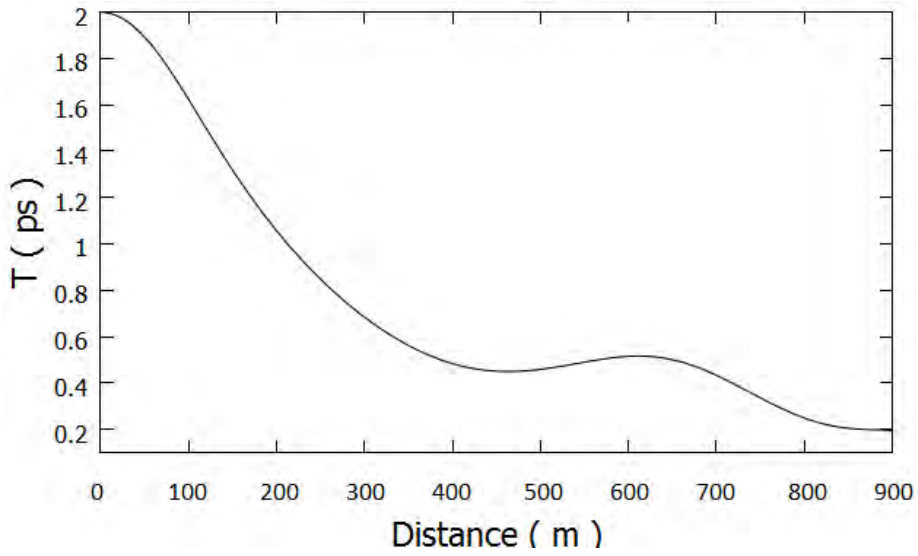

Fig. 5.6: Pulse width vs. distance curve for DDF (N=1).

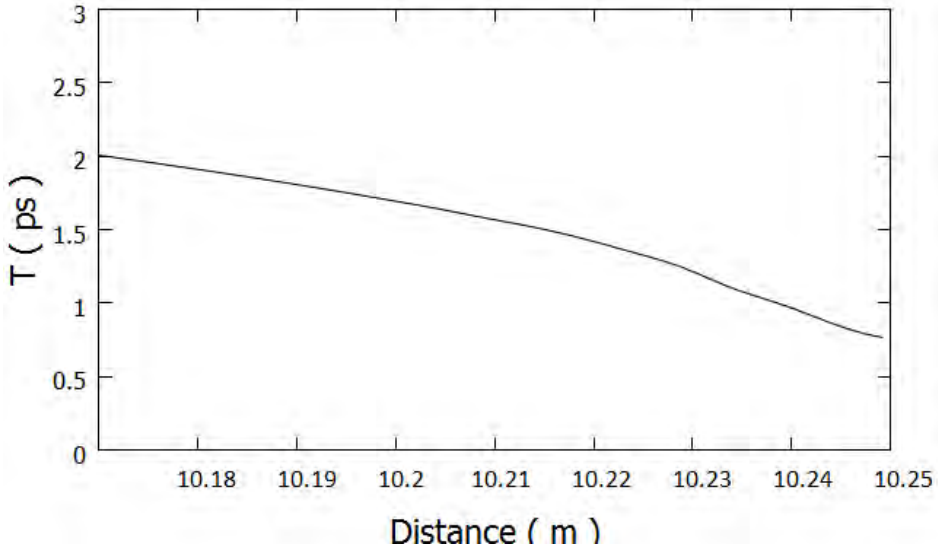

Fig. 5.7: Pulse width vs. distance curve for FBG (N=1).

Soliton compression can be obtained using DDF also. We have experienced fundamental soliton compression in linear DDF, whose dispersion profile has described by Eqn. (5.1). The temporal evolution shows the compressed pulse in Fig. 5.4 and spectral component has also been shown in Fig. 5.5. Parameters used in this analysis are T_{FWHM}=2ps, P_0=1.6w, β_{2P}=−10 ps^2 /km, β_{2L}=−1 ps^2/km, β_3 =0.029 ps^3/km, γ=5, s=0.29, τ_R=0.02. The time-bandwidth product is found on an average of 0.32 during the whole process. Linear DDF performs a good compression than that of DCF. In Fig. 5.6 we see that the 2ps pulse has been compressed and turn into 200fs, whereas this was only 700fs in case of DCF. Again Fig. 5.7 shows pulse compression using FBG. Where propagation through SSMF is done for 10m then compression is happened within 25cm of FBG. For the same 2ps pulse FBG compresses it up to 710fs pulse. Absolutely we can say from the above discussion that for fundamental soliton compression DDF is better than DCF and FBG. DCF has a constant dispersion profile whereas DDF maintains decreasing dispersion profile. This property makes the DDF better for soliton compression.

5.3 Compression of Higher-Order Soliton

Here we will see compression of higher-order soliton in DCF, FBG and DDF simultaneously. Using linear DDF the compression of 2nd order soliton is shown in Fig. 5.8. Parameters used in this analysis are T_{FWHM}=500fs, P_0=100w, β_{2P}=−10 ps^2/km, β_{2L}=−1 ps^2/km, β_3 =0.029 ps^3/km, γ=5, s=0.29, τ_R=0.02, N=2. What we have observed is that expansion happened within first 10m of DDF and then compression occurs in rest 15m the pulse has turned its shape from 800fs to 340fs after compression and propagation through DDF.

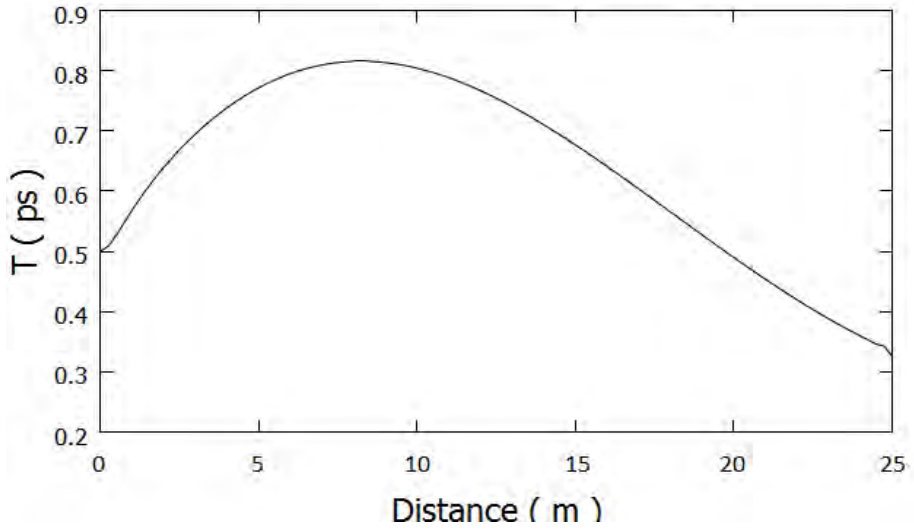

Fig. 5.8: Pulse width vs. distance curve for DDF(N=2).

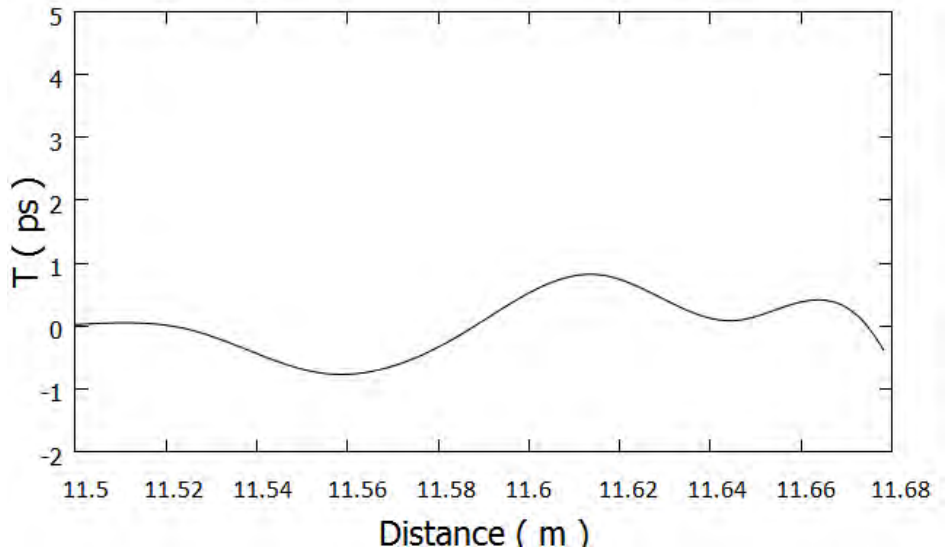

Fig. 5.9: Pulse width vs. distance curve for DCF(N=2).

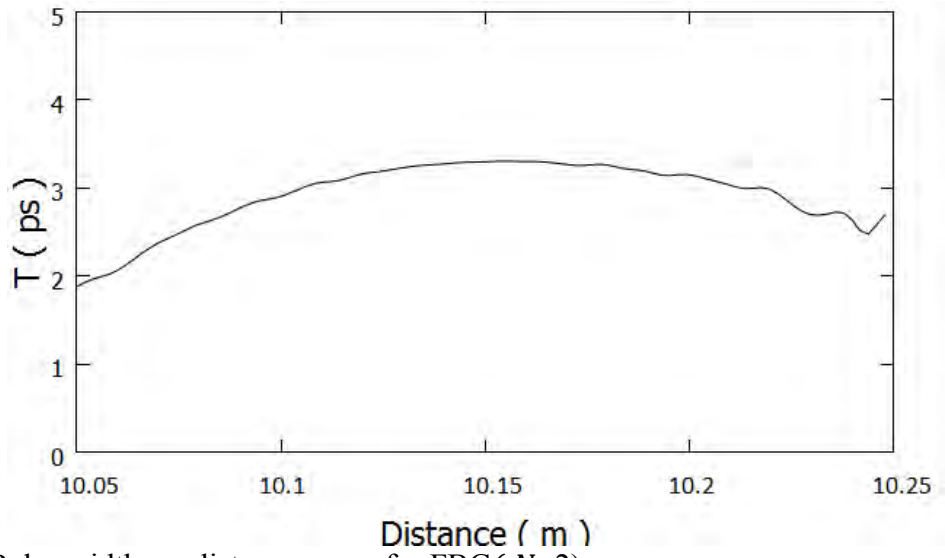

Fig. 5.10: Pulse width vs. distance curve for FBG(N=2).

On the contrary Fig. 5.9 shows what is happening in case of DCF with same parameter setting. The fiber shows compression for only 5cm then expansion for 7cm, again compression for 8cm that is in one word a peculiar nature. Fig. 5.10 shows second order soliton compression using FBG, where expansion is got beyond 3ps and then compression happened up to 2.5ps. In case of DDF it is 340fs after compression. Fig. 5.11, Fig. 5.12 and Fig. 5.13 stands for the 3rd order soliton compression in DDF, DCF and FBG respectively. Again a smooth curve observed in DDF that indicates compression of 3rd order soliton into 300fs. DCF starts with compression and after 11.6m expansion happens and continues as well shown in Fig. 5.12. Similarly alternatively compression and expansion is found for FBG shown in Fig. 5.13.

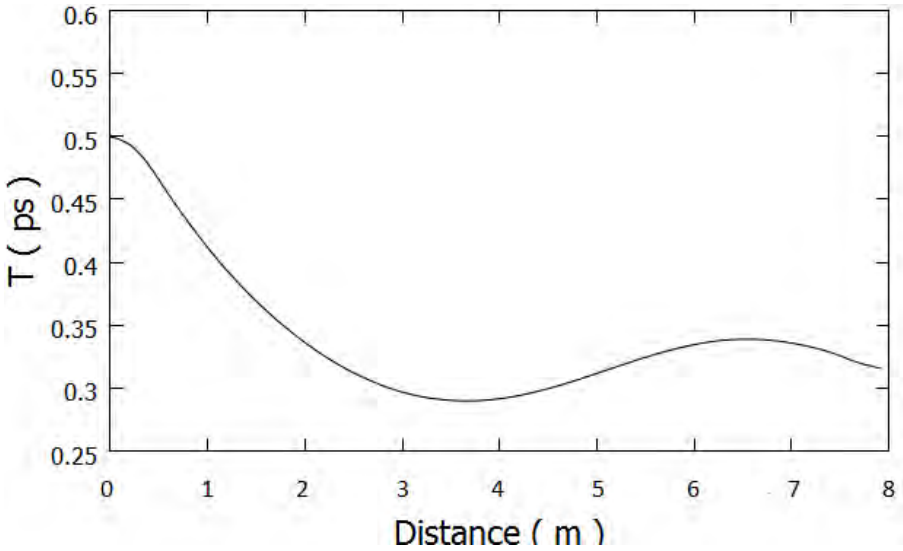

Fig. 5.11: Pulse width vs. distance curve for DDF(*N*=3).

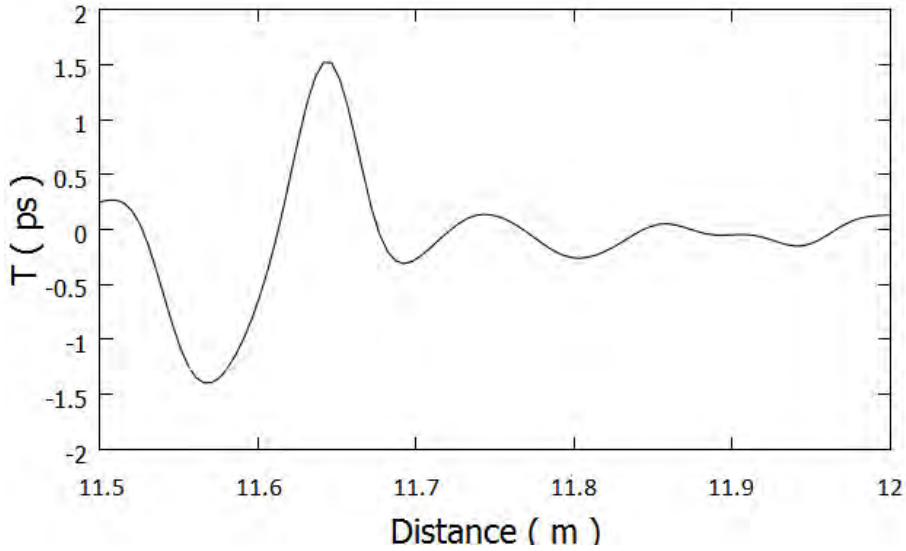

Fig. 5.12: Pulse width vs. distance curve for DCF(*N*=3).

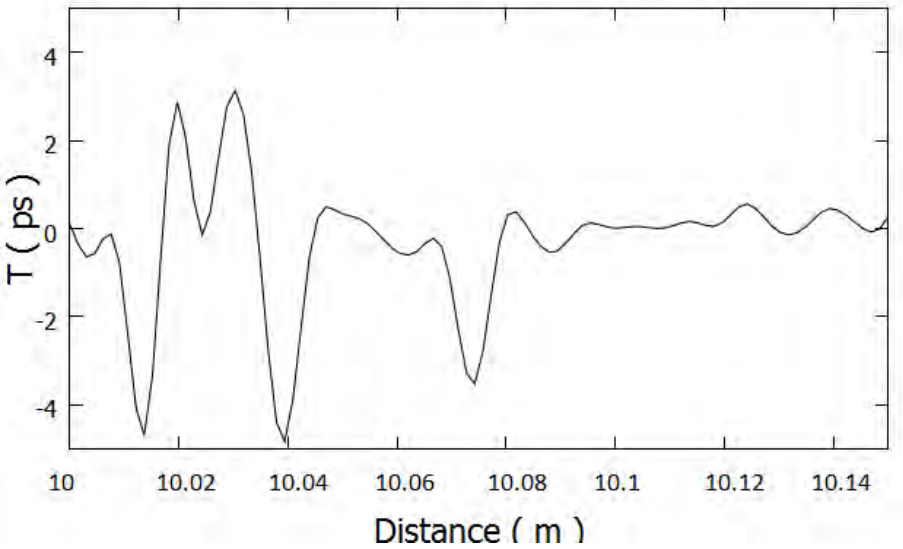

Fig. 5.13: Pulse width vs. distance curve for FBG(*N*=3).

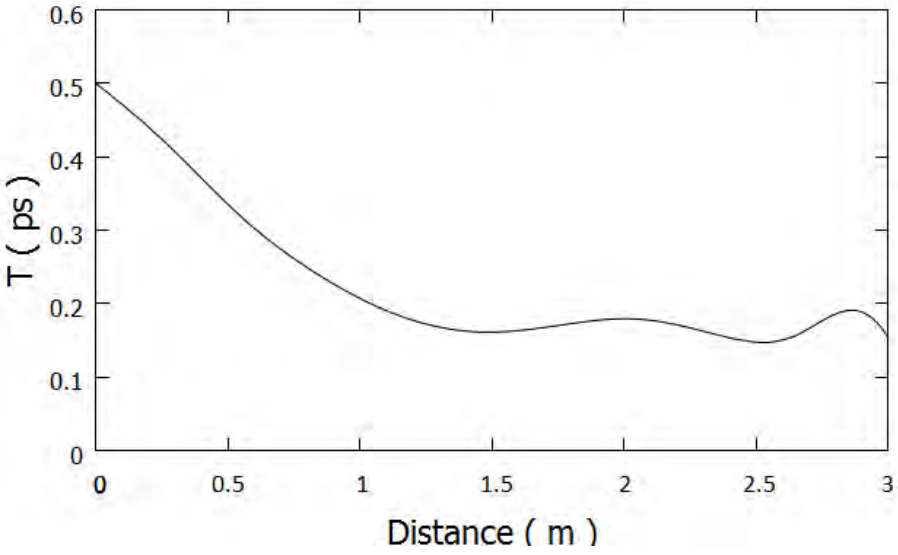

Fig. 5.14: Pulse width vs. distance curve for DDF(N=4).

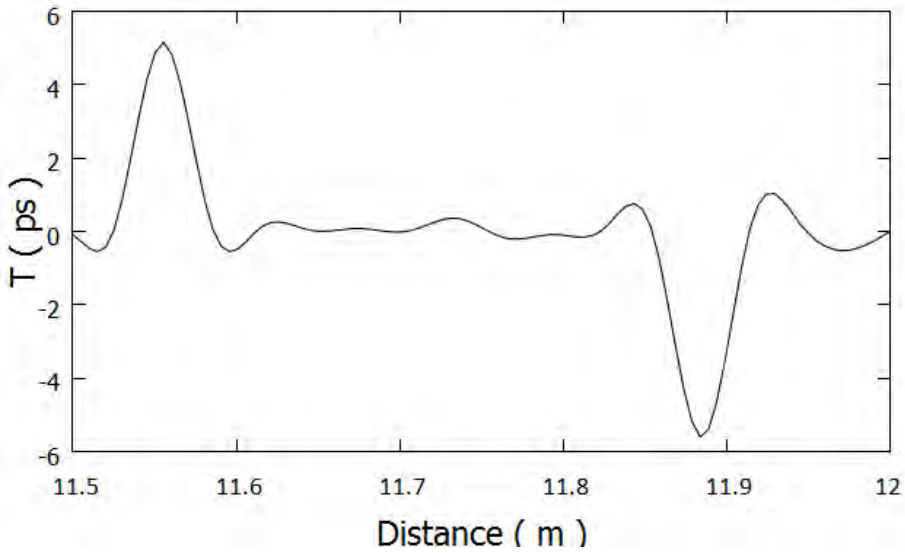

Fig. 5.15: Pulse width vs. distance curve for DCF(N=4).

Let us divert our concentration for newer outcome with 4th order sub-picosecond soliton compression experienced in Fig. 5.14, Fig. 5.15 and Fig. 5.16. In this regime we found a very good compression of 500fs pulse into 150fs in DDF. In the comparison to DCF and FBG with same pulse and parameter we get no more good compression shown in Fig. 5.15 and Fig. 5.16 respectively. Although the best result has been found above all of the analysis in Fig. 5.17, which shows the compression of ultrashort 5th order optical soliton in DDF, but it was not so smooth. The result gives us a compression up to approximately 90fs. Fig. 5.18 and Fig. 5.19 show the result for compression of ultrashort 5th order optical soliton in DCF and FBG as well.

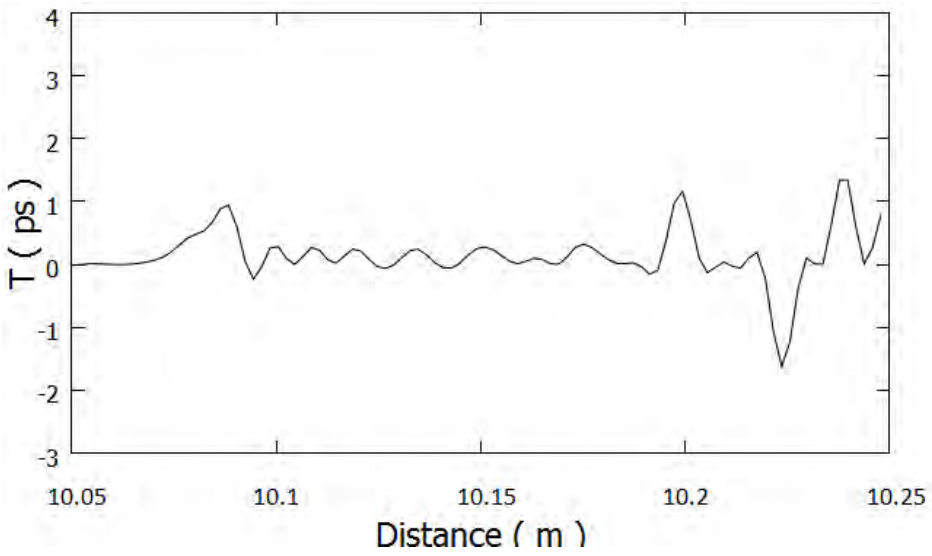

Fig. 5.16: Pulse width vs. distance curve for FBG(N=4).

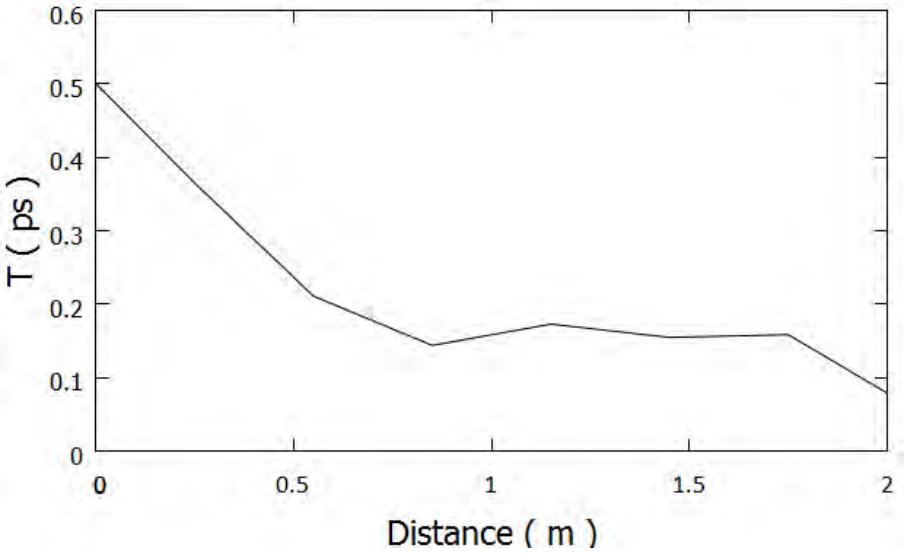

Fig. 5.17: Pulse width vs. distance curve for DDF(N=5).

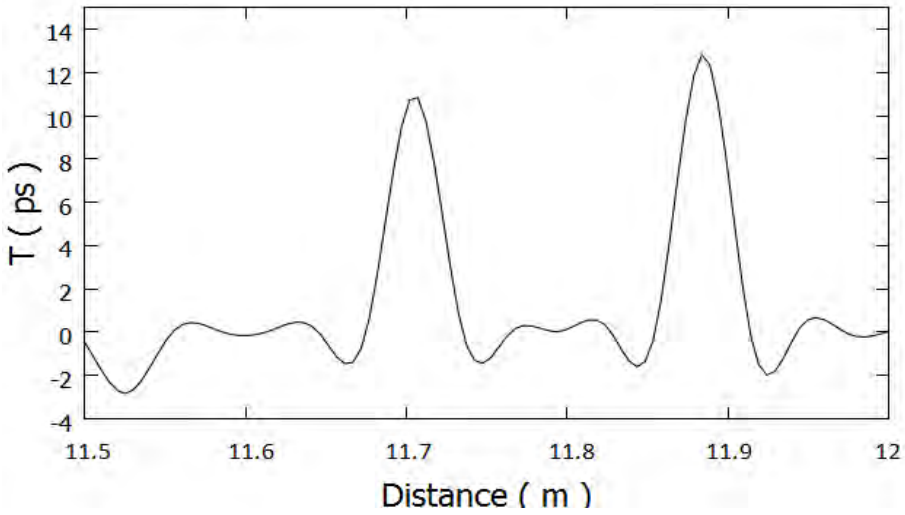

Fig. 5.18: Pulse width vs. distance curve for DCF(N=5).

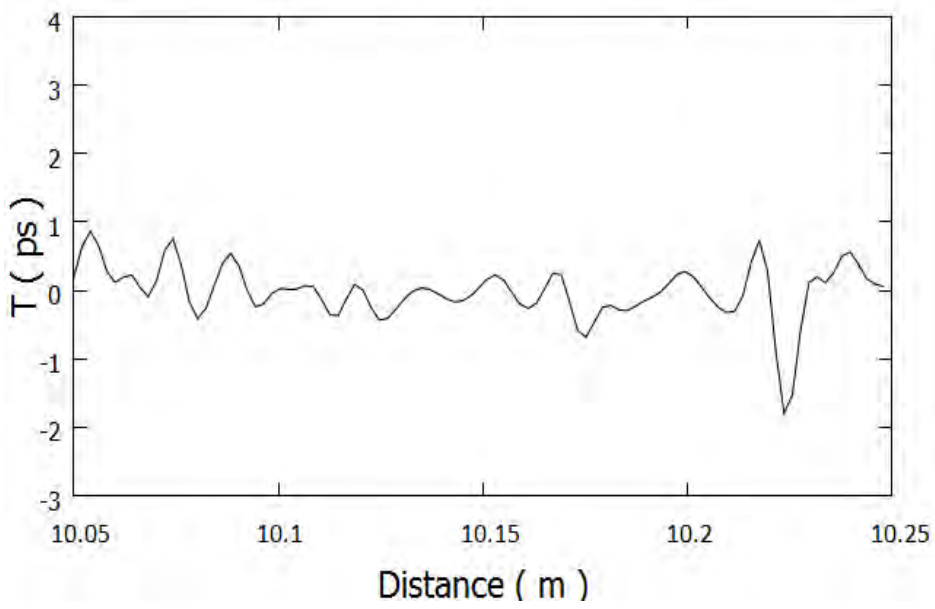

Fig. 5.19: Pulse width vs. distance curve for FBG(N=5).

We can summarize the data for ultrashort soliton compression in DCF, FBG and DDF as the following tabular format.

Table 5.2: Compression in DCF, FBG and DDF

Soliton order	Pulse width before compression	Pulse width after compression in DCF	Pulse width after compression in FBG	Pulse width after compression in DDF
Fundamental	2ps	700fs	500fs	200fs
Higher-order				
2^{nd}	500fs	480fs	Expansion (2.5ps)	340fs
3^{rd}	500fs	350fs	300fs	300fs
4^{th}	500fs	250fs	400fs	150fs
5^{th}	500fs	200fs	200fs	90fs

For 2ps pulse input, the compressed soliton width has been found 700fs, 500fs, 200fs in DCF, FBG and DDF respectively. Second order soliton compression has been explored with 500fs input pulse width. The compressed pulse width is about 480fs in DCF and 340fs in DDF,

whereas expansion happened in FBG. Again in fourth order soliton compression FBG causes expansion to pulse width. Finally in fifth order soliton compression the best output has been observed in DDF. The compressed pulse width is as low as 90fs whereas it has found 200fs in both FBG and DCF.

From all of the above comparison and outcomes for ultrashort optical soliton compression from fundamental and higher-order soliton up to 5^{th} order we can say it is obvious that DCF and FBG can not perform a good compression whereas DDF can perform it with excellence which has been clearly explored in the table. Now let us see the comparison of our study with previous work on DDF based compression [48], [50].

Table 5.3: Comparative statement of DDF based soliton compression

Study	Input Pulse Width	Output Pulse Width	Fiber length (m)	Compression Ratio
Previous study [48], [50]	3.5ps	230fs	1600	15.21
	630fs	115fs	100	5.47
	30ps	6.3ps	4860m	4.76
	1ps	100fs	480	10
Our study	2ps	200fs	900	10
	500fs	90fs	2	5.56

5.4 Medical Applications of the Compressed Ultrashort Soliton Pulse

With the passage of time medical field is becoming more challenging than that of anything. Before treatment the main concern prevails around diagnosis. To cope with this demand, newer technology is coming day by day with the name of biomedical equipment. Modern bio-photonics and microscopy techniques like coherent anti-stokes Raman Scattering (CARS) microscopy, optical coherence tomography etc. are extremely used for identification of chemical and biological species. Refractive surgery, surgery on the inner ear, dentistry, and cardiovascular surgery are now available and very popular. To accomplish this medical applications highly stable and high power pulse are needed. Ultrashort soliton pulse could be the best choice to the case mentioned above. The ability of precise and accurate cutting quality on different materials makes the femtosecond pulse a promising multifunctional

surgery tool. As the ultrashort soliton pulse possesses the properties of stability and high power, it can be used for the removal of abnormal tissues. Before exploring this we need to analyse the normal and abnormal cell size of human body.

Table 5.4: Normal and Abnormal (cancer affected) cell size.

Organs Name	Normal Cell Size	Cancer Cell Size
Liver	20-30 µm	50µm
Lung	7.54 - 8.77µm	Small cell lung cancer = 12.5µm Non-small cell lung cancer = 17.5µm
Breast	21.6±6.9µm	32.6±10.3µm

Table 5.5: Spatial dimension of compressed soliton.

Soliton order	Pulse width before compression	Pulse width after compression in DDF	Spatial soliton pulse in nanometer range after compression in DDF
Fundamental	2ps	200fs	1.61nm
Higher-order			
2^{nd}	500fs	340fs	2.72nm
3^{rd}	500fs	300fs	2.408nm
4^{th}	500fs	150fs	1.2nm
5^{th}	500fs	90fs	722.6pm

We observed maximum abnormal cell sizes are in micrometer range. From section 5.5 we have come to know about the spatial FWHM of compressed ultrashort pulse in DDF. The lowest one was about 722.6 picometer only shown in Table 5.5. Recently chemotherapy and radiotherapy are being used in cancer treatment to abolish the abnormal cells. But for a long period of time these two therapies is detrimental to health because of the side effect. Side effects associated with radiation therapy [81] in treatment of cancer occur because the high doses of radiation (which has spatial dispersion in mm [82] range) used to destroy cancer cells can also damage healthy cells and tissues located near the treatment area. That means the beam spot size of chemotherapy and radiotherapy is in mm^2 which can cause damage to healthy cells. So if it is possible to lessen the beam dimension of therapy than that of

abnormal cell size (μm range) then it will be much more precise to destroy the abnormal cells without affecting the healthy cells. Recently in 2014, a study [83] revealed 70-100 nm^2 for removal of tissue. What we have found in our study the compressed ultrashort soliton has spatial dimension (nm-pm range shown in Table 5.5) lower than that of cancer cell, hence it causes no side effect other then removing the specific affected tissue. In the above condition –soliton therapy" can be a viable technique for cancer cell treatment. More specifically the compressed soliton pulse will maintain small beam of the specific pico or nanometer range and as the cells size exceeds the range of soliton pulse, it will cause no effect to other cells. Hence we can use as small beam as nm^2 - pm^2 range. The specific cancer cell can be removed using high power of ultrashort soliton pulse beam without disturbing other cells of the body.

5.5 Conclusion

Compression of ultrashort fundamental and higher-order soliton and special application of that compressed pulse as Soliton therapy in field of medicine has been demonstrated in this chapter. In section 5.2 the compression characteristics of fundamental soliton and in section 5.3 compression characteristics of higher-order soliton up to 5^{th} order has been explored as well. The additional part in section 5.3 is the measurement of spatial FWHM of compressed pulse. How we can use this compressed pulse in medical treatment is described in section 5.4 and that makes the ending of this chapter.

Chapter 6

Conclusion

6.1 Summery

This thesis has been devoted to the investigation of characteristics of ultrashort soliton propagation, compression and applications of the compressed pulse. In this study, we have explored the impact of fiber nonlinearity, mainly SS and IRS, and third order dispersion on single fiber transmission. First analytical estimation has been deduced. Next changing different parameters we observed the characteristics of ultrashort soliton propagation. Finally, split step Fourier method (SSFM) is used for full numerical simulation. The outcome of this thesis is to simulate the best possible fiber for ultrashort soliton propagation among the different fibers and finding out the opportunity of DDF as ultrashort soliton compressor instead of DCF. We will also optimize the effect of self-steepening in order to achieve improved compression of higher-order ultrashort soliton pulse for precise medical applications.

First, we have discussed the specification of the different fibers used for our experiments. Then the analytic and numerical plots are given for these fibers with respect to different parameters. From the results obtained, it can be concluded that pulse shape fluctuations due to fiber nonlinearity might be a major limiting factor in the way to realize long-haul high speed phase modulated transmission systems. It is clearly seen that the performance degradations are mainly due to the nonlinear effects that occur when there is overlap between dispersed pulses regardless of whether dispersion compensation is deployed. Non-linear effects are due to the fact that the optical properties of the medium become dependent of the transmission length (distance between the transmitter and the receiver), the type of fiber, field intensity, cross-sectional area of the fiber, wavelength and duty cycle. Basically, these effects become more intensive when the optical power or the transmission length increases or when the pulse to pulse spacing becomes narrower. We have explored MCDSF as a viable means for ultrashort soliton propagation with per channel data rate of 1Tb/s.

A comparison between DDF, FBG and DCF based on compression of ultrashort soliton pulse has been explored. The medical applications of that compressed pulse for cancer cell treatment are also presented here named as soliton therapy.

6.2 Future Work

In this thesis we have investigated optical soliton pulse propagation in different optical fibers but we have not considered fiber loss, noise and residual dispersion. So this investigation needs further modification by considering amplifier and receiver noise .Again, we have only considered single channel transmission system. Corresponding transmitter and receiver and other supporting devices should be designed accordingly with this kind of system which we did not study in this thesis. So there are a lot of investigations yet to be done in this area. We have considered 400Gb/s and 1Tb/s here. But in the research arena bit rate is increasing beyond this nowadays. With increasing bit rate, SS and IRS effect will be more dominant in transmission line and contributing error along with the other errors. So, the ultrashort soliton propagation with SS, IRS, and TOD must be investigated for these high speed lines and also for different kinds of optical fibers (SSMF, NZDSF, LEAF, MCDSF, MCDFF).

References and links

1. Pave1 V. Mamyshev, Stanislav V. Chemikov, and E. M. Dianov, –Generation of Fundamental Soliton Trains for High-Bit-Rate Optical Fiber Communication Lines," *IEEE J. Quantum Electron.*, vol. 27, no. 10, pp. 2347-2355, 1991.
2. Ren´e-Jean Essiambre and Govind P. Agrawal, –Ultrahigh-bit-rate soliton communication systems using dispersion-decreasing fibers and parametric amplifiers," *Opt. Lett.*, vol. 21, no. 2, pp. 116-118, 1996.
3. Rene´-Jean Essiambre and Govind P. Agrawal, –Timing jitter of ultrashort solitons in high-speed communication systems. I. General formulation and application to dispersion-decreasing fibers," J. Opt. Soc. Am. B, Vol. 14, No. 2, 1997.
4. I. S. Amiri, S. E. Alavi, Sevia M. Idrus, A. Nikoukar, J. Ali, –IEEE 802.15.3c WPAN Standard Using Millimeter Optical Soliton Pulse Generated by a Panda Ring Resonator," *IEEE Photonics journal*, vol. 5, no. 5, 2013.
5. I. S. Amiri, S. E. Alavi and J. Ali, –High-capacity soliton transmission for indoor and outdoor communications using integrated ring resonators," *International Journal of Communication Systems*, vol. 28, no. 1, pp. 147–160, 2015.
6. M. J. Ablowitz, G. Biondini, L. A. Ostrovsky, –FOCUS ISSUE: Optical Solitons—Perspectives and Applications," *Chaos*, vol. 10, no. 3, pp. 471-474, 2000.
7. A. M. Zysk, F.T. Nguyen, A. L. Oldenburg, D. L. Marks, and S.A. Boppart, –Optical coherence tomography: A review of clinical development from bench to bedside," *J. Biomed. Opt.*, vol. 12, no. 5, pp. 051403(1–21), 2007.
8. Supatto, W., –Femtosecond pulse-induced microprocessing of live Drosophila embryos," *Medical Laser Application*, vol. 20, no. 3, pp. 207-216, 2005.
9. Chung, S.H. and E. Mazur, –Surgical applications of femtosecond lasers," *Journal of biophotonics*, vol. 2, no. 10, pp. 557-572, 2009.
10. Mian, S.I. and R.M. Shtein, –Femtosecond laser-assisted corneal surgery," *Current opinion in ophthalmology*, vol. 18, no. 4, pp. 295-299, 2007.
11. Schwab, B., –Bone ablation using ultrashort laser pulses. A new technique for middle ear surgery," *Laryngo-rhino-otologie*, vol. 83, no. 4, pp. 219-225, 2004.
12. Serbin, J., –Femtosecond lasers as novel tool in dental surgery," *Applied surface science*, vol. 197, pp. 737-740, 2002.
13. Lizarelli, R.F., –Selective ablation of dental enamel and dentin using femtosecond laser pulses," *Laser Physics Letters*, vol. 5, no. 1, pp. 63-69, 2008.

14. Lubatschowski, H., ―Medical applications for ultrafast laser pulses,‖ *Riken Review*, vol. 50, pp. 113-118, 2003.
15. J. Scott Russell, ―Report of 14th Meeting of the British Association for Advancement of Science,‖ New York, pp. 311–390, September 1844.
16. Korteweg, D. J.; de Vries, G. , ―On the Change of Form of Long Waves advancing in a Rectangular Canal and on a New Type of Long Stationary Waves,‖ *Philosophical Magazine*, vol. 39, no. 240, pp. 422–443, 1895.
17. N. J. Zabusky & M. D. Kruskal, ―Interaction of ―SOLITONS‖ in a Collisionless Plasma and the Recurrence of Initial States,‖ *Physical Review Letters*, vol. 15, no. 6, pp. 240-243, 1965.
18. Gardner, Clifford S., Greene, John M., Kruskal, Martin D., Miura, Robert M. ―Method for Solving the Korteweg–deVries Equation,‖ *Physical Review Letters,* vol. 19, no. 19, pp. 1095–1097, 1967.
19. wikipedia.org/wiki/Soliton.
20. Maxworthy, T., ―Experiments on collisions between solitary waves,‖ *Journal of Fluid Mechanics,* vol. 76, no. 1, pp. 177–186, 1976.
21. Fenton, J.D., Rienecker, M.M., ―A Fourier method for solving nonlinear water-wave problems: application to solitary-wave interactions,‖ *Journal of Fluid Mechanics*, vol. 118, pp. 411–443, 1982.
22. Craig, W., Guyenne, P., Hammack, J., Henderson, D., Sulem, C., ―Solitary water wave interactions,‖ *Physics of Fluids,* vol. 18, pp. 057106-25, 2006.
23. Cundiff, S. T., Collings, B. C., Akhmediev, N. N.; Soto-Crespo, J. M.; Bergman, K., Knox, W. H., ―Observation of Polarization-Locked Vector Solitons in an Optical Fiber,‖ *Physical Review Letters,* vol. 82, no. 20, 1999.
24. Tang, D. Y., Zhang, H., Zhao, L. M., Wu, X., ―Observation of high-order polarization-locked vector solitons in a fiber laser,‖ *Physical Review Letters,* vol. 101, no. 15, 2008.
25. X. Zhou, L. E. Nelson, P. Magill, R. Isaac, B. Zhu, D. W. Peckham, P. I. Borel, and K. Carlson, ―High spectral efficiency 400 Gb/s transmission using PDM time-domain hybrid 32–64 QAM and training-assisted carrier recovery,‖ *J. Lightwave Technol.* **,** vol. 31, no. 7, pp. 999-1005, 2013.
26. H. Zhang, J. Cai, H. G. Batshon, M. Mazurczyk, O. Sinkin, D. Foursa, A. Pilipetskii, G. Mohs, and N. Bergano, ―200 Gb/s and dual wavelength 400 Gb/s transmission

over transpacific distance at 6 b/s/Hz dpectral efficiency," *J. Lightwave Technol.* **,** vol. 32, no. 4, pp. 832-839, 2014.

27. T. J. Xia, G. Wellbrock, A. Tanaka, M. Huang, E. Ip, D. Qian, Y. Huang, S. Zhang, Y. Zhang, P. Ji, Y. Aono, S. Murakami, and T. Tajima, ―High capacity field trials of 40.5 Tb/s for LH distance of 1,822 km and 54.2 Tb/s for regional distance of 634 km," *Proceedings of OFC/NFOEC 2013*, paper PDP5A.4, CA, USA, March 17-21, 2013.
28. G. Bosco, V. Curri, A. Carena, P. Poggiolini, and F. Forghieri, ―On the performance of Nyquist-WDM terabit superchannels based on PM-BPSK, PM-QPSK, PM-8QAM or PM-16QAM subcarriers," *J. Lightwave Technol.,* vol. 29, no. 1, pp. 53–61, 2011.
29. J. Wang, C. Xie, and Z. Pan, ―Generation of spectrally efficient Nyquist-WDM QPSK signals using DSP techniques at transmitter," *Proceedings of OFC/NFOEC 2012*, paper OM3H.5, CA, USA, March 6-10, 2012.
30. O. Bertran-Pardo, J. Renaudier, P. Tran, H. Mardoyan, P. Brindel, A. Ghazisaeidi, M. T. Salsi, G. Charlet, and S. Bigo, ―Submarine transmissions with spectral efficiency higher than 3 b/s/Hz using Nyquist pulse-shaped channels," *Proceedings of OFC/NFOEC 2013*, paper OTu2B.1, CA, USA, March 17-21, 2013.
31. Q. Juan, B. Mao, N. Gonzalez, N. Binh, and N. Stojanovic, ―Generation of 28GBaud and 32GBaud PDMNyquist QPSK by a DAC with 11.3GHz analog bandwidth," *Proceedings of OFC/NFOEC 2013*, paper OTh1F.1, CA, USA, March 17-21, 2013.
32. J. Wang, C. Xie, and Z. Pan, ―Generation of spectrally efficient Nyquist-WDM QPSK signals using digital FIR or FDE filters at transmitters," *J. Lightwave Technol. ,* vol. 30, no. 23, pp. 3679–3686, 2012.
33. J.-X. Cai, ―100G Transmission Over Transoceanic Distance With High Spectral Efficiency and Large Capacity," *J. Lightwave Technol.,* vol. 30, no. 24, pp. 3845–3856, 2012.
34. ZHANG Xiaohong, YI Xiaobo, LIU Xiang, Peter J. Winzer, ―100G Transport Systems: Technology Bench-Mark Testing in China and Evolution to Terabit/s Interfaces," *china communications*, pp. 19-30, (April 2013).
35. Edson Silva, Luis Carvalho, Carolina Franciscangelis, Júlio Diniz, Aldário Bordonalli and Júlio Oliveira, ―Spectrally-Efficient 448-Gb/s dual-carrier PDM-16QAM channel in a 75-GHz grid," *Proceedings of OFC/NFOEC 2013*, paper JTh2A.39, CA, USA, March 17-21, 2013.

36. Zhang, J., Yu, J., and Chi, N., "Generation and transmission of 512-Gb/s quadcarrier digital super-Nyquist spectral shaped Signal," *OPTICS EXPRESS*, vol. 21, no. 25, pp. 31212-31217, 2013.
37. Daniel J. Blumenthal, "Terabit Optical Ethernet For Avionics," *Proceedings of (AVFOP), 2011 IEEE*, pp. 61-62, CA, USA, 4-6 Oct., 2011.
38. O'Sullivan, M., Laperle, C., Borowiec, A., Farley, K., "A 400G/1T High Spectral Efficiency Technology and Some Enabling Subsystems," *Proceedings of OFC/NFOEC 2012*, paper OM2H.1, CA, USA, March 6-10, 2012.
39. Zong, L., Liu, G., N., Lord, A., Zhou, Y., R., and Ma, T., "40/100/400 Gb/s Mixed Line Rate Transmission Performance in Flexgrid Optical Networks," *Proceedings of OFC/NFOEC 2013*, paper OTu2A.2, CA, USA, March 17-21, 2013.
40. V. A. J. M. Sleiffer, M.S.Alfiad, D. van den Borne,M. Kuschnerov, V. Veljanovski, M. Hirano, Y. Yamamoto, T. Sasaki, S. L. Jansen,T. Wuth, and H. de Waardt, "10 × 224-Gb/s POLMUX-16QAM Transmission Over 656 km of Large-A_{eff} PSCF With a Spectral Efficiency of 5.6 b/s/Hz," *IEEE Photonics Technology Letters,* vol. 23, no. 20, 2011.
41. G.M. Carter, R.-M. Mu, V.S. Grigoryan, C.R. Menyuk, P. Sinha, T.F. Carruthers, M.L. Dennis and Duling III, "Transmission of dispersion managed solitons at 20Gb/s over 20000km," *Electronics Letters*, vol. 35, no. 3, 1999.
42. Masataka Nakazawa, Hirokazu Kubota, Kenji Kurokawa, and Eiichi Yamada, "Femtosecond optical soliton transmission over long distances using adiabatic trapping and soliton standardization," *J. Opt. Soc. Am. B*, vol. 8, no. 9, 1991.
43. Z. Jiang, S.-D. Yang, D. E. Leaird, and A. M. Weiner, "Fully dispersion-compensated ~500 fs pulse transmission over 50 km single-mode fiber," *Opt. Lett.,* vol. 30, no. 12, pp. 1449-1451, 2005.
44. Vladimir Pechenkin and Frank R. Kschischang, "Higher Bit Rates for Dispersion-Managed Soliton Communication Systems via Constrained Coding," *Journal of Lightwave Technology,* vol. 24, no. 3, pp. 1149, 2006.
45. I. S. Amiri, D. Gifany, J. Ali, "Long Distance Communication Using Localized Optical Soliton via Entangled Photon," *IOSR Journal of Applied Physics* , vol. 3, no.1, pp. 32-39, 2013.
46. I. S. Amiri , D. Gifany , J. Ali, "Ultrashort Multi Soliton Generation for Application in Long Distance Communication," *J. Basic. Appl. Sci. Res.,* vol. 3, no. 3, pp. 442-451, 2013.

47. Amir Mostofi, Hamid Hatami-Hanza,and Pak L. Chu, ―Optimum Dispersion Profile for Compression of Fundamental Solitons in Dispersion Decreasing Fibers", *IEEE Journal of Quantum Electronics,* vol. 33, no. 4, 1997.
48. P. K. A. Wai, W. Cao **,** **"**Ultrashort soliton generation through higher-order soliton compression in a nonlinear optical loop mirror constructed from dispersion-decreasing fiber" *JOSA B*, vol. 20, no. 6, pp. 1346-1355, 2003.
49. P. Beaud, W. Hodel, B. Zysset, and H. P. Weber, ―Ultrashort pulse propagation, pulse breakup, and fundamental soliton formation in a single-mode optical fiber," *IEEE J. Quantum Electron.,* vol. 23, no. 11, pp. 1938-1946, 1987.
50. SV Chernikov, DJ Richardson, DN Payne, ―Soliton pulse compression in dispersion-decreasing fiber," *Opt. lett.,* vol. 18, no. 7, pp. 476-478, 1993.
51. Anu Sheetal , Ajay K.Sharma, R.S.Kaler ―Minimization of self-steepening of ultrashort higher-order soliton pulse at 40 Gb/s by the optimization of initial frequency chirp" *Optik - International Journal for Light and Electron Optics ,* vol. 121, no. 5, pp. 471–477, 2010.
52. F. Futami, K. Taira, K. Kikuchi, and A. Suzuki, ―Wideband fibre dispersion equalisation up to fourth-order for long-distance subpicosecond optical pulse transmission," *Electron. Lett.,* vol. 35, no. 25, pp. 2221-23, 1999.
53. M. D. Pelusi, F. Futami, K. Kikuchi, and A. Suzuki, ―Fourth-order dispersion compensation for 250-fs pulse transmission over 139-km optical fiber," *IEEE Photon. Technol. Lett.*, vol.12, no. 7, pp. 795-797, 2000.
54. T. Yamamoto, E. Yoshida, K. R. Tamura, K. Yonenaga, and M. Nakazawa, ―640-Gbit/s optical TDM transmission over 92 km through a dispersion-managed fiber consisting of single-mode fiber and "reverse dispersion fiber"," *IEEE* Photon. *Technol. Lett.,* vol. 12, no.3, pp. 353-355, 2000.
55. Akimaru, H. and M. R. Finley, ―Elements of the emerging broadband information highway," *IEEE Commun. Mag.*, vol. 35, pp. 84–94, 1997.
56. Chraplyvy, A. R. and R. W. Tkach, ―Terabit/second transmission experiments," *IEEE J. Quantum Electron.*, vol. 34, pp. 2103–2108, 1998.
57. Zon, X. Y., M. I. Hayee, S. M. Hwang, and A. E. Willner, ―Limitations in 10-Gb/s WDM optical fiber transmission when using a variety of fiber types to manage dispersion and nonlinearities," *J. Lightwave Tech.*, vol. 14, pp. 1144–1152, 1996.

58. Biswas, A. and S. Konar, "Soliton-solitons interaction with kerr law non-linearity," *Journal of Electromagnetic Waves and Applications*, vol. 19, no. 11, pp. 1443–1453, 2005.
59. Sawetanshumala, S. Jana, and S. Konar, "Propagation of a mixture of modes of a laser beam in a medium with saturable nonlinearity," *Journal of Electromagnetic Waves and Applications*, vol. 20, no. 1, pp. 65–77, 2006.
60. L. A. Ostrovskii, "Propagation Of Wave Packets And Space-Time Self-Focusing In A Nonlinear Medium," *Sov. Phys. JETP ,* vol. 24, no. 4, pp. 797, 1967.
61. R. J. Jonek and R. Landauer, "Laser pulse distortion in a nonlinear dielectric," *Phys. Lett.,* vol. 24, no. 4, pp. 228-229, 1967.
62. F. DeMartini, C. H. Townes, T. K. Gustafson, and P. L. Kelley, "Self-Steepening of Light Pulses," *Phys. Rev.,* vol. 164, no. 2, pp. 312, 1967.
63. D. Grischkowsky, E. Courtens, and J. A. Armstrong, "Observation of Self-Steepening of Optical Pulses with Possible Shock Formation," *Phys. Rev. Lett. ,* vol. 31, no. 7, pp. 422, 1973.
64. Md. Shariful Islam, Numerical Analysis of GVD and TOD Compensation at 160 Gb/s Long-Haul Transmission Using Fiber Bragg Grating, M.Sc Thesis, BUET, Dhaka, Bangladesh, March 2014.
65. Y.Aoki, K. Tajima, and I. Mito, "Input Power Limits of Single-Mode Optical Fibers due to Stimulated Brillouin Scattering in Optical Communication Systems," *J. of Lightwave Technol*., vol. 6, No. 10, pp. 710-719, 1998.
66. G.P. Agrawal, Nonlinear Fiber Optics, Academic Press, San Diego, CA, 2001.
67. N. Tzoar and M. Jain, "Self-phase modulation in long-geometry optical waveguides," *Phys. Rev. A ,* vol. 23, no. 3, pp. 1266, 1981.
68. E. M. Dianov, A. Y. Karasik, P. V. Mamyshev, A. M. Prokhorov, V. N. Serkin, M. F. Stel'makh, and A. A. Fomichev, "Stimulated-Raman conversion of multisoliton pulses in quartz optical fibers," *JETP Lett.,* vol. 41, no. 6, pp. 242-244, 1985.
69. M. J. Ablowitz and P. A. Clarkson, *Solitons, Nonlinear Evolution Equations, and Inverse Scattering* (Cambridge University Press, New York, 1991).
70. J. T. Taylor (ed.), *Optical Solitons—Theory and Experiment*, (Cambridge University Press, New York, 1992).
71. A. Hasegawa and F. Tappert, "Transmission of stationary nonlinear optical pulses in dispersive dielectric fibers. I. Anomalous dispersion," *Appl. Phys. Lett.* vol. 23, no. 3, pp. 142-144, 1973.

72. K. Tajima, –*Compensation of soliton broadening in nonlinear optical fibers with loss*," *Opt. Lett*., vol. 12, no. 1, pp. 54-56, 1987.
73. Finot C, Barviau B, Millot G, Guryanov A, Sysoliatin A and Wabnitz, –Parabolic pulse generation with active or passive dispersion decreasing optical fibers," *Opt. Express ,* vol.15,no. 24, pp. 15824-15835, 2007.
74. D. N. Christodoulides, and R. I. Joseph, –Slow Bragg solitons in nonlinear periodic structure", *Phys. Rev. Lett*., Vol. 62, No. 15, pp. 1746-1749, 1989.
75. H. Kogelnik and C. V. Shank, –Stimulated emission in a periodic structure," *Appl. Phys. Lett.,* Vol. 18, pp. 152–154, 1971.
76. Q. Li, P. K. A. Wai, K. Senthilnathan, –Modeling Self-Similar Optical Pulse Compression in Nonlinear Fiber Bragg Grating Using Coupled-Mode Equations," *Journal of Lightwave Technology*, vol. 29, no.9, pp. 1293-1305, 2011.
77. Q. Li, K. Senthilnathan, K. Nakkeeran, and P. K. A. Wai, –Nearly chirp- and pedestal-free pulse compression in nonlinear fiber Bragg gratings," *J. Opt. Soc. Am. B*, vol. 26, no. 3, pp. 432-443, 2009.
78. C. C. Chang, Weiner, Vengsarkar, D. W. Peckham, –Broadband fiber dispersion compensation for sub-100-fs pulses with a compression ratio of 300," *Opt. Lett.,* vol. 21, no. 15, pp. 1141-1143, 1996.
79. J. H. Lee, T. Kogure and D. J. Richardson, –Wavelength Tunable 10-GHz 3-ps Pulse Source Using a Dispersion Decreasing Fiber-Based Nonlinear Optical Loop Mirror," *IEEE J. Quantum Electron.*, vol. 10, no. 1, pp. 181-185, 2004.
80. D. Chao-Qing and C. Jun-Lang, –Ultrashort optical solitons in the dispersion-decreasing fibers," *Chin. Phys. B,* vol. 21, no. 8, pp. 080507(1-4), 2012.
81. J. R. Owen, A. Ashton, J. M. Bliss, J. Homewood, C. Harper, J. Hanson, J. Haviland, S. M. Bentzen, J. R. Yarnold, –Effect of radiotherapy fraction size on tumour control in patients with early-stage breast cancer after local tumour excision: long-term results of a randomised trial," *oncology.thelancet.com*, vol. 7, pp. 467-471, 2006.
82. T. Kondoh, J. Yang, Y. Yoshida, and S. Tagawa, –Electron Beam Pulse Processing Toward The Intensity Modified Radiation Therapy (IMRT)," *Proceedings of EPAC 2006*, paper WEPCH172, pp. 2334-2336, Edinburgh, Scotland, 18 September, 2006.
83. Afroozeh, Zeinalinezhad and S. Pourmand, –Optical Soliton Pulse Generation to Removal of Tissue," *IJBPAS*, vol. 3, no.11, pp. 2587-2594, 2014.